91602
new 82-10 LEGAL NOTICE

This report was prepared by Ontario Hydro and, while effort has been made to assure the accuracy and applicability of the material contained herein, neither Ontario Hydro nor any person acting on its behalf:

(a) makes any warranty, express or implied with respect to the use of any information, apparatus, method or process disclosed in this report or that such use may not infringe privately owned rights; or

(b) assumes any liabilities with respect to the use of, or for damages resulting from the use of, any information, apparatus, method or process disclosed in this report.

ontario hydro
research division

COMPLIMENTARY COPY
Please Credit Ontario Hydro Research if Reproduced in Whole or in Part

FRACTURE PROPERTIES OF BRUCE HEAVY WATER PLANT HYDROGEN-BLISTERED A516 Gr 70 CARBON STEEL

Report No. 89-135-K

O.E. Lepik and D.W. Carpenter
Nondestructive and Fracture Evaluation Section
Metallurgical Research Department

ABSTRACT

The fracture properties of hydrogen-blistered steel have been evaluated to assist in establishing repair or retirement criteria for hydrogen blistered pressure vessels at BHWP. The fracture toughness and crack growth resistance of hydrogen-charged A516 Gr 70 carbon steel containing hydrogen-induced blister cracks was characterized at 21 and 43°C. Results showed that the blister damage present did not have a significant effect on the material's fracture properties. Hydrogen-charged material exhibited a threefold reduction in J-resistance curve fracture toughness at 21°C, compared to nominally identical uncharged material. A fractographic examination indicated that the presence of hydrogen affected the fracture mode.

Hydrogen blister cracks in the BHWP H_2S absorber tower were assessed using a fracture mechanics approach. Critical crack lengths of postulated axial through-wall flaws, used to model the blister damage, are reported.

job	file	date	report no.
83-238-553	826.232	November 3, 1989	89-135-K

91602
new 82-10

90-01727/

ontario hydro
research division

EXECUTIVE SUMMARY

FRACTURE PROPERTIES OF BRUCE HEAVY WATER PLANT HYDROGEN-BLISTERED A516 Gr 70 CARBON STEEL

Report No. 89-135-K

O.E. Lepik and D.W. Carpenter
Nondestructive and Fracture Evaluation Section
Metallurgical Research Department

OBJECTIVE: To assist in establishing repair or retirement criteria for BHWP blistered steel pressure vessels, the objective of the present study was to determine the fracture properties of hydrogen-charged A516 Gr 70 carbon steel containing hydrogen-induced blister cracks. The material fracture properties were then used in a fracture mechanics assessment of hydrogen-induced blister cracking in the BHWP H_2S absorber tower.

MAJOR RESULTS OF STUDY:

1. Hydrogen-induced blister cracking in A516 Gr 70 steel removed from the old E1 absorber tower at BHWP had little or no effect on fracture toughness. The small effect of the blisters on the fracture behaviour may be attributed partly to the nature of blistering in this material because the material tested contained a single macroscopic blister or delamination in the plate through-thickness direction.

2. Hydrogen significantly affected the fracture toughness of A516 Gr 70 carbon steel at 21 and 43°C. At 21°C, hydrogen-charged material exhibited a three-fold reduction in J-Resistance curve fracture toughness, compared to nominally identical uncharged material.

3. Toughness of A516 Gr 70 carbon steel plate is dependent on inclusion orientation. Higher toughness (J_{Ic} and J-R curve) was exhibited in the C-R orientation than in the C-L orientation.

job	file	date	report no.
83-238-553	826.232	November 3, 1989	89-135-K

4. Repair or retirement criteria can be established for hydrogen blistered carbon steel pressure vessels by using elastic-plastic fracture mechanics. EPFM procedures proposed for the ASME Boiler and Pressure Vessel Code were used as guidelines in performing this evaluation. Blister cracking in the bottom section of H_2S absorber tower DA-3110 was assessed by this method and was modelled using a postulated axial through-wall flaw. Using a safety margin of 2.0 on internal design pressure, the allowable length of an axial through-wall flaw was determined to be 20.3 cm.

RECOMMENDATIONS:

1. It is recommended that additional fracture toughness J-tests be carried out on A516 Gr 70 steel plate known to contain numerous blisters in the same location in the through-thickness direction. Blister cracking of this severity would establish conclusively lower bound crack growth resistance J-R curves for blistered material.

2. Integrity assessments of blistered components using fracture mechanics principles are reliant on having accurate information available on the size of the blistered region in the component. In adopting such an assessment procedure, it is recommended that future nondestructive inspections determine the size of blistered areas known to contain step-wise cracking or closely-spaced blisters. A C-scan or a distance-coded C-scan (DC-scan) of highly blistered regions would provide the necessary information for such an assessment.

3. An elastic-plastic fracture mechanics analysis, which uses a postulated part-through wall flaw on the vessel's inside surface to model blister cracking, is recommended for future structural integrity assessments where leakage of the process medium is not tolerated. Analyses of this nature can more realistically estimate the allowable flaw size in a cracked component. However, this type of analysis places more stringent requirements on the nondestructive evaluation (NDE) of the component. For such an evaluation the NDE inspection must be capable of providing accurate information on the size of the blister group and the depth of the closest blister to the outside surface in the blister group.

TABLE OF CONTENTS

		Page
1.0	PURPOSE	1
2.0	CONCLUSIONS	1
3.0	RECOMMENDATIONS	2
4.0	BACKGROUND	2
5.0	EXPERIMENTAL PROGRAM	3
	5.1 Materials	3
	5.2 Specimen Details	3
	5.3 Mechanical Tests	5
	5.4 Fracture Toughness Tests	5
	5.5 Fractographic Examination	6
6.0	ANALYSIS OF J-R CURVE DATA	6
7.0	RESULTS	7
	7.1 Tensile Properties	7
	7.2 Fracture Toughness Properties	7
	7.2.1 J-R Curves	7
	7.3 Fractographic Features	11
8.0	INTEGRITY ASSESSMENT OF BLISTER DAMAGE IN H_2S ABSORBER TOWER DA-3110	12
	8.1 Nature of Hydrogen Damage in Low Strength Steels	12
	8.2 Failure Criteria	13
	8.3 Modelling Blister Damage	13
	8.4 Material Properties	14
	8.4.1 Tensile Properties	15
	8.4.2 Crack Growth Resistance J-R Curve	15
	8.5 Component Design Details and Stresses	15
	8.6 J-Integral/Tearing Modulus Approach	16
	8.6.1 J-Integral Resistance Curve Analysis	16
	8.6.2 J-Controlled Crack Growth	17
	8.6.3 Safety Factors	17
ACKNOWLEDGEMENTS		18
REFERENCES		19

Page

APPENDICES

A Graphs and Tables from All Tests A1

B Fracture Surfaces of All Tests B1

DISTRIBUTION last page

ontario hydro
research division

To G.D. Davidson
Manager
Bruce Heavy Water Plant

FRACTURE PROPERTIES OF BRUCE HEAVY WATER PLANT HYDROGEN-BLISTERED A516 Gr 70 CARBON STEEL

1.0 PURPOSE

The objective of the present study was to determine the fracture properties of hydrogen-charged A516 Gr 70 carbon steel containing hydrogen-induced blister cracks to assist in establishing repair or retirement criteria for BHWP blistered steel pressure vessels. The material fracture properties were then used in a fracture mechanics assessment of hydrogen-induced blister cracking in the BHWP H_2S absorber tower.

2.0 CONCLUSIONS

1. Hydrogen-induced blister cracking in A516 Gr 70 steel removed from the old E1 absorber tower at BHWP had little or no effect on fracture toughness. The small effect of the blisters on the fracture behaviour may be attributed partly to the nature of blistering in this material because the material tested contained a single macroscopic blister or delamination in the plate through-thickness direction.

2. Hydrogen significantly affected the fracture toughness of A516 Gr 70 carbon steel at 21 and 43°C. At 21°C, hydrogen-charged material exhibited a three-fold reduction in J-Resistance curve fracture toughness, compared to nominally identical uncharged material.

3. Toughness of A516 Gr 70 carbon steel plate is dependent on inclusion orientation. Higher toughness (J_{Ic} and J-R curve) was exhibited in the C-R orientation than in the C-L orientation.

4. Repair or retirement criteria can be established for hydrogen blistered carbon steel pressure vessels by using elastic-plastic fracture mechanics. EPFM procedures proposed for the ASME Boiler and Pressure Vessel Code were used as guidelines in performing this evaluation. Blister cracking in the bottom section of H_2S absorber tower DA-3110 was assessed by this method and was modelled using a postulated axial through-wall flaw. Using a safety margin of 2.0 on internal design pressure, the allowable length of an axial through-wall flaw was determined to be 20.3 cm.

3.0 RECOMMENDATIONS

1. It is recommended that additional fracture toughness J-tests be carried out on A516 Gr 70 steel plate known to contain numerous blisters in the same location in the through-thickness direction. Blister cracking of this severity would establish conclusively lower bound crack growth resistance J-R curves for blistered material.

2. Integrity assessments of blistered components using fracture mechanics principles are reliant on having accurate information available on the size of the blistered region in the component. In adopting such an assessment procedure, it is recommended that future nondestructive inspections determine the size of blistered areas known to contain step-wise cracking or closely-spaced blisters. A C-scan or a distance-coded C-scan (DC-scan) of highly blistered regions would provide the necessary information for such an assessment.

3. An elastic-plastic fracture mechanics analysis, which uses a postulated part-through wall flaw on the vessel's inside surface to model blister cracking, is recommended for future structural integrity assessments where leakage of the process medium is not tolerated. Analyses of this nature can more realistically estimate the allowable flaw size in a cracked component. However, this type of analysis places more stringent requirements on the nondestructive evaluation (NDE) of the component. For such an evaluation the NDE inspection must be capable of providing accurate information on the size of the blister group and the depth of the closest blister to the outside surface in the blister group.

4.0 BACKGROUND

Hydrogen-induced blister cracking of BHWP steel pressure vessels has been an ongoing concern since its discovery in the E1 absorber tower in 1975/1/. A number of vessels have since been taken out of service because of the severity of this damage while numerous others, with lesser amounts of damage, are presently in operation. While the ultimate solution to this problem is the use of inclusion shape-controlled steels of low inclusion content, the replacement of all existing susceptible vessels and piping is extremely costly. As a practical alternative, an approach based on fracture mechanics principles can be used to determine the degree of hydrogen blister cracking a particular component can sustain before the risk of leakage or component failure becomes unacceptable.

The present investigation was motivated by a request from BHWP to assist in establishing retirement criteria for hydrogen blistered pressure vessels. Results of a fracture test program on blistered steel plate, removed from the old E1 absorber tower at BHWP, are reported, and used in a fracture mechanics assessment of the hydrogen blister cracking in H_2S absorber tower DA-3110.

5.0 EXPERIMENTAL PROGRAM

5.1 Materials

The materials used in this study were samples of 19.0 mm thick plates of A516 Gr 70 carbon steel removed from the BHWP H_2S absorber tower. Prior to testing, each plate was ultrasonically inspected by the NDE unit at Research to map out the blistered regions. Details of the ultrasonic inspection are reported in Ref. 2. Plates identified as 'B', 'C', 'D' and the Research or 'R' plates in /2/ were selected for this investigation. Plates B, C and D contained blisters which were located near the inside surface while plate R contained extensive blistering and some stepwise cracks which were not near-surface.

All plate materials were heat treated in air at 250°C for 24 h. This "bake-out" treatment was used to remove most of the dissolved atomic hydrogen in the steel. Molecular hydrogen trapped at internal discontinuities in the steel was not removed by this heat treatment.

In machining the specimens, nearly all of the blister damage was removed from plates B, C and D. Thus, for the purposes of this investigation, specimens from these plates were considered to be free of blisters. Blisters were present in the specimens removed from plate R.

5.2 Specimen Details

Standard round tensile specimens (12.7 mm dia.) were machined from plates B and C from the mid-thickness location. The specimens were oriented such that the tensile axis was parallel to the rolling (hoop) direction.

Three-point bend specimens were used in the fracture test program. The specimen blanks were machined from the plates as shown in Figure 1. The crack plane was oriented such that the crack was in the radial-axial plane with crack growth in either the axial direction (C-L orientation) or the radial direction (C-R orientation). Specimen dimensions are shown in Figure 2. The bend specimen had a width of 15.87 mm, with the other in-plane dimensions in the proportions specified in ASTM E813-87/3/. The thickness of the specimen (15.87 mm) was larger than the specimen geometry recommendations of the ASTM specification to increase crack-tip constraint. All specimens were precracked and sidegrooved after precracking to promote flat fracture and a straight crack front. The average thickness reduction from sidegrooving was approximately 20%.

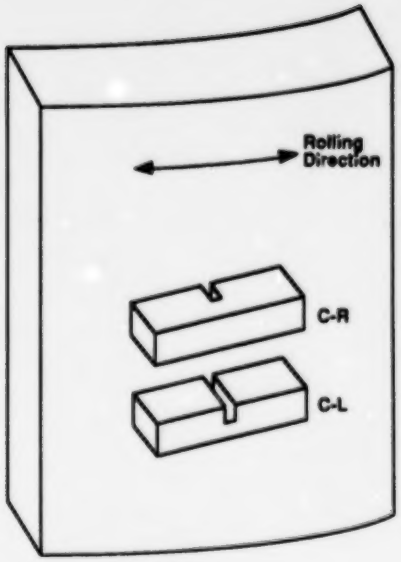

FIGURE 1 Specimen Orientation

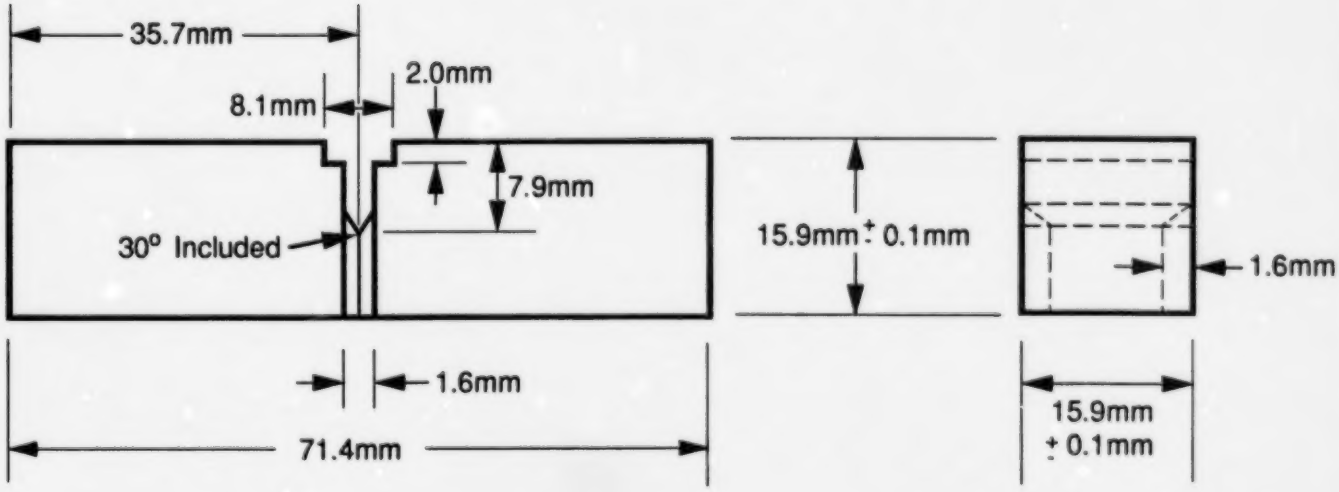

FIGURE 2 Three-Point Bend Specimen Dimensions

Specimens charged with hydrogen were cathodically charged at 21°C in a 1 N H_2SO_4 solution containing 2 g/l of $Na_2HAsO_4.7H_2O$ as the recombination inhibitor. The current densities and charging times ranged from 4 to 30 mA/cm^2 and from 14 to 24 h, respectively. A platinum anode electrode was used. All specimens charged with hydrogen were stored in liquid nitrogen before testing to minimize hydrogen outgassing.

5.3 Mechanical Tests

The tensile properties of plates B and C were determined at temperatures of 21 and 145°C spanning the operating temperature range of BHWP process components. The time required for heat-up was minimized to prevent excessive loss of hydrogen from the hydrogen-charged specimens. Heat-up time to 145°C was less than 35 minutes. All tensile tests were carried out at a strain rate of 10^{-4} s^{-1}.

5.4 Fracture Toughness Tests

A single specimen technique, performed according to the procedure outlined in ASTM test specification E1152-87/4/ was used to determine the J-resistance (J-R) curves. An MTS servohydraulic test machine, interfaced to a personal computer for test control and data acquisition, was used for testing. Specimens were tested in air at 21°C and at 43°C, the design temperature of the absorber tower. Specimen temperature was maintained by a box furnace and monitored by a thermocouple that was spot-welded to the surface of the specimen. Tests at 43°C were controlled to ±2°C. Specimen displacement was monitored by an LVDT. Stroke was corrected for machine and load fixture compliance using unnotched specimen blanks of blistered and blister-free material. Crack extension, monitored by a displacement gauge mounted on razor blades at the crack mouth, was estimated by using the unloading compliance method.

The J-tests were conducted at a slow loading displacement rate (i.e., strain rate) to enhance any potential hydrogen embrittlement that may occur in this material in this temperature range. A constant loading displacement rate of 8.3×10^{-5} mm/s was used. The test matrix, outlining the test temperatures and specimen details, is shown in Table 1.

TABLE 1

Program Test Matrix

Plate and Specimen ID	Specimen Orientation	Material Condition (1)	Test Temperature (°C)
C2, D3, R1	C-R	NH	21
R8	C-L	NH	21
B1, C1, D2, R4	C-R	H	21
R6	C-L	H	21
B3, C7	C-R	NH	43
C	C-R	H	43

Note: (1) NH: Not Hydrogen Charged
H: Hydrogen Charged

The onset of crack initiation was determined in a number of tests by using the d.c. potential drop (DCPD) technique. The potential measurement leads were placed diagonally across the crack mouth to minimize effects from crack bowing or tunnelling and the current leads were located on the ends of the specimen. The potential leads were spot-welded to the specimen while the current leads were fixed to the specimen with screws. Electrically insulated loading pins were used and the displacement gauge was not insulated from the razor blades on the specimen. Good sensitivity to crack extension was obtained by using a constant current of 8 or 10 A.

After testing the specimens were either heat tinted by a bunsen burner or fatigue cracked to mark the crack extension that had occurred. All specimens were then chilled in liquid nitrogen prior to being broken in two to expose the crack surfaces. The initial crack length after fatigue precracking and the final length were then measured on the fracture surface using the nine point average method described in ASTM E813-87. Following this the data was processed and plotted in the form of a J-R curve.

5.5 Fractographic Examination

The fracture surface of each specimen was examined in the stereomicroscope and photographed. The fracture surfaces of selected specimens were also examined in the scanning electron microscope to determine the effect of hydrogen and step-wise cracking on the fracture mode.

6.0 ANALYSIS OF J-R CURVE DATA

J_{Ic}, the fracture toughness near the initiation of slow stable crack growth, was determined in accordance with the method outlined in ASTM E813-87. J_{Ic} is defined by the intersection of a power law regression fit of the data between the 0.15 and 1.5 mm exclusion lines with a line that is parallel but offset by 0.2 mm from the blunting line. The blunting line is given by the relationship:

$$J = 2\sigma_f \Delta a \qquad (1)$$

where σ_f is the flow stress (the average of the 0.2% offset yield strength and ultimate tensile strength values) and Δa is the crack extension. The average tensile properties listed in Table 2 were used to define the blunting line.

The J-R curve was determined using the J-integral equation recommended in ASTM E1152-87. The J-R curve was established by a power law regression fit expressed by:

$$J = C_1 (\Delta a)^{C_2} \qquad (2)$$

of the experimental data points. This equation has been used extensively to establish J-R curves for ferritic steels/5/. Experimental data points from approximately the point of departure from the blunting line to the end of the test were used to calculate the constant C_1 and the exponent C_2.

7.0 RESULTS

7.1 Tensile Properties

The tensile properties of plates B and C were similar (see Table 2). As expected, the yield and ultimate strengths were unaffected by hydrogen charging, but tensile ductility, as reflected by % elongation and % reduction in area was markedly reduced by hydrogen charging.

The average tensile values in Table 2 were used for all the plate materials tested in this program. Values for the tensile flow stress and Young's modulus at 43°C were obtained from Ref. 6, and were estimated to be 438.0 MPa and 191.9 GPa, respectively.

TABLE 2

Tensile Properties of A516 Gr 70 Carbon Steel

Plate and Specimen ID	Test Temperature (°C)	Material Condition (1)	Yield Strength 0.2% Offset (MPa)	UTS (MPa)
C1	21	NH	366.9	-
C4	21	NH	366.5	530.0
C3	21	H	-	529.2
B3	21	H	366.5	526.0
B2	145	NH	297.1	493.3
B1	145	H	296.0	485.7
C2	148	H	306.6	482.6

Note:

(1) NH: Not Hydrogen Charged
H: Hydrogen Charged

7.2 Fracture Toughness Properties

7.2.1 J-R Curves

Representative J-R curves showing the effect of blister damage, specimen orientation and hydrogen are illustrated in Figures 3, 4 and 5, respectively. The hydrogen blister cracking present in plate R appeared to have little or no effect on the J-R curve crack growth resistance, as shown in Figure 3. The small effect of the blisters on the fracture behaviour may be attributed partly to the nature of blistering in this material: blister damage in the fractured specimens was manifest as a

single macroscopic blister or delamination in the plate through-thickness direction. A single blister can be expected to have little effect on the material's gross fracture properties.

A comparison of the C-L and C-R cracking orientations in Figure 4 showed that the crack growth resistance was higher in the C-R orientation. This difference in tearing behaviour reflects the orientation effects of non-metallic inclusions in rolled steels.

The presence of hydrogen significantly affected the fracture behaviour at 21 and 43°C, as shown in Figure 5. At 21°C hydrogen-charged material exhibited a threefold reduction in J-R curve fracture toughness, compared to nominally identical uncharged material.

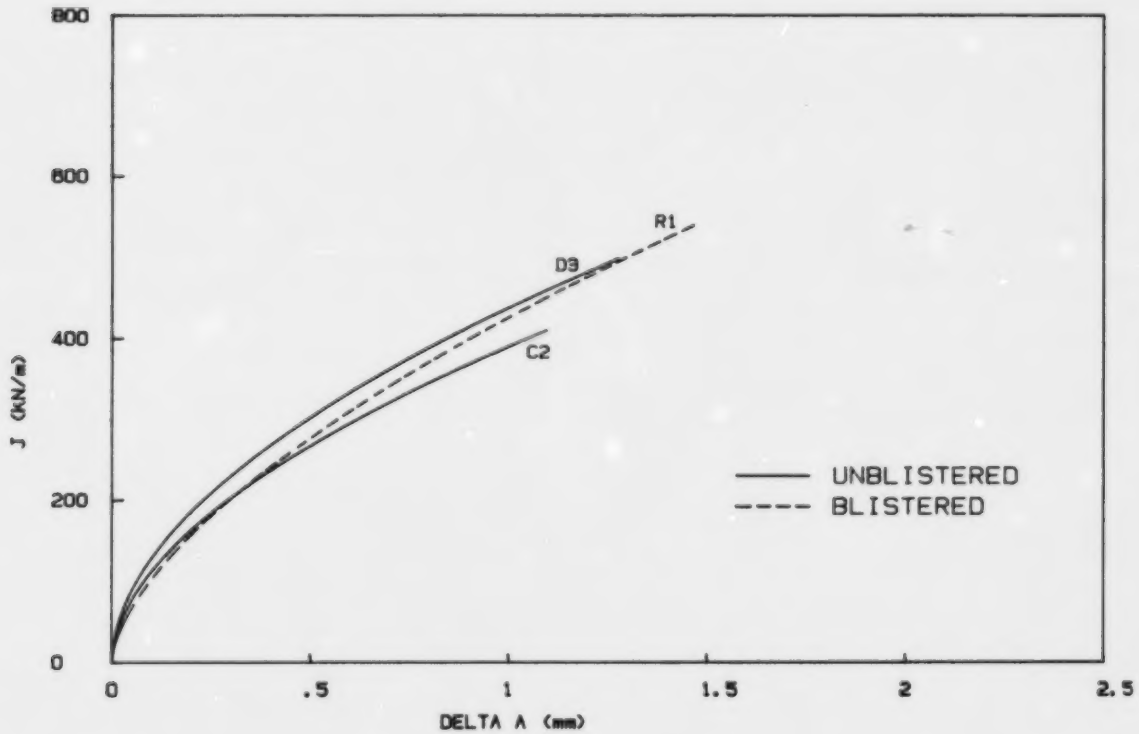

FIGURE 3 Effect of Blister Damage on J-R Curves.
(C-R Orientation, 21°C, Uncharged).

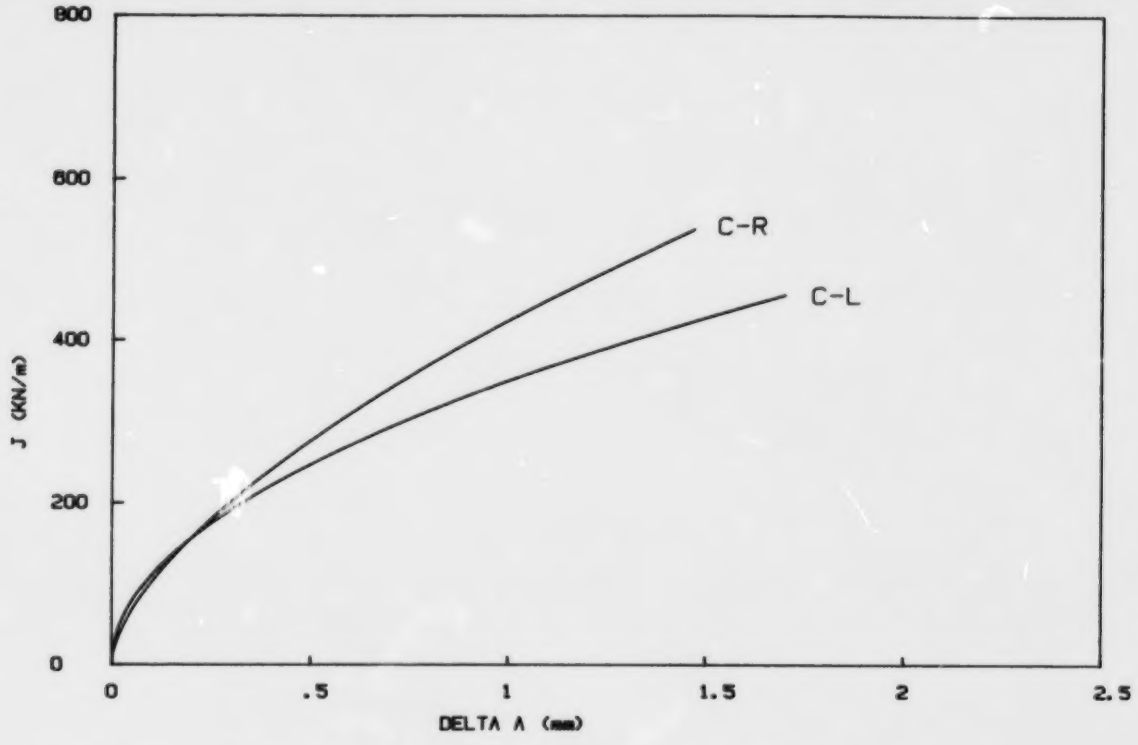

FIGURE 4 Effect of Specimen Orientation on J-R Curves. (Plate R, 21°C, Uncharged).

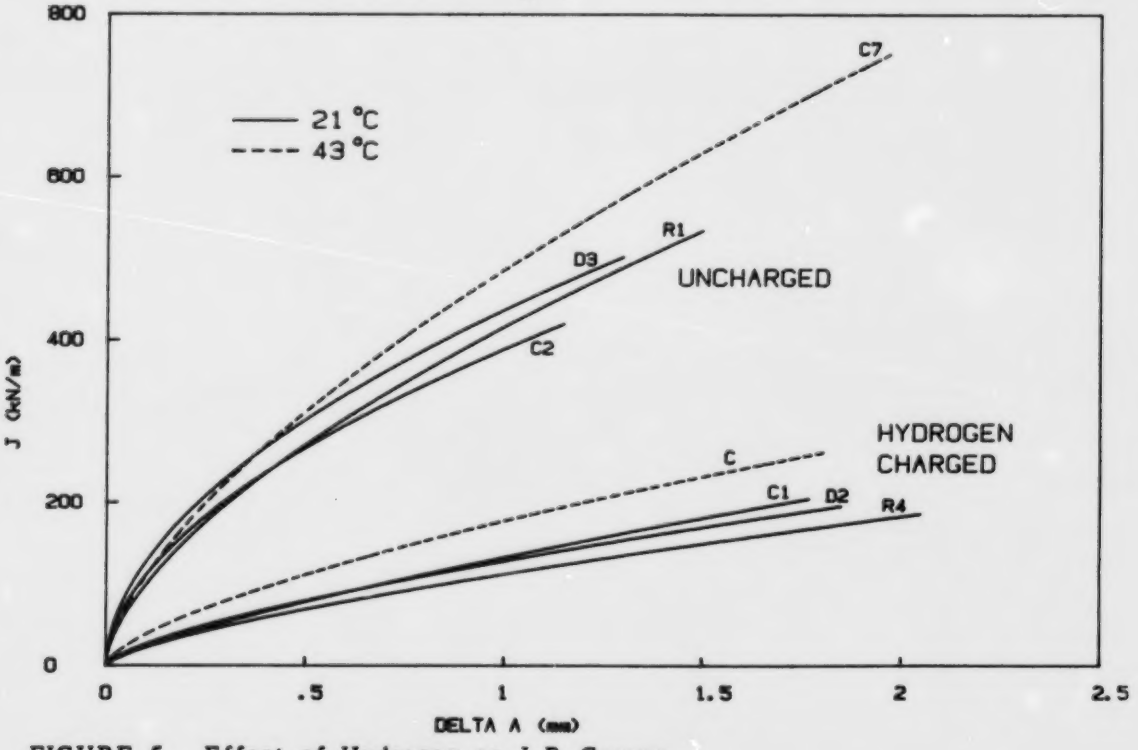

FIGURE 5 Effect of Hydrogen on J-R Curves. (C-R Orientation).

According to the validity requirements outlined in ASTM E813-87 valid J_{Ic} values could not be obtained for the specimens tested. Because of the small size of the specimens and the low strength of the material, plane strain conditions could not be established for most of the specimens. The initiation toughness values obtained, presented in Table 3 and referred to as J_Q, were mostly geometry dependent. However, the J_Q values can still be used to compare the relative initiation toughness of the different plates of A516 Gr 70 steel tested in this program.

TABLE 3

Summary of J-Resistance Curve Results

Specimen ID	J_Q[1] (kN/m)	J-R Curve Fit	
		Constant C1	Exponent C2
C2	266	388.96	.5417
D3	338	436.84	.5333
R1	289	415.94	.6189
R8	255	350.38	.5006
B1	33	118.02	.8792
C1	47	133.11	.7575
D2	50	128.63	.6833
R4	41	112.65	.7028
R6	40	107.46	.6495
B3	269	505.56	.7847
C7	368	485.98	.6424
C	70	177.10	.6642

Note:

1 Initiation toughness values are referred to as J_Q. Specimens did not meet the validity criteria of ASTM E813-87 for valid J_{Ic} values. See Appendix A for details on infractions of J_{Ic} validity requirements.

For archival purposes, all the individual load-displacement plots and J-R curves, with the experimental points and the construction outlined in ASTM E813-87 for determining J_{Ic}, are included in this report in Appendix A. In addition, the fracture surface of each specimen is shown in Appendix B.

7.3 Fractographic Features

The fracture surfaces of the uncharged material tested at 21°C showed a ductile dimpled topography, Figure 6, consisting of tear and equi-axed dimples of varying size. Hydrogen charging dramatically changed the fracture morphology, as shown in Figure 7. The fracture surface of the hydrogen-charged material exhibited features commonly referred to as quasi-cleavage. The entire fracture surface of all specimens charged with hydrogen showed quasi-cleavage fracture.

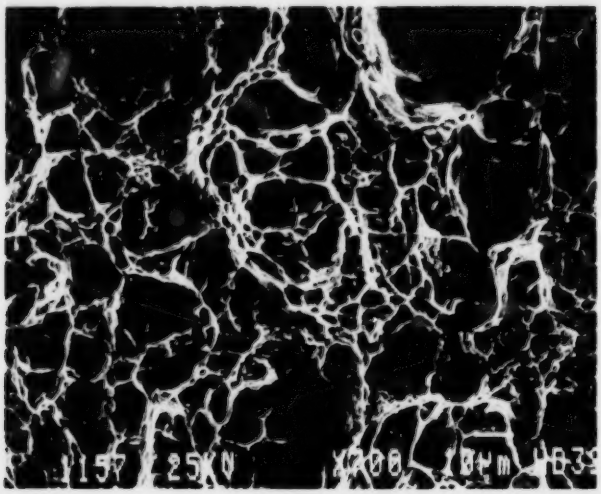

FIGURE 6 Fracture Surface of Uncharged Plate R Material Tested at 21°C. Typical Features are Shown in Region of Ductile Tearing. (Specimen R8).

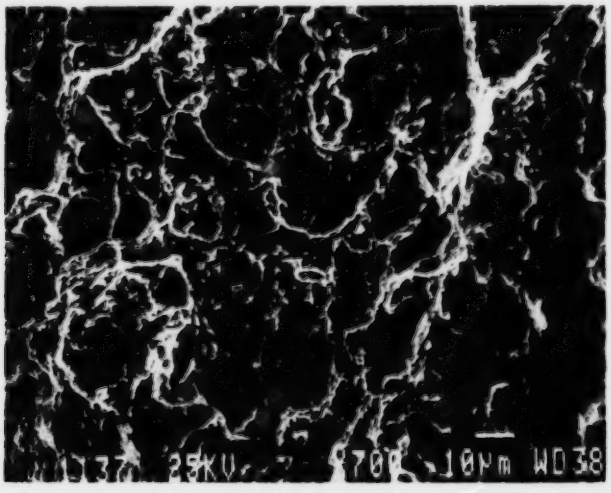

FIGURE 7 Fracture Surface of Hydrogen-Charged Plate R Material Tested at 21°C. Typical Features are Shown in Region of Ductile Tearing. (Specimen R6).

8.0 INTEGRITY ASSESSMENT OF BLISTER DAMAGE IN H_2S ABSORBER TOWER DA-3110

8.1 Nature of Hydrogen Damage in Low Strength Steels

In environments containing wet hydrogen sulphide (H_2S) the source of hydrogen causing damage is from corrosion of the inside surface of the steel vessel. This corrosion reaction produces atomic hydrogen that either is absorbed by the steel or recombines to form molecular hydrogen. In the absence of significant internal discontinuities the atomic hydrogen, because of the driving force, diffuses through the steel and into the outside atmosphere. In the process, the steel becomes saturated with hydrogen and is considered to be hydrogen charged.

Low strength plain-carbon or carbon-manganese steels, such as A516 Gr 70 carbon steel, are susceptible to blistering if internal defects are present such as voids, elongated inclusions, inclusion aggregates, or microcracks/7/. The flux of hydrogen diffusing through the steel can be trapped at these internal defects where it can recombine into molecular hydrogen. Once molecular hydrogen has formed within an internal defect it remains trapped because it cannot diffuse through the metal. As the concentration of molecular hydrogen increases, the pressure in the discontinuities increases and causes separation and growth of the flaw until an externally evident "blister" results.

Hydrogen blister cracks generally tend to be parallel to the surface of the steel plate in the rolling direction. The cracks normally do not appear to break the free surface to relax the stress exerted by the hydrogen pressure/8,9/. Instead, the blister cracks propagate along susceptible and hydrogen-embrittled microstructures and generate linking secondary cracks in the plate through-thickness direction. The linked blisters have a steplike appearance and are called "stepwise cracks". The secondary cracks, which connect the main cracks and lead to stepwise cracking (SWC), are caused by shear stresses at the main crack tip/10/. SWC has most commonly been observed to run towards the side of the pipe or vessel subject to hydrogen entry/8,11/, as shown in Figure 8.

In the presence of external stress, cracks may develop normal to the direction of external stress. Cracking of this nature is referred to as stress-oriented hydrogen-induced cracking (SOHIC). SOHIC can result in through-thickness cracks and is characterized by a stacked array of small hydrogen cracks that are normal to the applied stress. Tests of refinery steels have shown that SOHIC can occur if the steel is stressed greater than 30% of its yield strength/12/. These stress conditions can likely be expected to occur at the tip of sulphide-stress cracks or other crack-like defects in vessels.

Aside from hydrogen-induced blistering, low strength ferritic steels are also susceptible to embrittlement by dissolved atomic hydrogen. Embrittlement is manifested by a decrease in tensile ductility, a decrease in notched tensile strength, and delayed failure by fracture under static loading/13/. The embrittling effects are maximized when the steel is saturated with hydrogen. The dissolved atomic hydrogen affects the plastic properties, particularly the capacity for localized plastic flow (dislocation movement) in the presence of a notch/7/. Internal hydrogen has been also shown/14/ to facilitate void initiation at lower stresses and strains and accelerate void growth and coalescence.

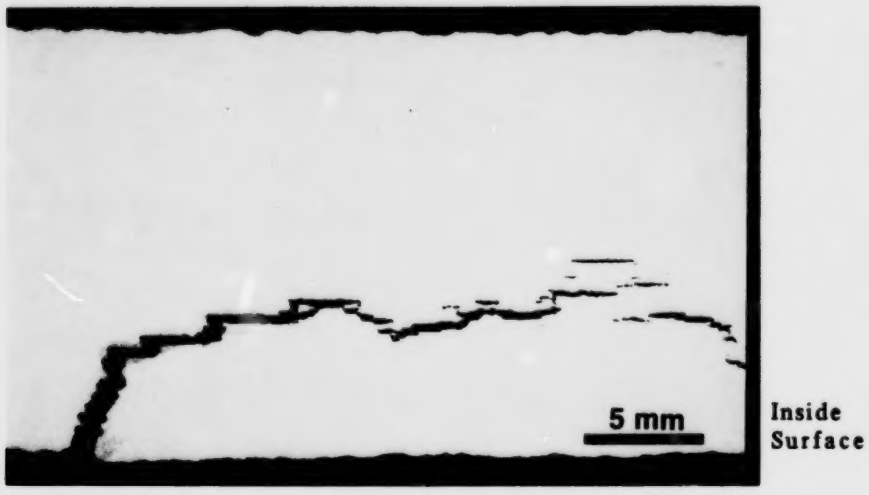

FIGURE 8 Cross-section of Plate R Showing A Stepwise Crack.

8.2 Failure Criteria

In proceeding with an assessment of the integrity of blistered pressure vessels a failure criterion must be specified. A failure criterion can be based on assessing the margin of safety for the following types of postulated flaws:

(i) A postulated through-wall flaw that conservatively characterizes the blister damage in a vessel. Implicit in this criterion is that leakage is occurring.

(ii) A postulated part-through-wall flaw that conservatively characterizes the blister damage in a vessel.

Depending on the margin of safety determined for the above flaw geometries, the vessel may be: (1) allowed to operate with periodic inspections, (2) repaired, or (3) retired. For the purposes of this study the analysis addresses the margin of safety for a postulated through-wall flaw in a vessel.

8.3 Modelling Blister Damage

Hydrogen-induced blisters and SWC were modelled in the vessel plate material as shown in Figure 9. Closely-spaced blisters or blisters connected by SWC were considered as a large interconnected group of blisters. This large group of blisters was modelled as an axially-oriented through-wall crack having the same axial length as that of the blister group. The through-wall crack model is conservative for low-stressed components, and bounds the case in high-stressed components where blister formation occurs by SOHIC.

The maximum length of the blister group in the axial and circumferential directions defines the respective lengths of axial and circumferential flaws. The axial through-wall defect was addressed in this study, primarily because the hoop stress

from pressure loading was twice that of the axial stress. If no external bending moments exist and orientation effects on fracture toughness are small, then the predicted critical crack length (CCL) at which instability occurs would be smaller for an axially-oriented crack. However, both crack geometries should be considered in a full assessment.

A knowledge of the blister depths is not required in this flaw model because it is conservatively assumed that the blister damage is idealized by a through-wall flaw.

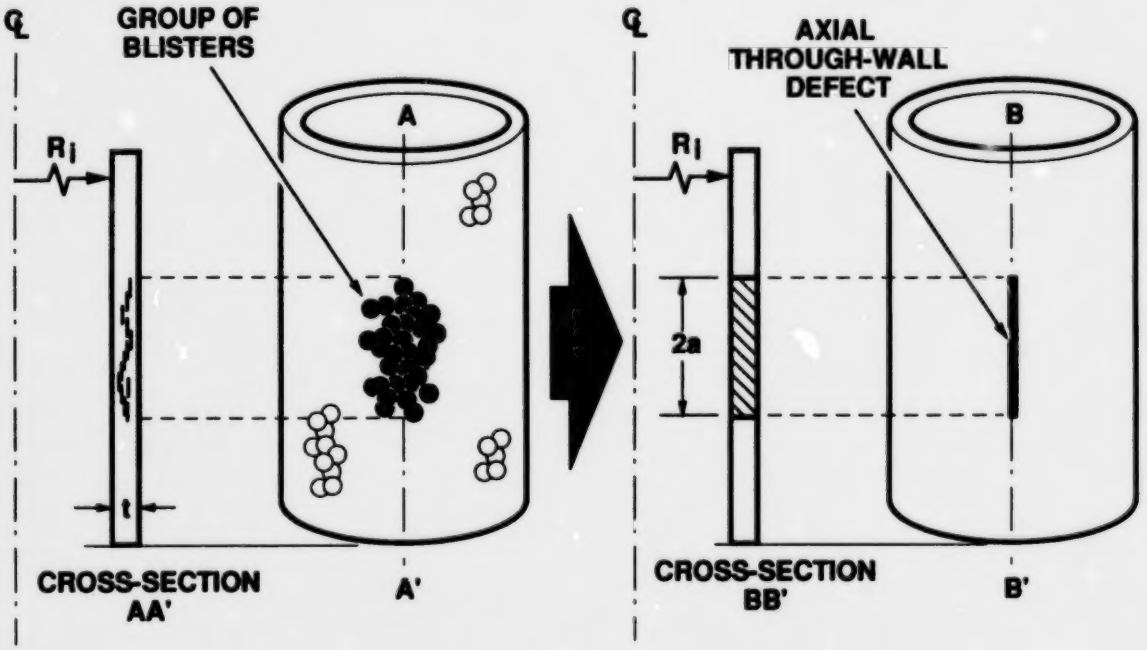

FIGURE 9 Idealization of Damage in a Blistered Pressure Vessel. A Blister Group is Modelled by an Axial Through-Wall Defect in the Vessel.

8.4 Material Properties

Material data from the current test program was used in the assessment. The plates in this test program were removed from BHWP absorber tower E1. For this reason, the material data was considered to be representative of the material properties of other A516 Gr 70 steel vessels currently in service at BHWP.

8.4.1 Tensile Properties

The average tensile properties determined at 21°C and listed in Table 4 were used.

TABLE 4

Material Tensile Properties of A516 Gr 70 Steel

Property	Value (at 21°C)
Young's Modulus, E (GPa)	192.3
Poisson's Ratio, ν	0.3
Yield Stress, σ_y (MPa)	366.6
Flow Stress, σ_f (MPa)	447.5

8.4.2 Crack Growth Resistance J-R Curve

The lowest J-R curve obtained in the test program was used. This curve corresponds to the crack growth resistance in the C-L orientation of hydrogen-charged and blistered A516 Gr 70 steel (the J-R curve of specimen R6). It is not certain that the J-R curve is a conservative lower-bound for the embrittling effects of dissolved hydrogen. However, similar reductions in fracture toughness have been reported for A516 Gr 70 steel in the presence of pressurized hydrogen gas/15/ or H_2S process environments/16/.

Certain restrictions apply to the use of the experimental J-R curve to ensure that only data corresponding to J-controlled crack growth is used in the analysis. The restrictions are specified in ASTM E1152-87 and are those outlined in Section 8.6.2 of this report. The permissible amount of crack extension, Δa, is $\Delta a = 0.1\ b_o$, where b_o is the original size of the uncracked ligament in the specimen. In compliance to this restriction, the J-R curve obtained from the 15.9 mm wide three-point bend specimen was considered only up to 0.63 mm of crack extension with a maximum J-integral value of J (Δa = 0.63 mm) = 79.6 kN/m.

8.5 Component Design Details and Stresses

For the purposes of this analysis the axial through-wall defect was postulated to be in the bottom section of the H_2S absorber tower. The design details of this section of the absorber tower are listed in Table 5.

The membrane hoop stress resulting from the design pressure of 0.662 MPa was used in the analysis. The internal pressure was added to this membrane stress to reflect pressurization of the crack faces. A total hoop stress of 80.43 MPa was used, which includes wall thickness reduction due to the corrosion allowance.

TABLE 5

Design Details of H_2S Absorber Tower DA-3110 (Bottom Section)

Diameter ID	304.80 cm
Wall Thickness	1.90 cm
Corrosion Allowance	0.63 cm
Operating Pressure	0.407 MPa
Design Pressure	0.662 MPa
MAWP	0.993 MPa
Operating Temperature	28.9 °C
Design Temperature	43.3 °C

8.6 J-Integral/Tearing Modulus Approach

8.6.1 J-Integral Resistance Curve Analysis

The ductile fracture response of the material was evaluated using an Elastic-Plastic Fracture Mechanics (EPFM) methodology. In this analysis, a crack driving force parameter, which is related to the applied loading geometry, and a flaw size in the component, is compared to the corresponding experimentally determined fracture resistance parameter to evaluate the integrity of the structure. This procedure is known as the J-integral/Tearing Modulus (J/T) approach and was used to assess the safety margin of the flawed component. The reader is referred to References 17 and 18 for details regarding this procedure. The application of EPFM procedures for flaw evaluation in pressure vessels is being addressed by the ASME and is currently being proposed for insertion in the Code as a nonmandatory Appendix/19/.

The critical length of an axial crack in a vessel was estimated by using the J/T approach. Crack driving force (CDF) curves were calculated for a postulated axial flaw by using the following relationship/20/:

$$J_{cdf} = \frac{8a\sigma_f^2}{\pi E} \ln\left[\sec\left(\frac{\pi M \sigma_H}{2\sigma_f}\right)\right] \quad (3)$$

where σ_H = applied hoop stress in the vessel

$2a$ = crack length

$$M = \left[1 + 1.255\left(\frac{a^2}{Rt}\right) - 0.0135\left(\frac{a^4}{R^2t^2}\right)\right]^{1/2} \quad (4)$$

where R = vessel radius

t = wall thickness.

M is known as the Folias factor/21/ and accounts for the additional stresses that arise at the crack tip due to bending from wall curvature.

The critical crack length was then calculated by a computer algorithm that determined the point of tangency between the J_{cdf} curve and the J-R curve. The CCL was the intercept of the J-R curve with the abscissa. In cases where the tangency condition was not met, the CCL was estimated by matching the J-R curve to the J_{cdf} curve.

8.6.2 J-Controlled Crack Growth

The concept of J-controlled crack growth is very important in the modelling of stable crack growth. J-controlled crack growth refers to the condition where the J-integral uniquely describes the crack tip, elastic-plastic deformation field. If the required conditions for J-controlled growth are not met the J-integral analysis is invalid. The required conditions are reviewed in /17/.

8.6.3 Safety Factors

Various safety margins on the applied load (pressure) were considered in the calculation of the allowable crack length of an axial through-wall flaw in the pressure vessel. The safety factor based on load is given by:

$$SF = \frac{P_{max}}{P_{app}} \qquad (5)$$

where P_{app} is the applied load and P_{max} is the load at flaw instability. Using a safety factor of 2.0 on load, the allowable length of an axial through-wall flaw in the bottom section of the absorber tower was determined to be 33.5 cm and 20.3 cm for operating and design pressures, respectively. The pressure dependence of the allowable flaw length for this particular flaw geometry is shown in Figure 10.

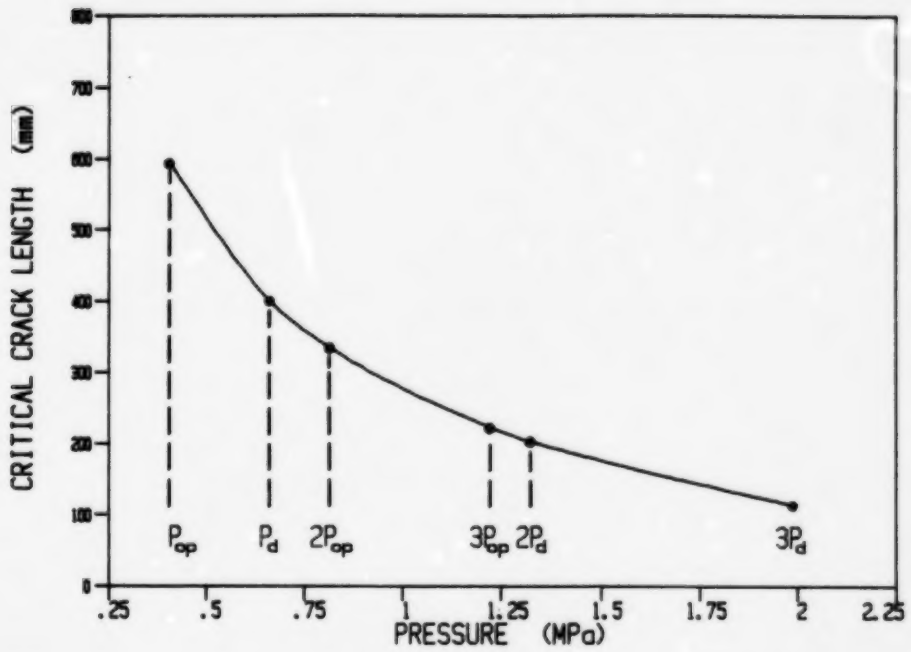

FIGURE 10 Effect of Pressure on the Critical Crack Length of an Axial Through-Wall Flaw in the Bottom Section of the E1 Absorber Tower.

ACKNOWLEDGEMENTS

We would like to thank Mrs. S. Sandloehken for coordinating the fractographic examination at Ecole Polytechnique.

Recommended:

B. Mukherjee
Acting Section Head
Nondestructive and Fracture
Evaluation Section

Prepared:

O.E. Lepik
Engineer
Nondestructive and Fracture
Evaluation Section

D.W. Carpenter
Technologist
Nondestructive and Fracture
Evaluation Section

Approved:

J. Brown
Manager
Metallurgical Research Dept

OEL/DWC:SEHG

REFERENCES

1. D.P. Dautovich and M.G. Hay, "Investigation of Hydrogen Damage in BHWP E1, Absorber Tower, Trim Section", Ontario Hydro Research Division Report No. 75-255-K, 1975.

2. M.D.C. Moles, "Ultrasonic Re-Inspection of Blistered BHWP Plates A-F", Ontario Hydro Research Division Report No. 87-97-K, May 1987.

3. "Standard Test Method for J_{Ic}, A Measure of Fracture Toughness", ASTM Standard E813-87, Vol. 03.01, 1988, pp. 686-700.

4. "Standard Test Method for Determining J-R Curves", ASTM Standard E1152-87, Vol. 03.01, 1988, pp. 800-810.

5. F.J. Loss, B.H. Monke, A.L. Hiser and H.E. Watson, "J-R Curve Characterization of Irradiated Low-Shelf Nuclear Vessel Steels", ASTM STP 803, C.F. Shih and J.P. Gudas (Eds.), American Society for Testing and Materials, 1983, pp. II-771-95.

6. ASME Boiler and Pressure Vessel Code, Section III, Division 1 - Appendices, 1980.

7. D. Warren, "Hydrogen Effects on Steel", Materials Performance, Vol. 26, No. 1, January 1987, pp. 38-48.

8. G.J. Biefer, "The Stepwise Cracking of Line-Pipe Steels in Sour Environments", Materials Performance, Vol. 21, No. 6, June 1982, pp. 19-34.

8. C.P. Ju and J.M. Rigsbee, "The Role of Microstructure for Hydrogen-Induced Blistering and Stepwise Cracking in a Plain Medium Carbon Steel", Materials Science and Engineering, Vol. 74, 1985, pp. 47-53.

10. M. Iino, "The Extension of Hydrogen Blister Crack-Array in Linepipe Steels", Met. Trans., Vol. 9A, November 1978, pp. 1581-90.

11. M.A. Clark, "Examination of Blistered Steel from Hydrotested E1, Absorber Tower, BHWP", Ontario Hydro Research Division Report No. 84-238-K, July, 1984.

12. R.D. Merrick, "An Overview of Hydrogen Damage to Steels at Low Temperatures", Materials Performance, Vol. 28, No. 2, February 1989, pp. 53-55.

13. C.D. Kim, "Hydrogen-Damage Failures", in ASM Metals Handbook, 9th Ed. Volume 11, 1986, pp. 245-251.

14. H. Cialone and R.J. Asaro, "The Role of Hydrogen in the Ductile Fracture of Plain Carbon Steels", Met. Trans., Vol. 10A, March 1979, pp. 367-375.

15. S.L. Robinson and R.E. Stoltz, "Toughness Losses and Fracture Behaviour of Low Strength Carbon-Manganese Steels in Hydrogen", in Hydrogen Effects in Metals, I.M. Bernstein and A.W. Thompson (Eds.), The Metallurgical Society of AIME, 1981, pp. 987-995.

16. H.I. McHenry, P.T. Purtscher and T.R. Shives, "Observations of Hydrogen Damage in a Failed Pressure Vessel", Corrosion Science, Vol. 27, No. 10/11, 1987, pp. 1041-1057.

17. V. Kumar, M.D. German and C.F. Shih, "An Engineering Approach for Elastic-Plastic Fracture Analysis", EPRI Report No. NP-1931, Research Project No. 1237-1, General Electric Co., July 1981.

18. D.A. Scarth, "EPFM Flaw Evaluation Procedures - Progress Report I on Development of EPFM Methodology Project", Ontario Hydro Research Division Report No. 85-310-K, December 1985.

19. "Assessment of Reactor Vessels with Low Upper Shelf Fracture Toughness", draft of proposed nonmandatory Appendix X to ASME Section XI, Revision 4, prepared by the ASME Section Working Group on Flaw Evaluation, November 30, 1988.

20. J.F. Kiefner, W.A. Maxey, R.J. Eiber and A.R. Duffy, "Failure Stress Levels of Flaws in Pressurized Cylinders", ASTM STP 536, J.G. Kaufman (Ed.), American Society for Testing and Materials, 1973, pp. 461-481.

21. E.S. Folias, "On the Theory of Fracture of Curved Sheets", Engineering Fracture Mechanics, Vol. 2, 1970, pp. 151-164.

APPENDIX A

Graphs and Tables From All Tests

ELASTIC-PLASTIC FRACTURE TOUGHNESS ANALYSIS

Specimen Id.	C2	Geometry	SE(B)
Contract #	BHWP	Orientation	C-R
Material	A516 Gr 70	Flow stress (MPa)	448
Temperature (C)	21	Modulus (GPa)	192
Environment	AIR	Stroke rate (mm/min)	0.005
		Loading rate (min)	6.513

Specimen Dimensions (mm)

Thickness	15.85	Notch depth	8.05
Net thickness	12.62	Gage length	4.00
Width	15.86	Alpha ratio	1.008
Span	63.5		

Initial Ligament(s) (mm)

5.89	5.84	5.80	5.73	5.73	5.71	5.74	5.79	5.84

Final Ligament(s) (mm)

4.59	4.43	4.52	4.59	5.22	4.97	4.68	4.65	4.65

Precrack Parameters

Pmax (kN)	1.90	Stress ratio (R)	0.10
Final a (mm)	10.01	Kmax (MPa sqr[m])	16.61

Test Parameters

Initial ligament	(mm)	5.77	J15limit	(kJ/m^2)	172
Final ligament	〃	4.71	J20limit	〃	129
Delta a (actual)	〃	1.07	J25limit	〃	103
Delta a (EvB/P)	〃	1.10	*JQ (813-81)	〃	0
Delta a error	〃	0.04	*JQ (813-81)(NV)	〃	173
Delta a error	(%)	3.3	*JQ (813-87)	〃	0
Compliance Adjustment		1.363	*JQ (813-87)(NV)	〃	266
CTODi (mm)		0.178	Tearing modulus		294.1

POWER LAW REGRESSION CONSTANT C +4.1747E+02
POWER LAW REGRESSION EXPONENT N +6.4402E-01

Comments * Computed from E813-87 form for J

Tested November 1988.
Precrack load > 40% of limit load (Sec 7.6.2)
Less than 4 data pts for JIc fit (Sec 9.2.2)
Thickness < 25*JQ/flowstress (Sec 9.4.1.1)
Ligament < 25*JQ/flowstress (Sec 9.4.1.2)
Crk ext edge to ctr > 2% of W (sec 9.4.1.6)
Em differs from E by > 10%
Improper data group for E1152-87 (Sec 8.4.1)

Specimen Id. C2

Index	Load (kN)	Disp. (mm)	Delta a (mm)	CTOD (mm)	K399 (MPa sqr[m])	K813	J813-81	J813-87 (kJ/m^2)	J1152	Jmod
0	0.0	-0.015		0.000	0.0	0.0	0.0	0.0	0.0	0.0
1	1.5	0.034		0.002	14.7	10.6	0.7	0.6	0.6	0.6
2	1.7	0.023		0.002	16.6	4.6	0.2	0.1	0.1	0.1
3	1.9	0.033		0.003	18.6	10.4	0.7	0.6	0.6	0.6
4	2.1	0.047		0.004	20.6	15.7	1.5	1.3	1.3	1.3
5	2.6	0.054	0.000	0.006	25.5	17.7	1.9	1.6	1.6	1.6
6	3.1	0.085		0.011	30.4	27.4	4.3	3.9	3.9	3.9
7	3.3	0.181	0.006	0.023	32.4	48.7	12.8	12.3	12.3	12.3
8	3.5	0.220	-0.001	0.031	34.3	55.3	16.5	15.9	15.9	15.9
9	3.6	0.267	0.012	0.037	35.4	62.6	20.9	20.4	20.4	20.4
10	3.7	0.303	0.003	0.044	36.3	67.9	24.6	24.0	24.0	24.0
11	3.7	0.352	0.003	0.050	36.3	74.6	29.6	29.0	29.0	29.0
12	3.8	0.398	-0.011	0.057	37.1	80.6	34.5	33.7	33.8	33.7
13	3.9	0.440	0.002	0.064	38.2	85.5	38.7	38.0	38.1	38.1
14	4.0	0.486	0.027	0.070	39.5	90.9	43.6	43.0	42.9	43.0
15	4.1	0.527	-0.002	0.077	40.1	95.7	48.4	47.6	47.7	47.6
16	4.2	0.578	-0.014	0.085	41.0	101.3	54.3	53.3	53.5	53.4
17	4.2	0.618	0.007	0.092	41.2	105.5	58.7	57.9	57.9	57.9
18	4.3	0.663	-0.005	0.099	42.1	110.2	64.1	63.2	63.3	63.2
19	4.3	0.727	0.022	0.107	42.4	116.6	71.3	70.7	70.5	70.7
20	4.4	0.779	0.026	0.115	43.4	121.5	77.4	76.7	76.6	76.8
21	4.4	0.823	0.035	0.123	43.5	125.6	82.7	82.0	81.8	82.1
22	4.5	0.873	0.071	0.130	44.9	130.1	88.3	88.0	87.4	88.2
23	4.6	0.914	0.078	0.138	46.0	133.8	93.5	93.1	92.5	93.4
24	4.6	0.968	0.069	0.145	45.9	138.6	100.5	99.9	99.5	100.3
25	4.6	1.012	0.087	0.152	46.1	142.4	105.8	105.4	104.8	105.9
26	4.7	1.074	0.094	0.159	47.2	147.5	113.6	113.2	112.6	113.8
27	4.8	1.119	0.093	0.169	48.2	151.3	119.7	119.0	118.6	119.8
28	4.8	1.163	0.128	0.176	48.6	154.8	124.8	124.7	123.7	125.6
29	4.8	1.212	0.135	0.183	48.7	158.8	131.3	131.1	130.1	132.2
30	4.8	1.256	0.132	0.191	48.7	162.2	137.3	136.9	136.2	138.1
31	4.8	1.305	0.146	0.197	48.9	166.0	143.5	143.3	142.4	144.7
32	4.8	1.354	0.163	0.204	49.1	169.6	149.7	149.7	148.6	151.3
33	4.8	1.398	0.167	0.212	49.2	172.9	155.6	155.4	154.4	157.2
34	4.9	1.449	0.183	0.219	50.4	176.6	162.2	162.1	161.0	164.2
35	4.9	1.502	0.223	0.227	51.0	180.3	168.4	169.1	167.1	171.4
36	4.9	1.551	0.226	0.235	51.0	183.8	175.1	175.6	173.9	178.3
37	4.9	1.600	0.230	0.242	51.1	187.2	181.8	182.2	180.6	185.1
38	4.9	1.649	0.265	0.251	51.6	190.5	187.5	188.6	186.3	191.9
39	4.9	1.693	0.300	0.259	52.1	193.3	192.6	194.4	191.3	198.0
40	4.9	1.742	0.307	0.266	52.2	196.6	199.3	200.9	198.0	204.9
41	4.9	1.781	0.337	0.273	52.6	199.0	203.7	206.0	202.4	210.4
42	4.9	1.820	0.352	0.278	52.8	201.5	208.7	211.2	207.4	215.9
43	4.9	1.874	0.374	0.285	53.2	204.9	215.6	218.3	214.2	223.6
44	4.9	1.918	0.391	0.294	53.4	207.6	221.2	224.2	219.9	229.8
45	4.9	1.966	0.393	0.301	53.4	210.6	228.0	230.6	226.7	236.8
46	4.9	2.005	0.425	0.308	53.9	212.9	232.3	235.7	230.9	242.3
47	4.9	2.045	0.420	0.315	53.8	215.3	238.4	241.1	237.0	248.1
48	4.9	2.089	0.435	0.321	54.1	217.9	244.1	246.9	242.7	254.4
49	5.0	2.140	0.463	0.328	55.6	220.8	250.2	253.5	248.7	261.7

Specimen Id. C2

Index	Load (kN)	Disp. (mm)	Delta a (mm)	CTOD (mm)	K399 (MPa sqr[m])	K813	J813-81	J813-87 (kJ/m^2)	J1152	Jmod
50	5.0	2.194		0.337	55.6	225.0	258.2	263.2	261.8	274.8
51	4.9	2.235	0.509	0.345	55.2	226.3	262.1	266.4	260.7	275.8
52	4.9	2.274	0.504	0.351	55.2	228.6	268.1	271.7	266.7	281.6
53	4.9	2.323	0.543	0.358	55.8	231.2	273.3	278.0	271.8	288.7
54	4.9	2.357	0.531	0.365	55.6	233.2	279.0	282.7	277.5	293.8
55	4.8	2.404	0.537	0.371	54.6	235.7	285.5	289.0	284.1	300.6
56	4.8	2.453	0.569	0.378	55.1	238.3	290.9	295.3	289.4	307.6
57	4.8	2.551	0.615	0.394	55.8	243.3	302.6	307.9	301.1	321.8
58	4.8	2.653	0.673	0.411	56.8	248.5	314.2	321.0	312.6	336.7
59	4.7	2.759	0.741	0.428	56.7	253.6	325.6	334.6	324.0	352.2
60	4.7	2.857	0.785	0.445	57.5	258.3	337.1	346.9	335.5	366.5
61	4.7	2.959	0.829	0.461	58.3	263.0	349.4	359.8	347.7	381.6
62	4.6	3.064	0.881	0.478	58.0	267.9	361.4	373.2	359.8	397.2
63	4.6	3.157	0.908	0.494	58.5	272.0	373.2	384.8	371.5	411.0
64	4.6	3.259	0.933	0.511	58.9	276.5	386.6	397.5	384.9	426.2
65	4.6	3.357	0.961	0.528	59.4	280.7	399.1	409.7	397.3	440.9
66	4.5	3.458	1.002	0.544	58.9	284.9	410.8	422.2	409.0	455.9
67	4.5	3.555	1.042	0.560	59.7	288.9	421.8	433.9	420.0	470.2
68	4.5	3.658	1.069	0.577	60.2	293.0	434.9	446.5	433.1	485.6
69	4.4	3.764	1.101	0.594	59.5	297.2	447.7	459.4	445.9	501.4

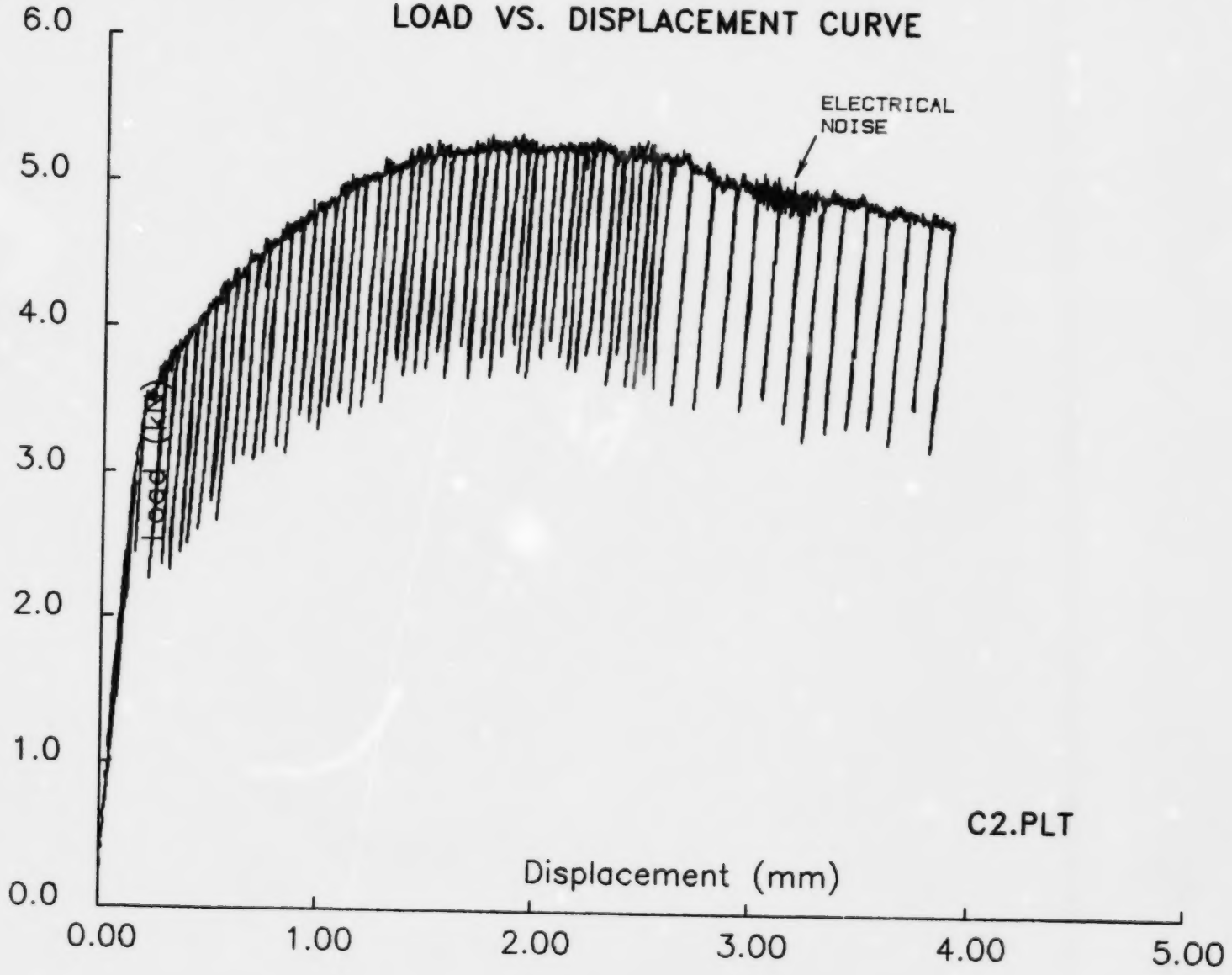
LOAD VS. DISPLACEMENT CURVE
ELECTRICAL NOISE
6.0
5.0
4.0
3.0
2.0
1.0
0.0
Load (KN)
0.00
1.00
2.00
3.00
4.00
5.00
Displacement (mm)
C2.PLT

A5

89-135

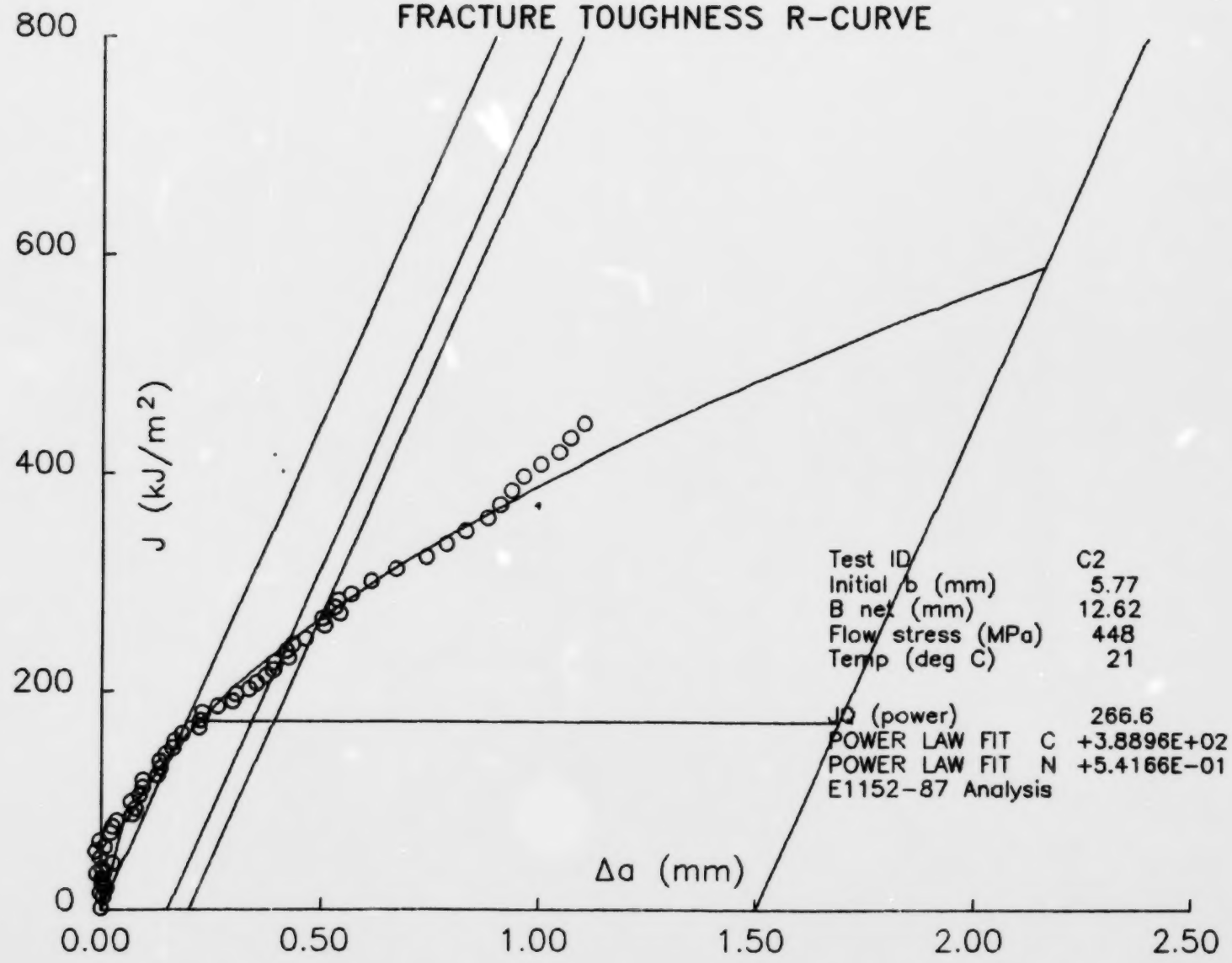
FRACTURE TOUGHNESS R-CURVE
800
600
400
200
0
J (kJ/m²)
Δa (mm)
0.00
0.50
1.00
1.50
2.00
2.50
Test ID C2
Initial b (mm) 5.77
B net (mm) 12.62
Flow stress (MPa) 448
Temp (deg C) 21
JQ (power) 266.6
POWER LAW FIT C +3.8896E+02
POWER LAW FIT N +5.4166E-01
E1152-87 Analysis

A6

89-135

ELASTIC-PLASTIC FRACTURE TOUGHNESS ANALYSIS

Specimen Id.	D3	Geometry	SE(B)
Contract #	BHWP	Orientation	C-R
Material	A516 Gr 70	Flow stress (MPa)	448
Temperature (C)	21	Modulus (GPa)	192
Environment	AIR	Stroke rate (mm/min)	0.005
		Loading rate (min)	6.835

Specimen Dimensions (mm)

Thickness	15.84	Notch depth	8.00
Net thickness	12.69	Gage length	4.00
Width	15.85	Alpha ratio	1.008
Span	63.5		

Initial Ligament(s) (mm)

5.89	5.78	5.71	5.76	5.70	5.67	5.69	5.74	5.85

Final Ligament(s) (mm)

3.80	4.31	4.55	4.51	4.19	4.22	4.05	4.28	3.70

Precrack Parameters

Pmax (kN)	1.90	Stress ratio (R)	0.10
Final a (mm)	9.97	Kmax (MPa sqr[m])	16.77

Test Parameters

Initial ligament	(mm)	5.74	J15limit	(kJ/m^2)	171
Final ligament	"	4.23	J20limit	"	128
Delta a (actual)	"	1.51	J25limit	"	103
Delta a (EvB/P)	"	1.28	*JQ (813-81)	"	0
Delta a error	"	-0.23	*JQ (813-81)(NV)	"	269
Delta a error	(%)	-15.1	*JQ (813-87)	"	0
Compliance Adjustment		1.305	*JQ (813-87)(NV)	"	338
CTODi (mm)		0.220	Tearing modulus		260.3

POWER LAW REGRESSION CONSTANT C +4.6191E+02
POWER LAW REGRESSION EXPONENT N +5.6773E-01

Comments

* Computed from E813-87 form for J

Tested November 1988.
Precrack load > 40% of limit load (Sec 7.6.2)
Less than 4 data pts for JIc fit (Sec 9.3.2)
Thickness < 25*JQ/flowstress (Sec 9.4.1.1)
Ligament < 25*JQ/flowstress (Sec 9.4.1.2)
Crk ext edge to ctr > 2% of W (sec 9.4.1.6)
Final delta a error > 15% of a (Sec 9.4.1.7)
Em differs from E by > 10%
Improper data group for E1152-87 (Sec 8.4.1)

Specimen Id. D3

Index	Load (kN)	Disp. (mm)	Delta a (mm)	CTOD (mm)	K399 (MPa sqr[m])	K813	J813-81	J813-87 (kJ/m^2)	J1152	Jmod
0	0.0	-0.015		0.000	0.0	0.0	0.0	0.0	0.0	0.0
1	1.7	0.007		-0.000	16.8	2.4	0.2	0.0	0.0	0.0
2	1.8	0.026		0.001	17.8	13.4	1.1	0.9	0.9	0.9
3	1.9	0.030		0.000	18.7	14.6	1.3	1.1	1.1	1.1
4	2.4	0.064		0.002	23.7	24.1	3.3	3.0	3.0	3.0
5	2.9	0.078	0.000	0.005	28.6	27.5	4.3	3.9	3.9	3.9
6	3.4	0.127	-0.009	0.010	33.4	39.3	8.5	8.0	8.0	8.0
7	3.8	0.328		0.036	37.4	73.1	28.4	27.8	27.7	27.7
8	4.1	0.520		0.066	40.3	96.6	49.2	48.5	48.4	48.4
9	4.5	0.712		0.094	44.3	116.9	71.8	71.0	70.9	70.9
10	4.7	0.905	0.066	0.123	47.2	135.2	95.2	95.0	94.2	95.2
11	4.9	1.094	0.112	0.151	49.8	151.7	119.6	119.6	118.5	120.2
12	5.0	1.283	0.020	0.179	49.6	167.4	147.7	145.7	146.6	146.5
13	5.1	1.473	0.121	0.208	52.0	181.6	171.5	171.5	170.3	172.8
14	5.2	1.667	0.084	0.236	52.5	195.6	200.6	199.0	199.4	200.8
15	5.3	1.857	0.313	0.266	56.9	208.0	219.9	225.1	218.5	228.3
16	5.3	1.959	0.376	0.281	58.0	214.6	233.0	239.5	231.5	243.8
17	5.3	2.062	0.341	0.297	57.4	221.3	250.6	254.7	249.1	259.9
18	5.3	2.160	0.385	0.313	58.1	227.3	263.7	268.7	262.2	275.0
19	5.3	2.262	0.411	0.328	58.5	233.5	278.3	283.4	276.8	290.8
20	5.3	2.360	0.486	0.344	59.8	239.1	289.7	297.2	288.1	306.0
21	5.3	2.453	0.483	0.360	59.8	244.5	304.7	310.7	303.1	320.8
22	5.3	2.555	0.489	0.374	59.9	250.2	320.5	325.5	318.9	336.9
23	5.3	2.648	0.476	0.392	59.7	255.4	336.1	339.2	334.5	351.8
24	5.3	2.722		0.403	59.7	260.4	347.8	352.7	352.2	369.5
25	5.3	2.797		0.415	59.7	264.4	359.7	363.6	364.1	381.4
26	5.3	2.871		0.427	59.7	268.3	371.5	374.4	375.9	393.2
28	5.2	2.947	0.689	0.438	62.3	270.8	367.7	381.3	365.8	398.3
29	5.1	3.041		0.454	61.1	276.9	382.8	398.7	390.0	422.5
30	5.2	3.133	0.767	0.469	63.8	279.8	391.6	407.0	389.4	427.8
31	4.8	3.230	0.865	0.486	60.7	284.4	399.1	420.5	397.1	443.1
32	4.8	3.332	0.844	0.501	60.3	288.9	416.7	434.1	414.7	459.0
33	4.8	3.430	0.975	0.518	62.8	292.9	420.4	446.1	418.2	473.6
34	4.7	3.534	0.960	0.534	61.2	297.4	438.0	460.1	436.0	490.1
35	4.6	3.632	1.056	0.551	61.8	301.3	444.1	472.2	441.9	504.8
36	4.6	3.725	1.088	0.567	62.5	305.0	455.4	483.7	453.2	519.1
37	4.5	3.814	1.146	0.583	62.3	308.4	463.3	494.7	461.2	532.6
38	4.3	4.041	1.252	0.619	61.7	316.8	486.6	522.0	484.5	566.8
39	3.7	4.076	1.281	0.626	53.6	318.5	488.5	527.5	486.8	572.1

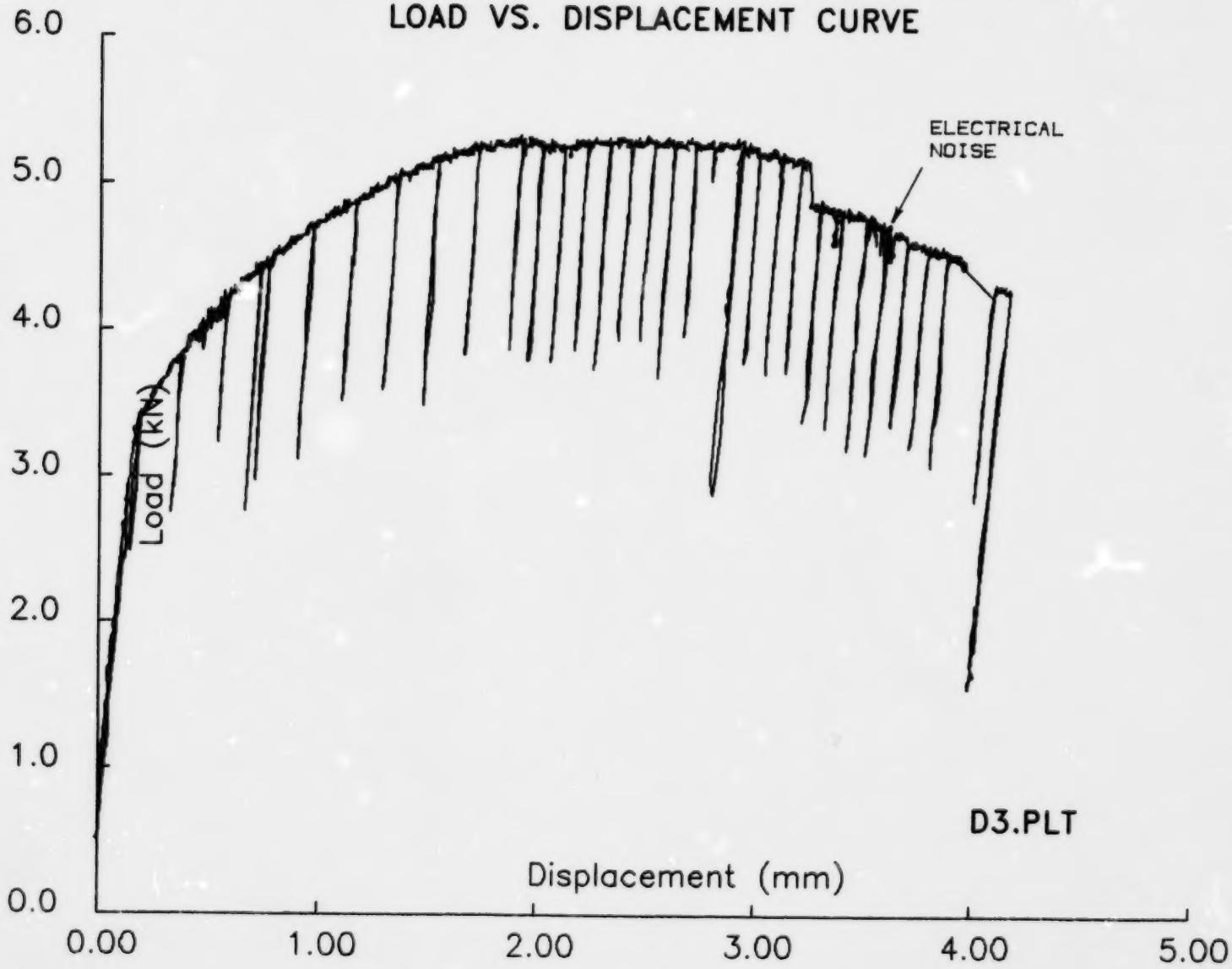
LOAD VS. DISPLACEMENT CURVE
ELECTRICAL NOISE
Load (kN)
Displacement (mm)
D3.PLT
6.0
5.0
4.0
3.0
2.0
1.0
0.0
0.00
1.00
2.00
3.00
4.00
5.00

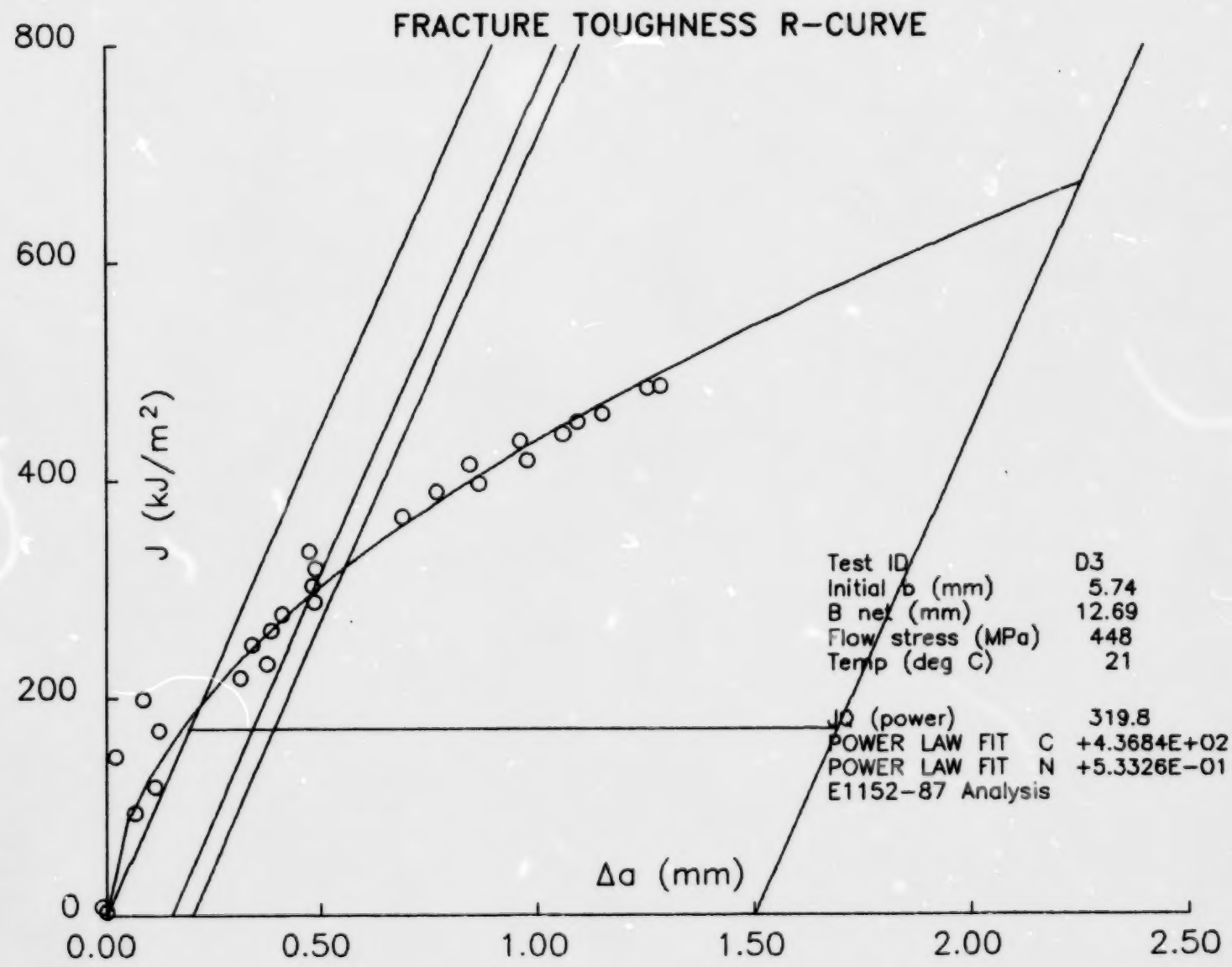
FRACTURE TOUGHNESS R-CURVE
800
600
400
200
0
J (kJ/m²)
Δa (mm)
0.00
0.50
1.00
1.50
2.00
2.50
Test ID D3
Initial b (mm) 5.74
B net (mm) 12.69
Flow stress (MPa) 448
Temp (deg C) 21
JQ (power) 319.8
POWER LAW FIT C +4.3684E+02
POWER LAW FIT N +5.3326E-01
E1152-87 Analysis

A10

89-135

ELASTIC-PLASTIC
FRACTURE TOUGHNESS ANALYSIS

Specimen Id.	R1	Geometry	SE(B)
Contract #	BHWP	Orientation	C-R
Material	A516 Gr 70	Flow stress (MPa)	448
Temperature (C)	21	Modulus (GPa)	192
Environment	AIR	Stroke rate (mm/min)	0.005
		Loading rate (min)	7.435

Specimen Dimensions (mm)

Thickness	15.66	Notch depth	7.78
Net thickness	12.94	Gage length	5.00
Width	15.89	Alpha ratio	1.008
Span	63.5		

Initial Ligament(s) (mm)

6.24	6.15	6.13	6.07	6.09	6.05	6.03	6.00	6.00

Final Ligament(s) (mm)

4.03	4.35	4.55	4.72	4.51	4.61	4.44	4.37	3.82

Precrack Parameters

Pmax (kN)	1.90	Stress ratio (R)	0.10
Final a (mm)	9.76	Kmax (MPa sqr[m])	15.54

Test Parameters

Initial ligament	(mm)	6.08	J15limit	(kJ/m^2)	181
Final ligament	"	4.44	J20limit	"	136
Delta a (actual)	"	1.64	J25limit	"	109
Delta a (EvB/P)	"	1.49	*JQ (813-81)	"	0
Delta a error	"	-0.15	*JQ (813-81)(NV)	"	217
Delta a error	(%)	-9.2	*JQ (813-87)	"	0
Compliance Adjustment		1.197	*JQ (813-87)(NV)	"	289
CTODi (mm)		0.188	Tearing modulus		265.1

POWER LAW REGRESSION CONSTANT C +4.3306E+02
POWER LAW REGRESSION EXPONENT N +6.2338E-01

Comments * Computed from E813-87 form for J

Tested December 14 1988.
Precrack load > 40% of limit load (Sec 7.6.2)
Less than 4 data pts for JIc fit (Sec 9.3.2)
Thickness < 25*JQ/flowstress (Sec 9.4.1.1)
Ligament < 25*JQ/flowstress (Sec 9.4.1.2)
Crk ext edge to ctr > 2% of W (sec 9.4.1.6)
Em differs from E by > 10%
Improper data group for E1152-87 (Sec 8.4.1)

Specimen Id. R1

Index	Load (kN)	Disp. (mm)	Delta a (mm)	CTOD (mm)	K399 (MPa sqr[m])	K813	J813-81	J813-87 (kJ/m^2)	J1152	Jmod
0	0.0	-0.020		0.000	0.0	0.0	0.0	0.0	0.0	0.0
1	3.0	0.087		0.005	27.0	24.1	3.3	3.0	3.0	3.0
2	3.4	0.124		0.010	30.6	33.9	6.4	6.0	6.0	6.0
3	3.9	0.180	0.000	0.017	35.1	46.0	11.5	11.0	11.0	11.0
4	4.3	0.267	0.003	0.030	38.7	62.0	20.6	20.0	20.0	20.0
5	4.6	0.361	0.006	0.044	41.4	76.7	31.3	30.6	30.6	30.6
6	4.8	0.454	0.019	0.060	43.4	89.4	42.3	41.5	41.5	41.6
7	5.0	0.551	0.008	0.074	45.1	101.5	54.4	53.5	53.6	53.6
8	5.2	0.648	0.037	0.090	47.2	112.7	66.9	66.0	66.0	66.2
9	5.3	0.749	0.061	0.106	48.4	123.5	80.1	79.3	79.1	79.6
10	5.4	0.848	0.082	0.122	49.6	133.5	93.5	92.7	92.4	93.2
11	5.5	0.943	0.116	0.139	51.0	142.6	106.3	105.7	105.2	106.5
12	5.5	1.046	0.149	0.154	51.4	151.9	120.4	119.9	119.3	121.1
13	5.6	1.146	0.188	0.172	52.9	160.3	134.0	133.7	132.8	135.4
14	5.6	1.249	0.228	0.188	53.4	168.8	148.2	148.2	147.0	150.4
15	5.7	1.343	0.224	0.205	54.3	176.3	162.4	161.7	161.2	164.5
16	5.7	1.441	0.255	0.221	54.8	183.8	176.3	175.7	175.0	179.2
17	5.8	1.541	0.270	0.237	55.9	191.3	191.1	190.2	189.8	194.4
18	5.8	1.638	0.302	0.255	56.4	198.2	205.0	204.4	203.7	209.3
19	5.8	1.736	0.326	0.270	56.8	205.1	219.4	218.7	218.0	224.5
20	5.8	1.834	0.359	0.287	57.3	211.6	233.4	232.9	232.0	239.7
21	5.8	1.932	0.431	0.302	58.4	217.9	245.8	247.0	244.3	254.8
22	5.8	2.034	0.469	0.319	59.0	224.4	260.3	261.8	258.8	270.9
23	5.8	2.137	0.480	0.336	59.2	230.8	276.3	276.9	274.8	287.4
24	5.7	2.242	0.529	0.353	58.9	237.0	290.4	292.1	289.0	303.9
25	5.7	2.340	0.572	0.371	59.6	242.6	303.7	306.0	302.2	319.3
26	5.7	2.438	0.604	0.389	60.2	248.1	317.6	320.0	316.1	334.9
27	5.7	2.540	0.658	0.404	61.1	253.6	330.9	334.4	329.3	351.2
28	5.7	2.643	0.669	0.422	61.3	259.2	346.9	349.3	345.3	367.9
29	2.4	2.833		0.449	25.8	268.0	368.9	373.4	371.0	393.5
30	2.9	2.834		0.450	31.2	268.0	369.0	373.4	371.3	393.9
31	3.4	2.850		0.453	36.6	268.4	370.4	374.5	373.0	395.5
32	3.9	2.872		0.456	41.9	269.1	372.7	376.4	375.5	398.1
33	4.4	2.883		0.459	47.3	269.4	373.9	377.4	377.1	399.7
34	4.9	2.898		0.464	52.7	270.0	376.0	379.1	379.6	402.1
35	5.4	2.929		0.470	58.1	271.4	380.5	383.0	384.5	407.1
36	5.6	3.022	0.846	0.487	63.3	274.3	382.2	391.2	378.3	413.3
37	5.5	3.127	0.882	0.504	62.9	279.4	396.9	406.1	393.0	430.6
38	5.4	3.227	0.933	0.522	62.7	284.1	409.1	419.7	405.2	446.6
39	5.4	3.330	0.977	0.540	63.5	288.8	422.3	433.6	418.4	463.2
40	5.3	3.436	1.042	0.558	63.5	293.4	434.0	447.7	430.1	480.1
41	5.2	3.535	1.085	0.576	63.1	297.7	446.3	461.0	442.4	496.1
42	5.1	3.636	1.136	0.593	62.9	301.9	457.7	474.1	453.9	512.0
43	5.0	3.737	1.223	0.611	63.4	305.9	465.4	486.7	461.6	527.6
44	5.0	3.839	1.255	0.629	64.0	309.9	478.6	499.4	474.7	543.7
45	4.8	3.947	1.342	0.648	63.2	314.0	486.8	512.9	483.0	560.5
46	4.7	4.052	1.397	0.667	62.9	317.9	497.3	525.4	493.5	576.6
47	4.7	4.155	1.462	0.686	64.3	321.4	506.3	537.3	502.4	592.3
48	4.6	4.260	1.492	0.704	63.6	325.2	519.4	549.9	515.6	608.7

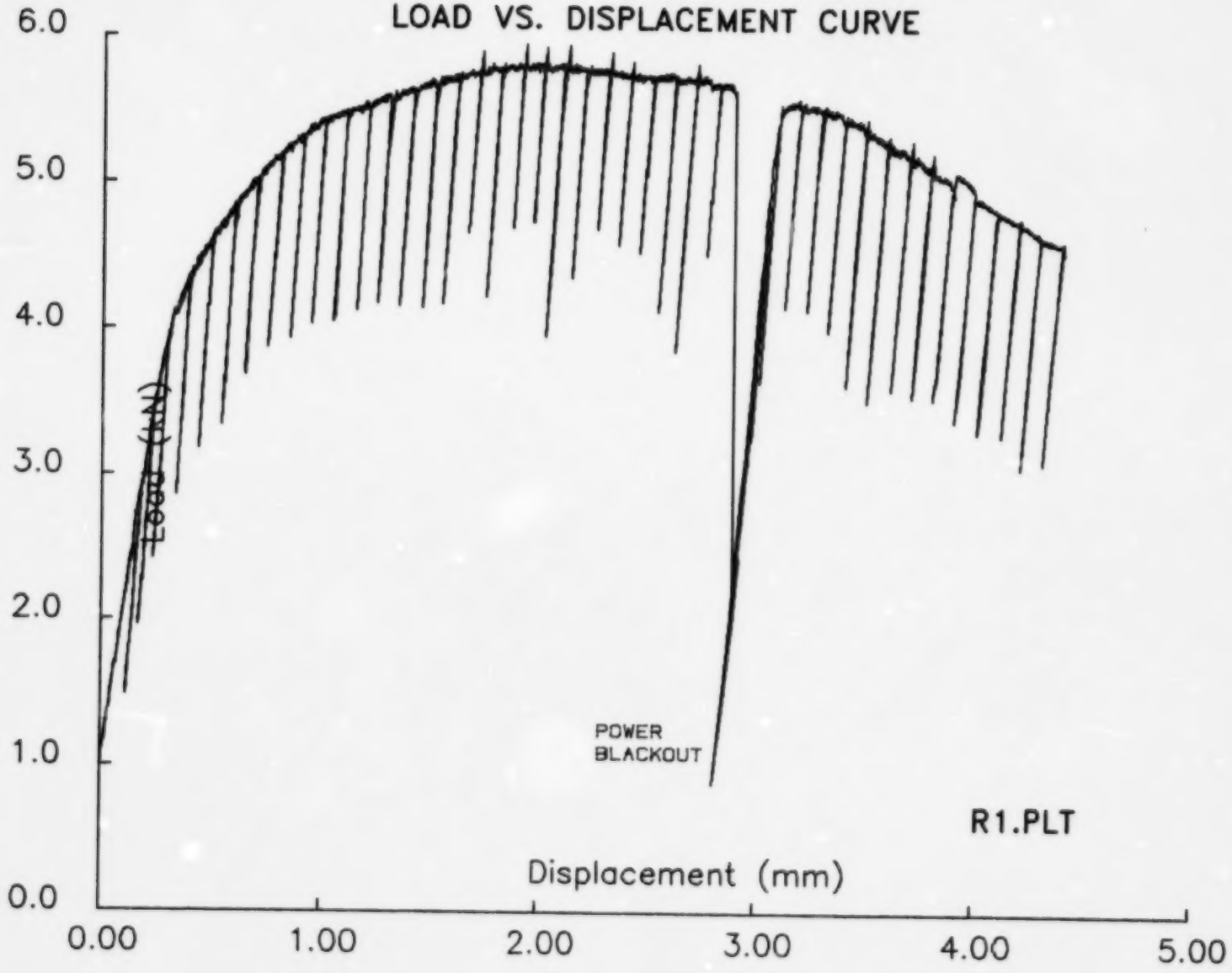
LOAD VS. DISPLACEMENT CURVE
6.0
5.0
4.0
3.0
2.0
1.0
0.0
Load (kN)
POWER
BLACKOUT
R1.PLT
Displacement (mm)
0.00
1.00
2.00
3.00
4.00
5.00

A13

89-135

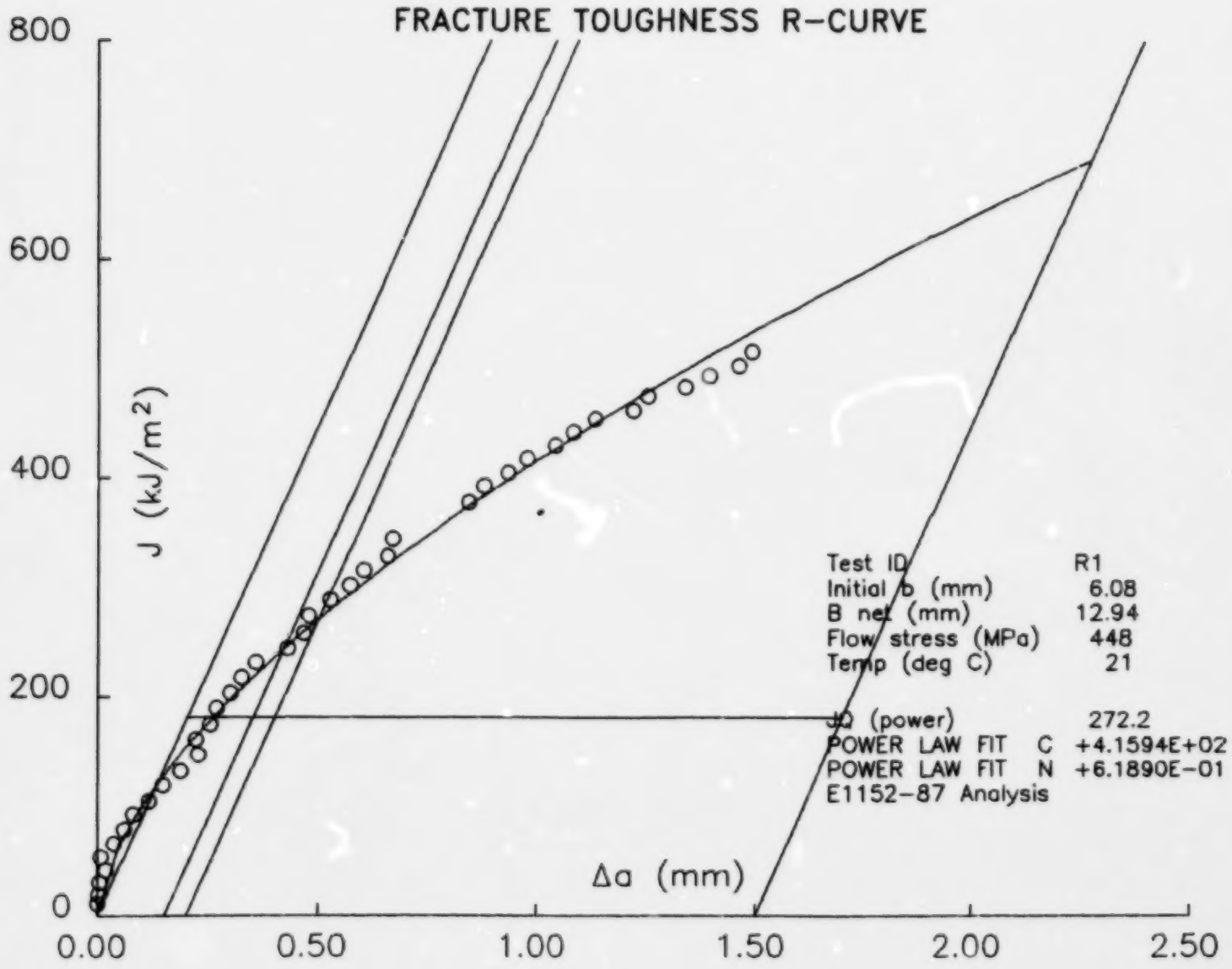
FRACTURE TOUGHNESS R-CURVE
800
600
400
200
0
J (kJ/m²)
Δa (mm)
0.00
0.50
1.00
1.50
2.00
2.50
Test ID R1
Initial b (mm) 6.08
B net (mm) 12.94
Flow stress (MPa) 448
Temp (deg C) 21
dQ (power) 272.2
POWER LAW FIT C +4.1594E+02
POWER LAW FIT N +6.1890E-01
E1152-87 Analysis

A14

89-135

ELASTIC-PLASTIC FRACTURE TOUGHNESS ANALYSIS

Specimen Id.	R8	Geometry	SE(B)
Contract #	BHWP	Orientation	C-L
Material	A516 Gr 70	Flow stress (MPa)	448
Temperature (C)	21	Modulus (GPa)	192
Environment	AIR	Stroke rate (mm/min)	0.005
		Loading rate (min)	7.046

Specimen Dimensions (mm)

Thickness	15.86	Notch depth	8.00
Net thickness	12.66	Gage length	5.00
Width	15.89	Alpha ratio	1.008
Span	63.5		

Initial Ligament(s) (mm)

6.07	6.01	6.04	6.02	6.00	5.96	6.01	6.03	6.08

Final Ligament(s) (mm)

3.78	4.14	4.51	4.23	3.98	4.12	4.00	4.30	3.83

Precrack Parameters

Pmax (kN)	1.90	Stress ratio (R)	0.10
Final a (mm)	9.30	Kmax (MPa sqr[m])	15.59

Test Parameters

Initial ligament	(mm)	6.02	J15limit	(kJ/m^2)	179
Final ligament	"	4.14	J20limit	"	135
Delta a (actual)	"	1.88	J25limit	"	108
Delta a (EvB/P)	"	1.70	*JQ (813-81)	"	0
Delta a error	"	-0.18	*JQ (813-81)(NV)	"	218
Delta a error	(%)	-9.7	*JQ (813-87)	"	0
Compliance Adjustment		1.241	*JQ (813-87)(NV)	"	255
CTODi (mm)		0.196	Tearing modulus		184.3

POWER LAW REGRESSION CONSTANT C +3.7084E+02
POWER LAW REGRESSION EXPONENT N +5.1883E-01

Comments * Computed from E813-87 form for J

Tested January 10 1989.
Precrack load > 40% of limit load (Sec 7.6.2)
Less than 4 data pts for JIc fit (Sec 9.3.2)
Thickness < 25*JQ/flowstress (Sec 9.4.1.1)
Ligament < 25*JQ/flowstress (Sec 9.4.1.2)
Crk ext edge to ctr > 2% of W (sec 9.4.1.6)
Em differs from E by > 10%
Improper data group for E1152-87 (Sec 8.4.1)

Specimen Id. R8

Index	Load (kN)	Disp. (mm)	Delta a (mm)	CTOD (mm)	K399 (MPa sqr[m])	K813	J813-81	J813-87 (kJ/m^2)	J1152	Jmod
0	0.0	-0.020		0.000	0.0	0.0	0.0	0.0	0.0	0.0
1	3.0	0.052		0.005	27.5	18.0	2.0	1.7	1.7	1.7
2	3.5	0.093		0.010	32.1	31.1	5.5	5.0	5.0	5.0
3	4.0	0.162		0.019	36.7	47.5	12.4	11.8	11.8	11.8
4	4.3	0.257	0.000	0.033	39.5	65.1	22.7	22.0	22.0	22.0
5	4.5	0.350	0.001	0.046	41.3	79.2	33.4	32.6	32.6	32.6
6	4.7	0.447	-0.003	0.060	43.1	92.3	45.1	44.3	44.3	44.3
7	4.9	0.544	0.005	0.075	45.0	104.2	57.4	56.5	56.4	56.5
8	5.1	0.641	0.010	0.091	46.9	115.2	70.0	69.1	69.0	69.1
9	5.2	0.736	0.026	0.106	48.1	125.5	82.8	81.9	81.7	81.9
10	5.2	0.834	0.053	0.122	48.4	135.2	95.8	95.1	94.7	95.3
11	5.3	0.934	0.079	0.137	49.7	144.5	109.2	108.7	108.1	109.1
12	5.4	1.029	0.123	0.153	51.2	153.0	122.0	121.8	120.8	122.5
13	5.4	1.127	0.157	0.168	51.6	161.4	135.5	135.5	134.2	136.7
14	5.5	1.221	0.177	0.185	52.9	169.2	148.9	148.9	147.6	150.4
15	5.5	1.319	0.224	0.200	53.5	176.9	162.2	162.8	160.9	164.9
16	5.5	1.422	0.257	0.216	54.0	184.7	176.8	177.5	175.4	180.3
17	5.5	1.524	0.289	0.233	54.5	192.2	191.1	192.0	189.7	195.6
18	5.5	1.622	0.337	0.251	55.1	199.0	204.4	205.9	203.0	210.4
19	5.5	1.720	0.391	0.267	56.0	205.6	217.4	219.8	215.9	225.2
20	5.5	1.822	0.421	0.284	56.4	212.3	232.0	234.4	230.5	240.9
21	5.4	1.928	0.483	0.301	56.3	218.9	245.7	249.3	244.2	257.1
22	5.4	2.030	0.511	0.318	56.8	225.1	260.2	263.6	258.6	272.7
23	5.4	2.133	0.586	0.336	58.0	231.1	272.5	277.7	270.9	288.5
24	5.3	2.239	0.632	0.353	57.6	237.1	286.6	292.5	285.0	304.9
25	5.2	2.343	0.674	0.371	57.2	242.9	300.5	306.8	298.9	320.9
26	5.1	2.449	0.731	0.389	57.1	248.4	313.3	320.9	311.7	336.9
27	5.0	2.554	0.804	0.407	57.1	253.6	324.8	334.6	323.2	352.6
28	5.0	2.657	0.884	0.426	58.5	258.5	335.3	347.6	333.6	367.9
29	4.9	2.757	0.926	0.444	58.1	263.4	347.8	360.7	346.2	383.2
30	4.8	2.862	1.013	0.461	58.4	268.1	357.5	373.7	355.9	398.8
31	4.7	2.968	1.075	0.481	58.3	272.7	368.9	386.7	367.2	414.5
32	4.6	3.072	1.153	0.499	58.4	277.1	378.6	399.3	376.8	429.8
33	4.5	3.178	1.213	0.517	58.2	281.4	389.5	411.8	387.7	445.3
34	4.4	3.284	1.299	0.536	58.5	285.5	397.8	423.9	396.1	460.6
35	4.3	3.383	1.373	0.555	58.6	289.3	406.0	435.1	404.2	474.9
36	4.2	3.489	1.473	0.574	59.1	293.1	412.3	446.6	410.5	489.9
37	4.1	3.590	1.510	0.593	58.4	296.7	423.4	457.7	421.6	504.4
38	4.0	3.689	1.584	0.611	58.5	300.0	430.5	468.1	428.7	518.3
39	3.9	3.790	1.640	0.629	58.1	303.4	439.2	478.6	437.4	532.3
40	3.8	3.896	1.699	0.648	57.8	306.7	447.8	489.3	446.1	546.9

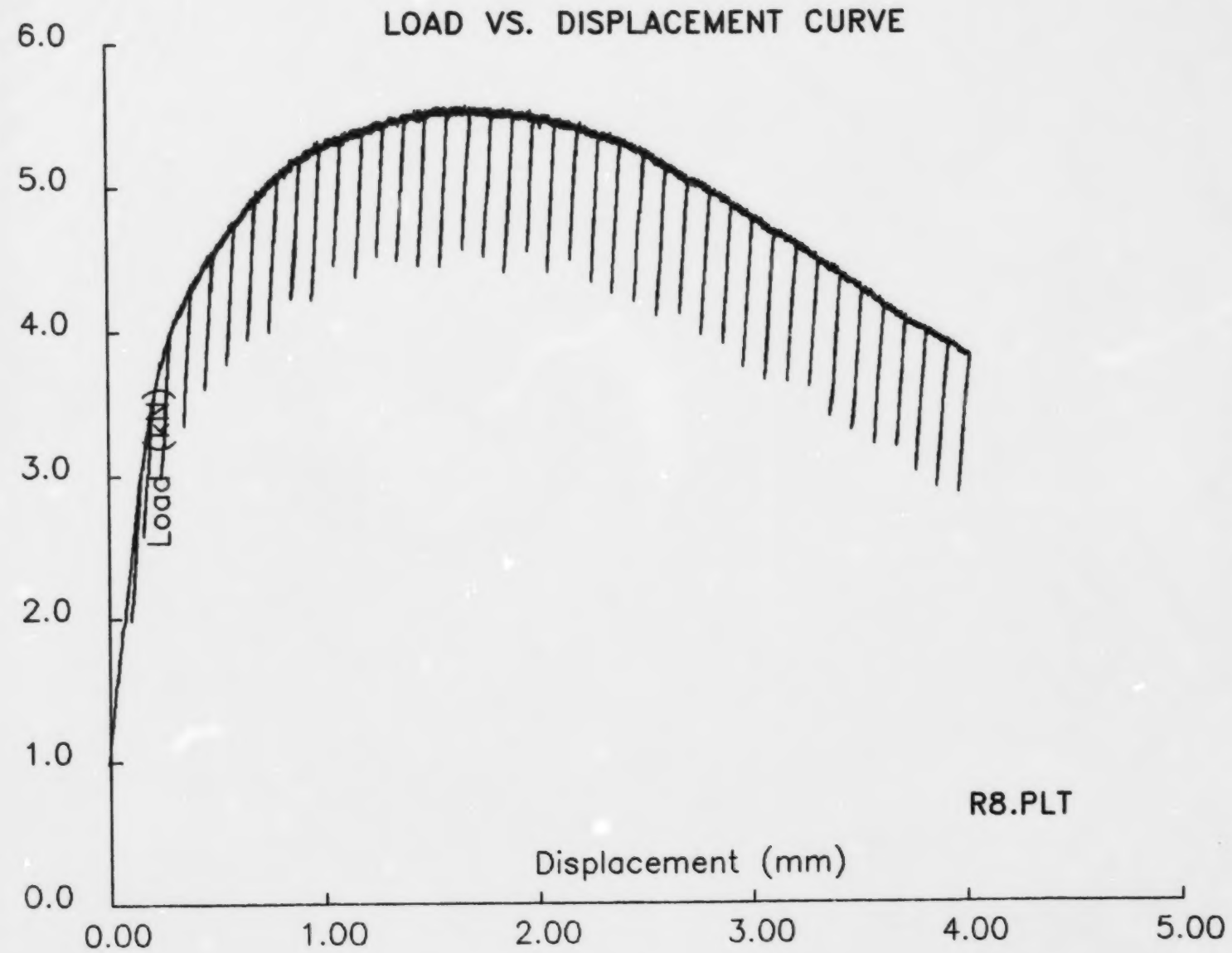
LOAD VS. DISPLACEMENT CURVE
6.0
5.0
4.0
3.0
2.0
1.0
0.0
Load (kN)
R8.PLT
Displacement (mm)
0.00
1.00
2.00
3.00
4.00
5.00

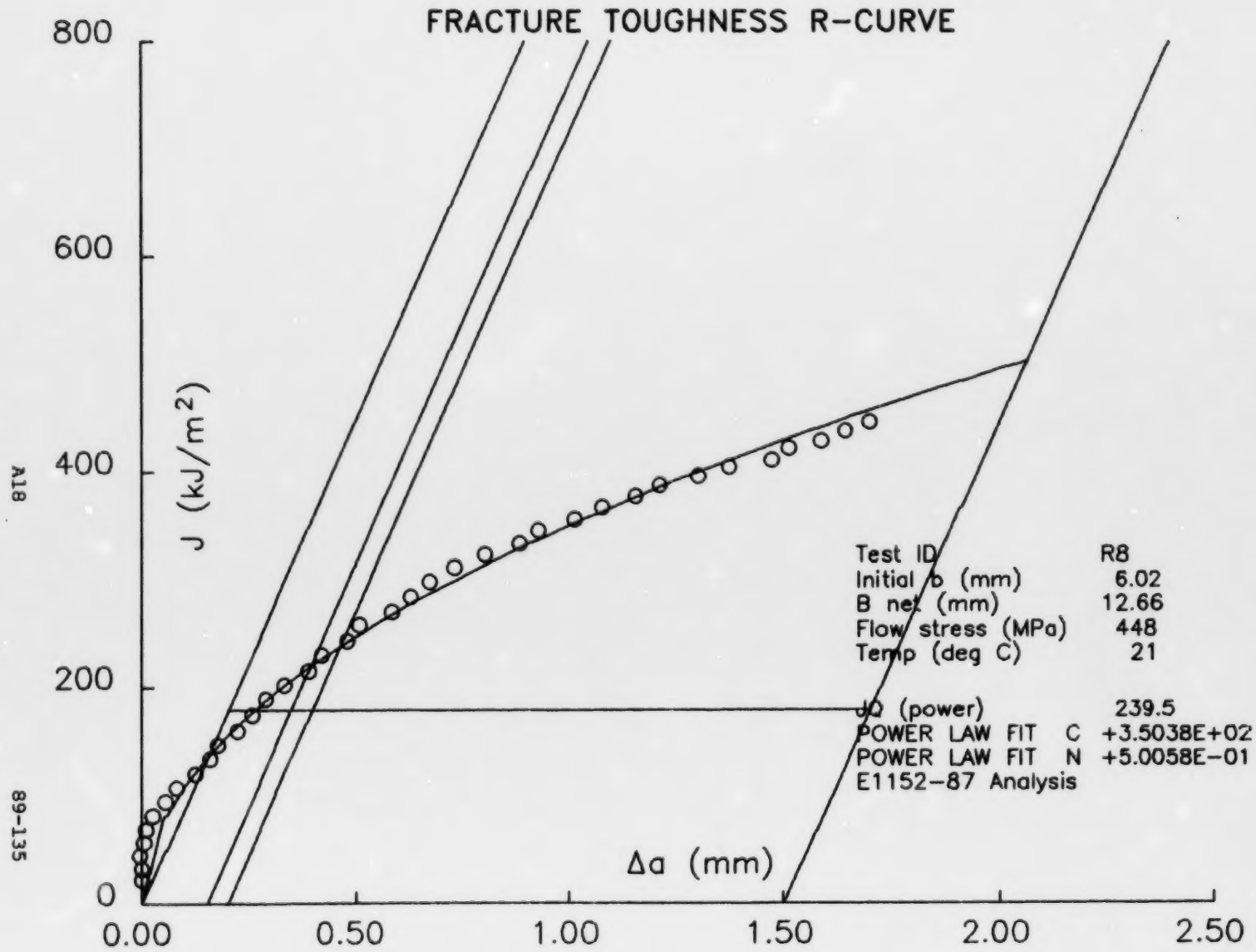
FRACTURE TOUGHNESS R-CURVE
800
600
400
200
0
J (kJ/m²)
Δa (mm)
0.00
0.50
1.00
1.50
2.00
2.50
Test ID R8
Initial b (mm) 6.02
B net (mm) 12.66
Flow stress (MPa) 448
Temp (deg C) 21
JQ (power) 239.5
POWER LAW FIT C +3.5038E+02
POWER LAW FIT N +5.0058E-01
E1152-87 Analysis
A18
89-135

ELASTIC-PLASTIC
FRACTURE TOUGHNESS ANALYSIS

Specimen Id.	B1	Geometry	SE(B)
Contract #	BHWP	Orientation	C-R
Material	A516 Gr 70	Flow stress (MPa)	448
Temperature (C)	21	Modulus (GPa)	192
Environment	AIR	Stroke rate (mm/min)	0.005
		Loading rate (min)	7.237

Specimen Dimensions (mm)

Thickness	15.84	Notch depth	7.80
Net thickness	12.48	Gage length	5.00
Width	15.89	Alpha ratio	1.008
Span	63.5		

Initial Ligament(s) (mm)

6.17	6.13	6.09	6.09	6.07	6.07	6.12	6.21	6.30

Final Ligament(s) (mm)

3.02	4.03	4.29	4.24	4.47	4.27	4.52	4.31	3.15

Precrack Parameters

Pmax (kN)	1.90	Stress ratio (R)	0.10
Final a (mm)	8.80	Kmax (MPa sqr[m])	15.17

Test Parameters

Initial ligament	(mm)	6.13	J15limit	(kJ/m^2)	183
Final ligament	〃	4.15	J20limit	〃	137
Delta a (actual)	〃	1.97	J25limit	〃	110
Delta a (EvB/P)	〃	1.93	*JQ (813-81)	〃	12
Delta a error	〃	-0.04	*JQ (813-81)(NV)	〃	12
Delta a error	(%)	-2.2	*JQ (813-87)	〃	33
Compliance Adjustment		1.187	*JQ (813-87)(NV)	〃	33
CTODi	(mm)	0.009	Tearing modulus		101.7

POWER LAW REGRESSION CONSTANT C +1.1772E+02
POWER LAW REGRESSION EXPONENT N +8.7948E-01

Comments * Computed from E813-87 form for J

Tested November 16 1988.
Precrack load > 40% of limit load (Sec 7.6.2)
Crk ext edge to ctr > 2% of W (sec 9.4.1.6)
Em differs from E by > 10%
Improper data group for E1152-87 (Sec 8.4.1)

Specimen Id. B1

Index	Load (kN)	Disp. (mm)	Delta a (mm)	CTOD (mm)	K399 (MPa sqr[m])	K813	J813-81	J813-87 (kJ/m^2)	J1152	Jmod
0	0.0	-0.015		0.000	0.0	0.0	0.0	0.0	0.0	0.0
1	2.4	0.049		0.003	21.6	15.9	1.5	1.3	1.3	1.3
2	2.9	0.065		0.005	26.1	21.0	2.6	2.3	2.3	2.3
3	3.4	0.087		0.008	30.6	27.7	4.4	4.0	4.0	4.0
4	3.9	0.117	0.000	0.013	35.1	35.9	7.3	6.7	6.7	6.7
5	4.0	0.217		0.027	36.0	57.2	17.7	17.0	17.0	17.0
6	4.2	0.315	0.168	0.043	39.4	72.1	27.6	27.0	26.9	27.3
7	4.2	0.412	0.270	0.058	40.5	84.8	38.1	37.4	37.3	38.2
8	4.3	0.512	0.373	0.074	42.6	96.2	49.1	48.1	48.2	49.7
9	4.3	0.615	0.464	0.091	43.6	106.9	60.6	59.4	59.7	61.9
10	4.3	0.717	0.554	0.107	44.7	116.5	72.1	70.6	71.1	74.2
11	4.3	0.815	0.611	0.124	45.4	125.1	83.4	81.4	82.4	86.3
12	4.3	0.913	0.739	0.140	47.1	133.0	93.7	92.0	92.6	98.3
13	4.2	0.969	0.772	0.149	46.4	137.4	100.1	98.2	99.1	105.3
14	4.1	1.020	0.866	0.158	46.5	141.1	104.8	103.6	103.7	111.6
15	4.1	1.069	0.956	0.166	47.8	144.4	109.0	108.5	107.9	117.5
16	4.1	1.123	0.999	0.175	48.4	148.1	115.0	114.1	113.8	124.2
17	4.0	1.179	1.061	0.185	48.1	151.8	120.6	119.9	119.4	131.1
18	3.9	1.231	1.129	0.193	47.9	155.1	125.4	125.2	124.2	137.5
19	4.0	1.282	1.159	0.203	49.5	158.2	131.2	130.1	129.9	143.8
20	3.9	1.334	1.202	0.212	48.9	161.4	136.6	135.5	135.4	150.4
21	3.9	1.388	1.226	0.221	49.3	164.6	142.8	140.9	141.5	157.1
22	3.9	1.441	1.283	0.230	50.2	167.6	147.9	146.1	146.6	163.7
23	3.8	1.492	1.314	0.239	49.4	170.6	153.5	151.4	152.2	170.3
24	3.8	1.541	1.363	0.248	50.2	173.2	158.1	156.0	156.8	176.3
25	3.8	1.595	1.407	0.257	50.9	176.1	163.5	161.2	162.2	183.1
26	3.7	1.652	1.451	0.267	50.2	179.1	169.2	166.8	167.9	190.2
27	3.7	1.700	1.515	0.277	51.3	181.4	173.0	171.2	171.6	196.1
28	3.6	1.757	1.544	0.286	50.4	184.3	179.0	176.7	177.7	203.3
29	3.6	1.811	1.610	0.296	51.5	186.8	183.2	181.5	181.8	209.8
30	3.5	1.867	1.670	0.306	51.1	189.5	187.9	186.8	186.5	216.9
31	3.5	1.920	1.701	0.316	51.6	191.9	193.2	191.5	191.8	223.4
32	3.4	1.972	1.750	0.326	51.0	194.3	197.5	196.2	196.1	229.8
33	3.4	2.026	1.797	0.334	51.9	196.5	202.1	200.8	200.6	236.3
34	3.3	2.082	1.857	0.345	51.4	198.9	206.3	205.8	204.8	243.2
35	3.2	2.138	1.931	0.356	51.2	201.2	209.4	210.5	207.9	249.8

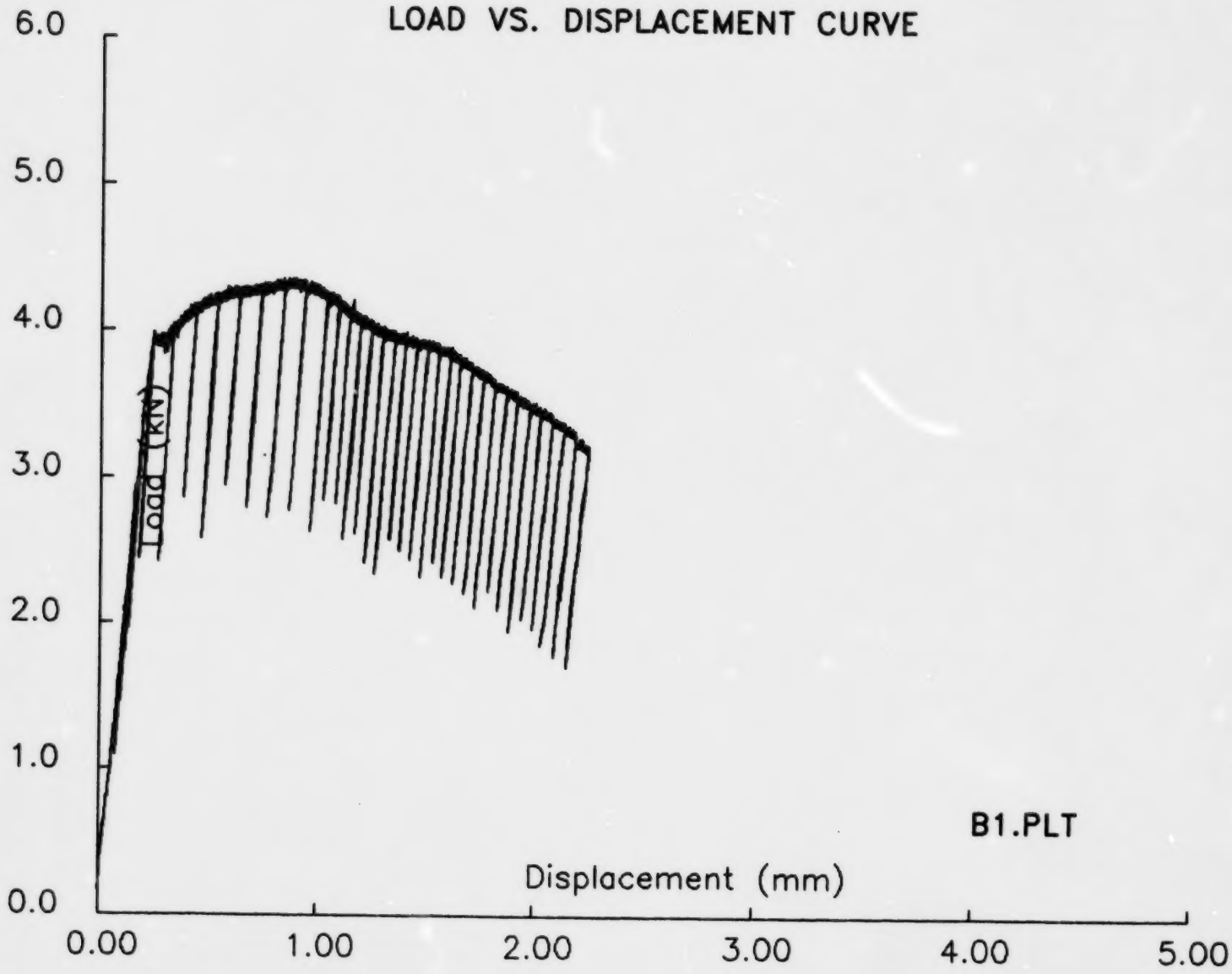
LOAD VS. DISPLACEMENT CURVE
6.0
5.0
4.0
3.0
2.0
1.0
0.0
Load (kN)
B1.PLT
Displacement (mm)
0.00
1.00
2.00
3.00
4.00
5.00

A21

89-135

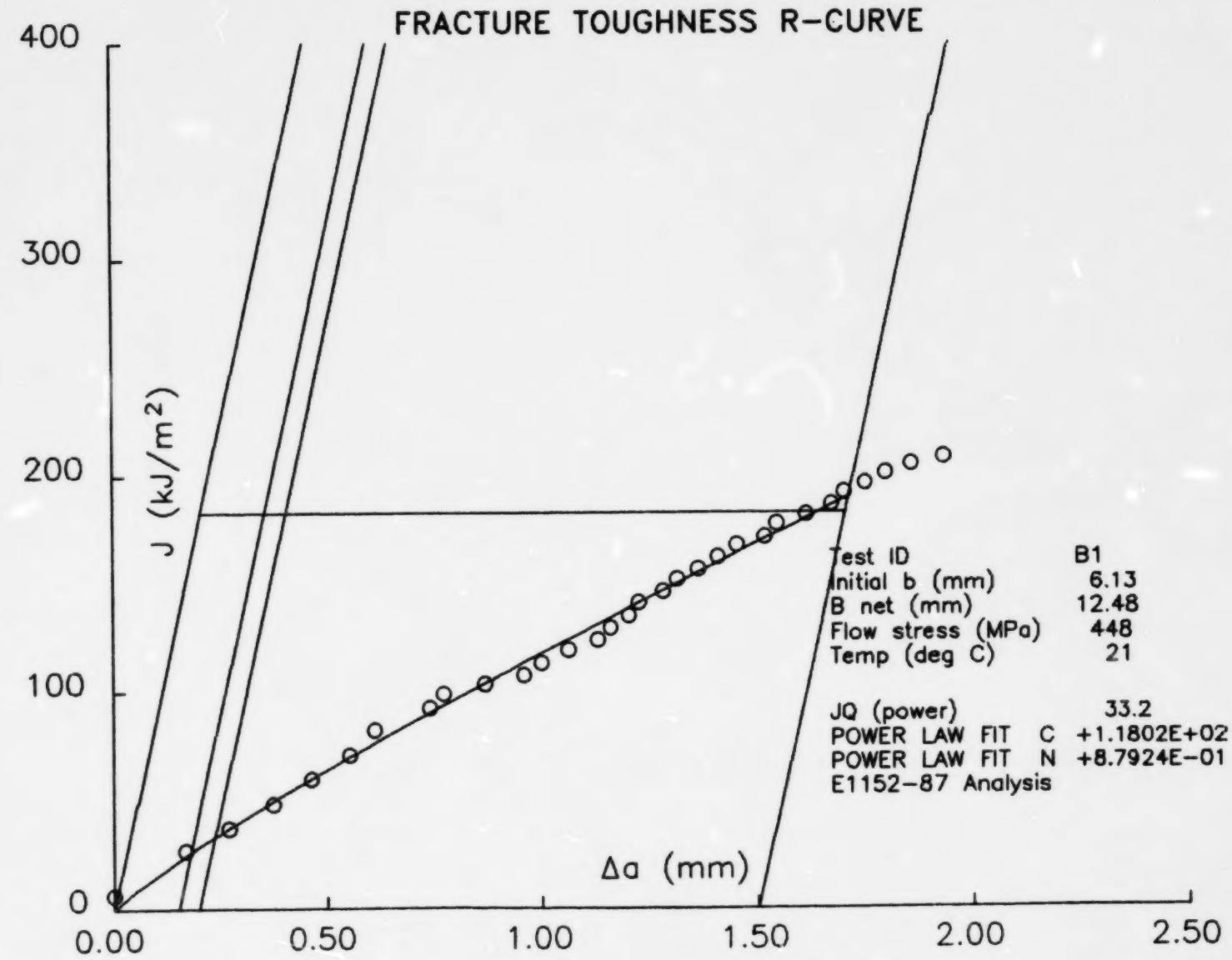
FRACTURE TOUGHNESS R-CURVE
400
300
200
100
0
J (kJ/m²)
0.00
0.50
1.00
1.50
2.00
2.50
Δa (mm)
Test ID B1
Initial b (mm) 6.13
B net (mm) 12.48
Flow stress (MPa) 448
Temp (deg C) 21
JQ (power) 33.2
POWER LAW FIT C +1.1802E+02
POWER LAW FIT N +8.7924E-01
E1152-87 Analysis

A22

89-135

ELASTIC-PLASTIC FRACTURE TOUGHNESS ANALYSIS

Specimen Id.	C1	Geometry	SE(B)
Contract #	BHWP	Orientation	C-R
Material	A516 Gr 70	Flow stress (MPa)	448
Temperature (C)	21	Modulus (GPa)	192
Environment	AIR	Stroke rate (mm/min)	0.005
		Loading rate (min)	7.016

Specimen Dimensions (mm)

Thickness	15.84	Notch depth	7.80
Net thickness	12.70	Gage length	5.00
Width	15.88	Alpha ratio	1.008
Span	63.5		

Initial Ligament(s) (mm)

5.84	5.80	5.76	5.80	5.81	5.80	5.94	6.01	6.06

Final Ligament(s) (mm)

3.84	4.10	4.01	4.00	3.86	3.80	3.84	4.01	3.46

Precrack Parameters

Pmax (kN)	1.90	Stress ratio (R)	0.10
Final a (mm)	8.80	Kmax (MPa sqr[m])	16.26

Test Parameters

Initial ligament	(mm)	5.86	J15limit	(kJ/m^2)	175
Final ligament	"	3.91	J20limit	"	131
Delta a (actual)	"	1.95	J25limit	"	105
Delta a (EvB/P)	"	1.75	*JQ (813-81)	"	24
Delta a error	"	-0.20	*JQ (813-81)(NV)	"	26
Delta a error	(%)	-10.1	*JQ (813-87)	"	47
Compliance Adjustment		1.264	*JQ (813-87)(NV)	"	46
CTODi (mm)		0.027	Tearing modulus		104.4

POWER LAW REGRESSION CONSTANT C	+1.3416E+02
POWER LAW REGRESSION EXPONENT N	+7.6750E-01

Comments * Computed from E813-87 form for J

Tested November 17 1988.
Precrack load > 40% of limit load (Sec 7.6.2)
Crk ext edge to ctr > 2% of W (sec 9.4.1.6)
Em differs from E by > 10%

Specimen Id. C1

Index	Load (kN)	Disp. (mm)	Delta a (mm)	CTOD (mm)	K399 (MPa sqr[m])	K813	J813-81	J813-87 (kJ/m^2)	J1152	Jmod
0	0.0	-0.015		0.000	0.0	0.0	0.0	0.0	0.0	0.0
1	2.6	0.044		0.003	24.8	15.5	1.5	1.2	1.2	1.2
2	3.1	0.065		0.006	29.6	22.9	3.1	2.7	2.7	2.7
3	3.6	0.096	0.000	0.010	34.4	32.1	5.9	5.4	5.4	5.4
4	3.9	0.186	0.013	0.022	37.4	52.5	15.0	14.3	14.4	14.4
5	4.1	0.282	0.099	0.036	40.2	68.5	25.2	24.4	24.5	24.6
6	4.1	0.385	0.162	0.050	40.9	82.7	36.5	35.6	35.7	36.1
7	4.2	0.437	0.213	0.058	42.5	88.9	42.0	41.1	41.2	41.9
8	4.2	0.491	0.231	0.066	42.7	95.2	48.2	47.1	47.4	48.2
9	4.2	0.544	0.316	0.075	43.7	100.8	53.7	52.8	52.8	54.3
10	4.2	0.598	0.375	0.083	44.4	106.3	59.6	58.7	58.7	60.6
11	4.3	0.644	0.387	0.091	45.6	110.8	65.1	63.9	64.1	66.2
12	4.3	0.698	0.413	0.099	45.9	116.0	71.5	70.0	70.5	72.9
13	4.3	0.751		0.107	45.9	122.1	78.1	77.6	80.1	82.5
14	4.2	0.808	0.531	0.116	46.4	125.8	83.3	82.3	82.3	86.2
15	4.3	0.859	0.569	0.124	48.0	130.0	89.2	87.9	88.1	92.5
16	4.3	0.913	0.621	0.133	48.7	134.4	95.2	93.9	94.0	99.3
17	4.2	0.964	0.682	0.141	48.5	138.4	100.5	99.6	99.4	105.7
18	4.2	1.018	0.725	0.149	49.1	142.4	106.6	105.5	105.4	112.5
19	4.1	1.074	0.776	0.158	48.7	146.6	112.7	111.7	111.6	119.6
20	4.1	1.128	0.857	0.167	49.9	150.2	117.8	117.3	116.5	126.3
21	4.0	1.184		0.176	48.6	155.9	124.9	126.5	130.6	140.3
22	4.0	1.238	0.959	0.185	50.2	157.5	129.1	128.9	127.8	140.0
23	4.0	1.287	1.013	0.194	51.0	160.5	133.9	133.9	132.6	146.1
24	3.9	1.344	1.069	0.202	50.6	164.0	139.6	139.9	138.3	153.3
25	3.9	1.393	1.104	0.211	51.2	166.9	144.9	144.9	143.5	159.5
26	3.8	1.443	1.155	0.219	50.7	169.9	149.8	150.1	148.4	165.8
27	3.8	1.497	1.195	0.228	51.4	172.9	155.3	155.4	154.0	172.6
28	3.8	1.551	1.254	0.237	52.4	175.8	160.3	160.7	158.9	179.3
29	3.7	1.608	1.301	0.247	51.8	178.9	165.9	166.4	164.5	186.5
30	3.6	1.664	1.364	0.256	51.5	181.8	170.6	171.8	169.2	193.3
31	3.6	1.713	1.414	0.265	52.4	184.1	174.8	176.3	173.4	199.3
32	3.5	1.769	1.446	0.273	51.5	187.0	180.7	181.9	179.3	206.4
33	3.5	1.823	1.513	0.282	52.7	189.4	184.7	186.6	183.2	212.9
34	3.4	1.879	1.567	0.292	52.2	192.1	189.3	191.8	187.8	219.8
35	3.3	1.930	1.640	0.302	51.9	194.4	192.4	196.4	190.9	225.9
36	3.2	1.987	1.680	0.310	51.1	196.9	197.4	201.5	195.9	232.7
37	3.2	2.041	1.753	0.320	52.5	198.9	200.4	205.8	198.9	239.0

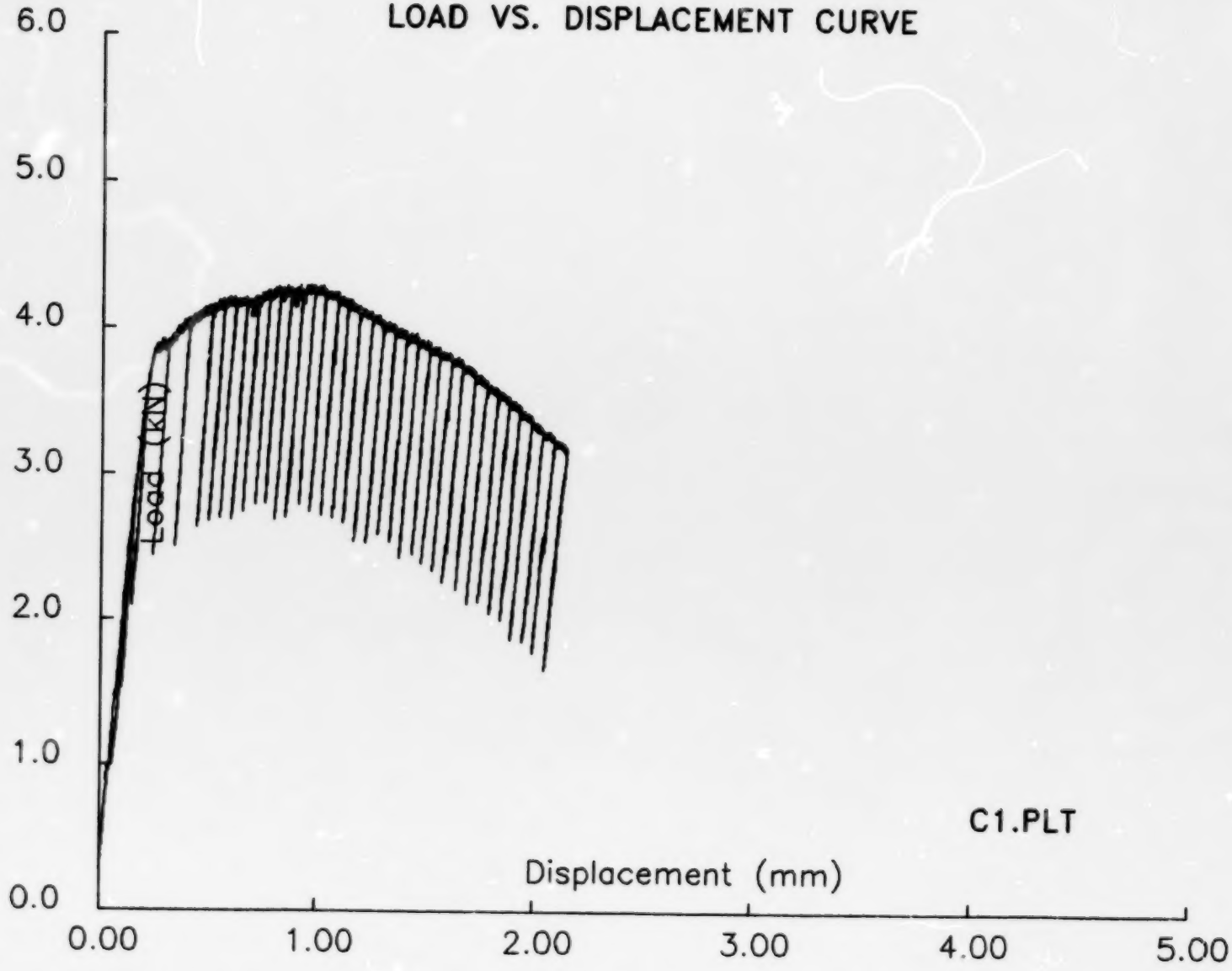
LOAD VS. DISPLACEMENT CURVE
6.0
5.0
4.0
3.0
2.0
1.0
0.0
Load (KN)
C1.PLT
Displacement (mm)
0.00
1.00
2.00
3.00
4.00
5.00

A25

89-135

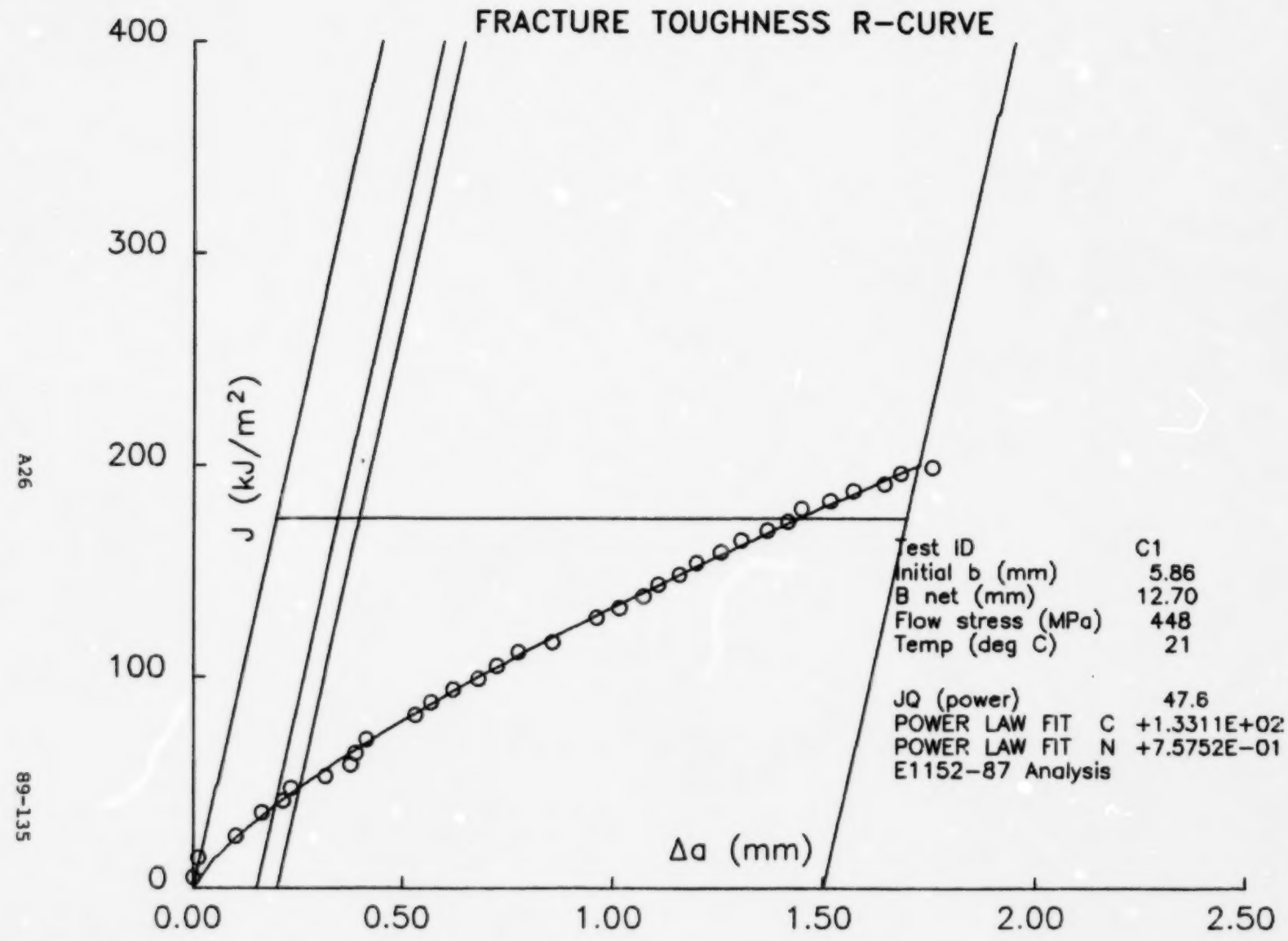
FRACTURE TOUGHNESS R-CURVE
400
300
200
100
0
J (kJ/m²)
0.00
0.50
1.00
1.50
2.00
2.50
Δa (mm)
Test ID C1
Initial b (mm) 5.86
B net (mm) 12.70
Flow stress (MPa) 448
Temp (deg C) 21
JQ (power) 47.6
POWER LAW FIT C +1.3311E+02
POWER LAW FIT N +7.5752E-01
E1152-87 Analysis

A26

89-135

ELASTIC-PLASTIC
FRACTURE TOUGHNESS ANALYSIS

Specimen Id.	D2	Geometry	SE(B)
Contract #	BHWP	Orientation	C-R
Material	A516 Gr 70	Flow stress (MPa)	448
Temperature (C)	21	Modulus (GPa)	192
Environment	AIR	Stroke rate (mm/min)	0.005
		Loading rate (min)	6.837

Specimen Dimensions (mm)

Thickness	15.82	Notch depth	7.85
Net thickness	12.64	Gage length	5.00
Width	15.90	Alpha ratio	1.008
Span	63.5		

Initial Ligament(s) (mm)

5.76	5.64	5.59	5.59	5.59	5.56	5.64	5.65	5.66

Final Ligament(s) (mm)

2.91	3.14	3.64	3.66	3.74	3.59	3.79	3.20	3.39

Precrack Parameters

Pmax (kN)	1.90	Stress ratio (R)	0.10
Final a (mm)	9.00	Kmax (MPa sqr[m])	17.34

Test Parameters

Initial ligament	(mm)	5.62	J15limit	(kJ/m^2)	168
Final ligament	"	3.49	J20limit	"	126
Delta a (actual)	"	2.13	J25limit	"	101
Delta a (EvB/P)	"	1.81	*JQ (813-81)	"	32
Delta a error	"	-0.32	*JQ (813-81)(NV)	"	30
Delta a error	(%)	-15.2	*JQ (813-87)	"	50
Compliance Adjustment		1.321	*JQ (813-87)(NV)	"	49
CTODi (mm)		0.029	Tearing modulus		99.6

POWER LAW REGRESSION CONSTANT C +1.3018E+02
POWER LAW REGRESSION EXPONENT N +6.9703E-01

Comments * Computed from E813-87 form for J

Tested November 18 1988.
Precrack load > 40% of limit load (Sec 7.6.2)
Crk ext edge to ctr > 2% of W (sec 9.4.1.6)
Final delta a error > 15% of a (Sec 9.4.1.7)
Em differs from E by > 10%

Specimen Id. D2

Index	Load (kN)	Disp. (mm)	Delta a (mm)	CTOD (mm)	K399 (MPa sqr[m])	K813	J813-81	J813-87 (kJ/m^2)	J1152	Jmod
0	0.0	-0.015		0.000	0.0	0.0	0.0	0.0	0.0	0.0
1	2.0	0.054		0.002	20.4	16.1	1.5	1.3	1.3	1.3
2	2.5	0.070		0.004	25.5	20.8	2.5	2.2	2.2	2.2
3	3.0	0.097		0.007	30.6	28.4	4.6	4.2	4.2	4.2
4	3.5	0.127	0.000	0.011	35.7	36.1	7.4	6.8	6.8	6.8
5	3.8	0.217	0.022	0.023	39.0	55.2	16.6	15.9	15.9	15.9
6	3.9	0.318	0.107	0.036	41.0	71.3	27.3	26.4	26.5	26.7
7	4.0	0.412	0.162	0.050	42.7	84.0	37.7	36.7	36.8	37.3
8	4.0	0.461	0.213	0.057	43.3	89.9	43.0	42.0	42.1	42.9
9	4.1	0.512	0.243	0.064	44.8	95.8	48.8	47.7	47.9	48.9
10	4.1	0.561	0.260	0.072	45.0	101.2	54.6	53.3	53.7	54.8
11	4.1	0.615	0.317	0.079	45.7	106.8	60.5	59.3	59.6	61.2
12	4.1	0.668	0.380	0.087	46.6	111.9	66.3	65.2	65.3	67.5
13	4.1	0.722	0.411	0.095	47.0	117.1	72.6	71.3	71.6	74.1
14	4.1	0.776	0.455	0.103	47.6	121.9	78.7	77.3	77.6	80.8
15	4.1	0.830	0.519	0.111	48.5	126.5	84.5	83.3	83.4	87.4
16	4.1	0.883	0.557	0.119	49.1	131.0	90.6	89.2	89.5	94.0
17	4.0	0.935	0.617	0.127	48.7	135.1	96.0	95.0	94.9	100.4
18	4.0	0.989	0.704	0.135	50.1	139.1	101.2	100.6	100.0	107.0
19	3.9	1.041	0.758	0.143	49.6	143.0	106.6	106.3	105.4	113.5
20	3.9	1.090	0.825	0.151	50.7	146.3	111.3	111.4	110.1	119.5
21	3.9	1.143	0.872	0.159	51.4	150.0	117.1	117.0	115.8	126.2
22	3.8	1.194	0.936	0.168	51.2	153.5	122.1	122.5	120.8	132.7
23	3.7	1.251	0.984	0.176	50.6	157.1	128.0	128.4	126.7	139.8
24	3.7	1.300	1.051	0.185	51.7	160.0	132.3	133.2	130.9	145.7
25	3.6	1.357	1.116	0.193	51.4	163.5	137.6	138.9	136.2	152.7
26	3.6	1.410	1.181	0.202	52.6	166.4	142.2	144.0	140.8	159.2
27	3.5	1.461	1.213	0.210	51.7	169.4	147.7	149.2	146.3	165.7
28	3.5	1.515	1.270	0.218	52.7	172.2	152.6	154.3	151.1	172.3
29	3.5	1.564	1.308	0.227	53.4	174.8	157.5	158.9	156.0	178.4
30	3.4	1.620	1.354	0.235	52.7	177.8	162.8	164.4	161.4	185.3
31	3.4	1.669	1.398	0.244	53.6	180.2	167.3	168.8	165.8	191.3
32	3.4	1.723	1.422	0.251	54.0	182.8	173.2	173.8	171.7	198.1
33	3.3	1.779	1.453	0.260	53.0	185.7	179.1	179.3	177.6	205.2
34	3.3	1.833	1.499	0.269	53.9	188.2	183.9	184.1	182.3	211.8
35	3.2	1.884	1.537	0.278	53.0	190.6	188.4	188.9	186.9	218.0
36	3.2	1.938	1.579	0.287	53.9	192.9	193.2	193.5	191.6	224.6
37	3.1	1.995	1.648	0.296	53.6	195.4	196.8	198.5	195.2	231.3
38	3.0	2.046	1.695	0.305	52.8	197.6	200.7	203.1	199.2	237.5
39	3.0	2.099	1.747	0.314	53.9	199.7	204.4	207.3	202.8	243.7
40	2.9	2.156	1.808	0.323	53.3	201.9	208.0	212.1	206.4	250.3

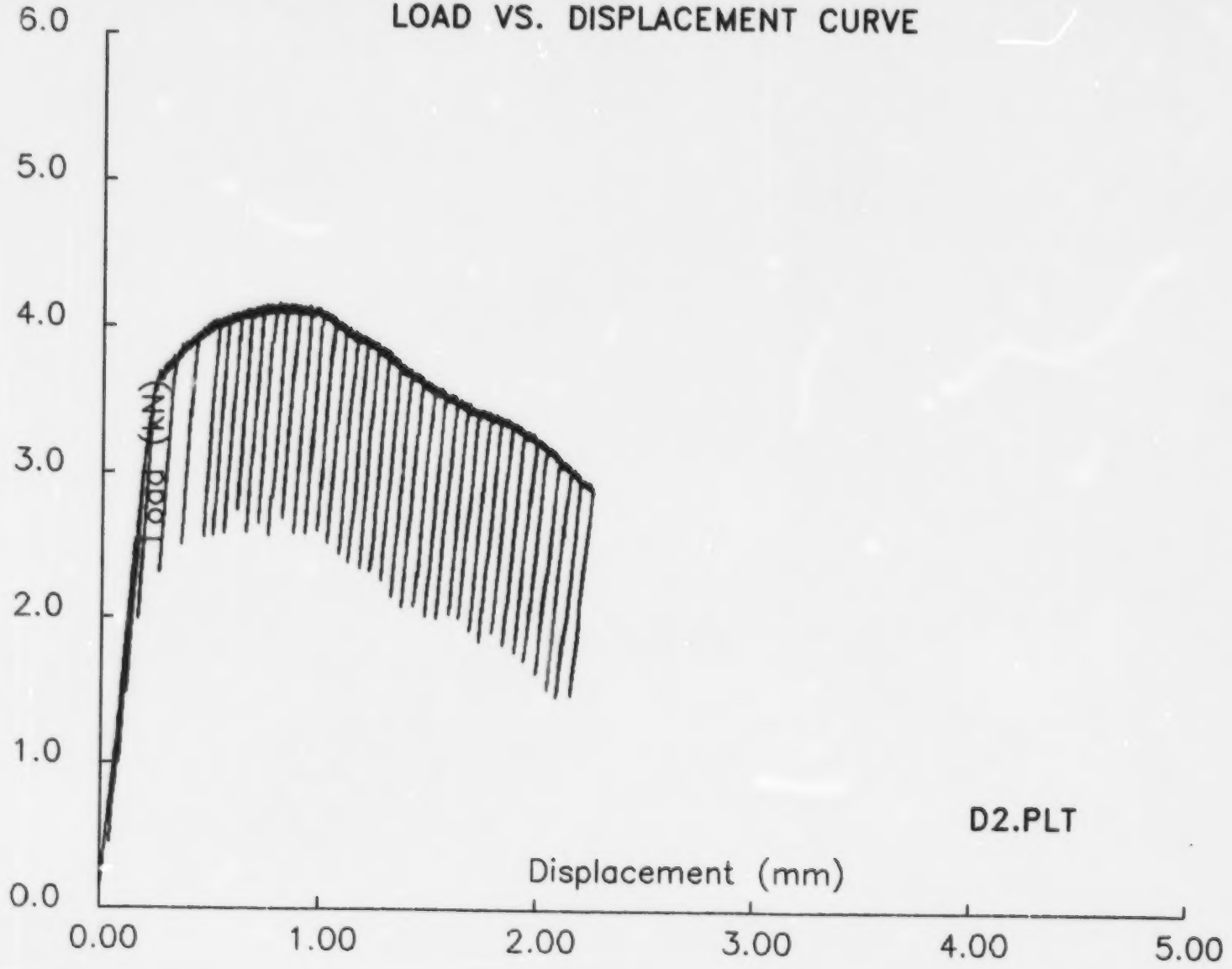
LOAD VS. DISPLACEMENT CURVE
6.0
5.0
4.0
3.0
2.0
1.0
0.0
Load (kN)
D2.PLT
Displacement (mm)
0.00
1.00
2.00
3.00
4.00
5.00

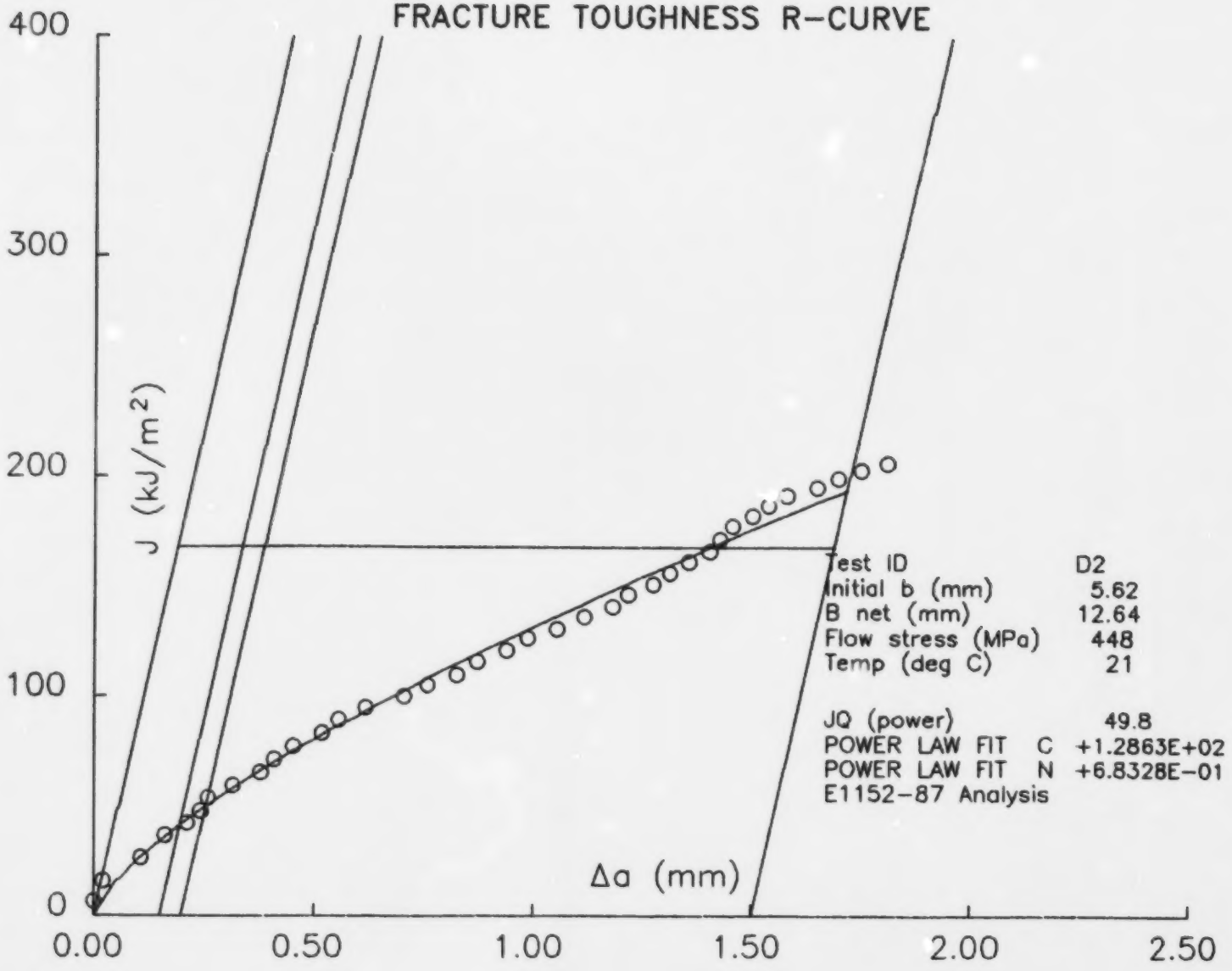
FRACTURE TOUGHNESS R-CURVE
400
300
200
100
0
J (kJ/m²)
Δa (mm)
0.00
0.50
1.00
1.50
2.00
2.50
Test ID D2
Initial b (mm) 5.62
B net (mm) 12.64
Flow stress (MPa) 448
Temp (deg C) 21
JQ (power) 49.8
POWER LAW FIT C +1.2863E+02
POWER LAW FIT N +6.8328E-01
E1152-87 Analysis

A30

89-135

ELASTIC-PLASTIC FRACTURE TOUGHNESS ANALYSIS

Specimen Id.	R4	Geometry	SE(B)
Contract #	BHWP	Orientation	C-R
Material	A516 Gr 70	Flow stress (MPa)	448
Temperature (C)	21	Modulus (GPa)	192
Environment	AIR	Stroke rate (mm/min)	0.005
		Loading rate (min)	7.202

Specimen Dimensions (mm)

Thickness	15.89	Notch depth	7.80
Net thickness	12.73	Gage length	5.00
Width	15.89	Alpha ratio	1.008
Span	63.5		

Initial Ligament(s) (mm)

6.27	6.21	6.16	6.10	6.10	6.18	6.16	6.17	6.27

Final Ligament(s) (mm)

3.15	3.80	3.82	4.16	4.15	4.12	4.06	4.02	3.38

Precrack Parameters

Pmax (kN)	1.90	Stress ratio (R)	0.10
Final a (mm)	8.80	Kmax (MPa sqr[m])	14.97

Test Parameters

Initial ligament	(mm)	6.17	J15limit	(kJ/m^2)	184
Final ligament	"	3.92	J20limit	"	138
Delta a (actual)	"	2.24	J25limit	"	110
Delta a (EvB/P)	"	2.02	*JQ (813-81)	"	28
Delta a error	"	-0.22	*JQ (813-81)(NV)	"	28
Delta a error	(%)	-9.7	*JQ (813-87)	"	41
Compliance Adjustment		1.202	*JQ (813-87)(NV)	"	41
CTODi (mm)		0.036	Tearing modulus		83.0

POWER LAW REGRESSION CONSTANT C +1.1372E+02
POWER LAW REGRESSION EXPONENT N +7.1967E-01

Comments * Computed from E813-87 form for J

Tested December 21 1988.
Precrack load > 40% of limit load (Sec 7.6.2)
Crk ext edge to ctr > 2% of W (sec 9.4.1.6)
Em differs from E by > 10%

Specimen Id. R4

Index	Load (kN)	Disp. (mm)	Delta a (mm)	CTOD (mm)	K399 (MPa sqr[m])	K813	J813-81	J813-87 (kJ/m^2)	J1152	Jmod
0	0.0	-0.020		0.000	0.0	0.0	0.0	0.0	0.0	0.0
1	2.9	0.094	0.000	0.007	25.5	24.8	3.5	3.2	3.2	3.2
2	3.4	0.129	0.006	0.012	30.0	33.5	6.3	5.9	5.9	5.9
3	3.9	0.190	0.017	0.020	34.5	46.7	11.9	11.3	11.4	11.4
4	4.3	0.276	0.094	0.034	38.8	62.1	20.8	20.0	20.1	20.2
5	4.5	0.374	0.163	0.049	41.3	76.8	31.7	30.7	30.9	31.2
6	4.6	0.469	0.251	0.065	43.2	89.3	42.6	41.4	41.7	42.5
7	4.7	0.530	0.291	0.075	44.6	96.4	49.7	48.4	48.8	49.8
8	4.7	0.594	0.367	0.085	45.5	103.6	57.1	55.8	56.1	57.7
9	4.7	0.657	0.432	0.095	46.3	110.1	64.5	63.1	63.5	65.6
10	4.6	0.718	0.498	0.105	46.1	116.2	71.6	70.2	70.6	73.4
11	4.6	0.781	0.609	0.116	47.5	121.8	78.2	77.2	77.1	81.2
12	4.5	0.843	0.687	0.127	47.5	127.2	85.0	84.2	83.9	89.0
13	4.5	0.902	0.773	0.137	48.6	132.0	91.2	90.6	90.1	96.4
14	4.5	0.960	0.811	0.148	49.2	136.6	98.2	97.1	97.0	104.0
15	4.4	1.022	0.878	0.158	49.0	141.4	105.0	103.9	103.8	111.9
16	4.4	1.080	0.953	0.168	50.1	145.5	111.1	110.1	109.9	119.3
17	4.3	1.141	1.068	0.179	50.6	149.8	116.6	116.7	115.4	127.1
18	4.3	1.205	1.100	0.189	51.1	154.1	124.4	123.5	123.1	135.5
19	4.2	1.266	1.183	0.200	51.2	158.1	130.3	129.9	129.0	143.3
20	4.0	1.335	1.306	0.212	50.6	162.3	135.9	137.1	134.7	152.1
21	3.9	1.401	1.383	0.223	50.6	166.2	142.1	143.6	140.9	160.3
22	3.9	1.465	1.456	0.235	51.8	169.6	148.1	149.6	146.8	168.3
23	3.8	1.531	1.533	0.247	51.7	173.2	154.1	155.9	152.8	176.5
24	3.7	1.597	1.609	0.259	51.6	176.6	160.0	162.2	158.7	184.8
25	3.6	1.658	1.678	0.270	51.4	179.7	165.2	167.8	163.8	192.3
26	3.6	1.722	1.720	0.282	52.2	182.7	171.7	173.5	170.3	200.2
27	3.5	1.788	1.786	0.294	51.9	185.8	177.3	179.4	176.0	208.3
28	3.4	1.849	1.886	0.305	52.2	188.5	180.8	184.7	179.4	215.7
29	3.3	1.911	1.974	0.317	52.2	191.1	184.6	189.9	183.2	223.0
30	3.2	1.972	2.025	0.328	51.6	193.7	189.7	195.0	188.3	230.3

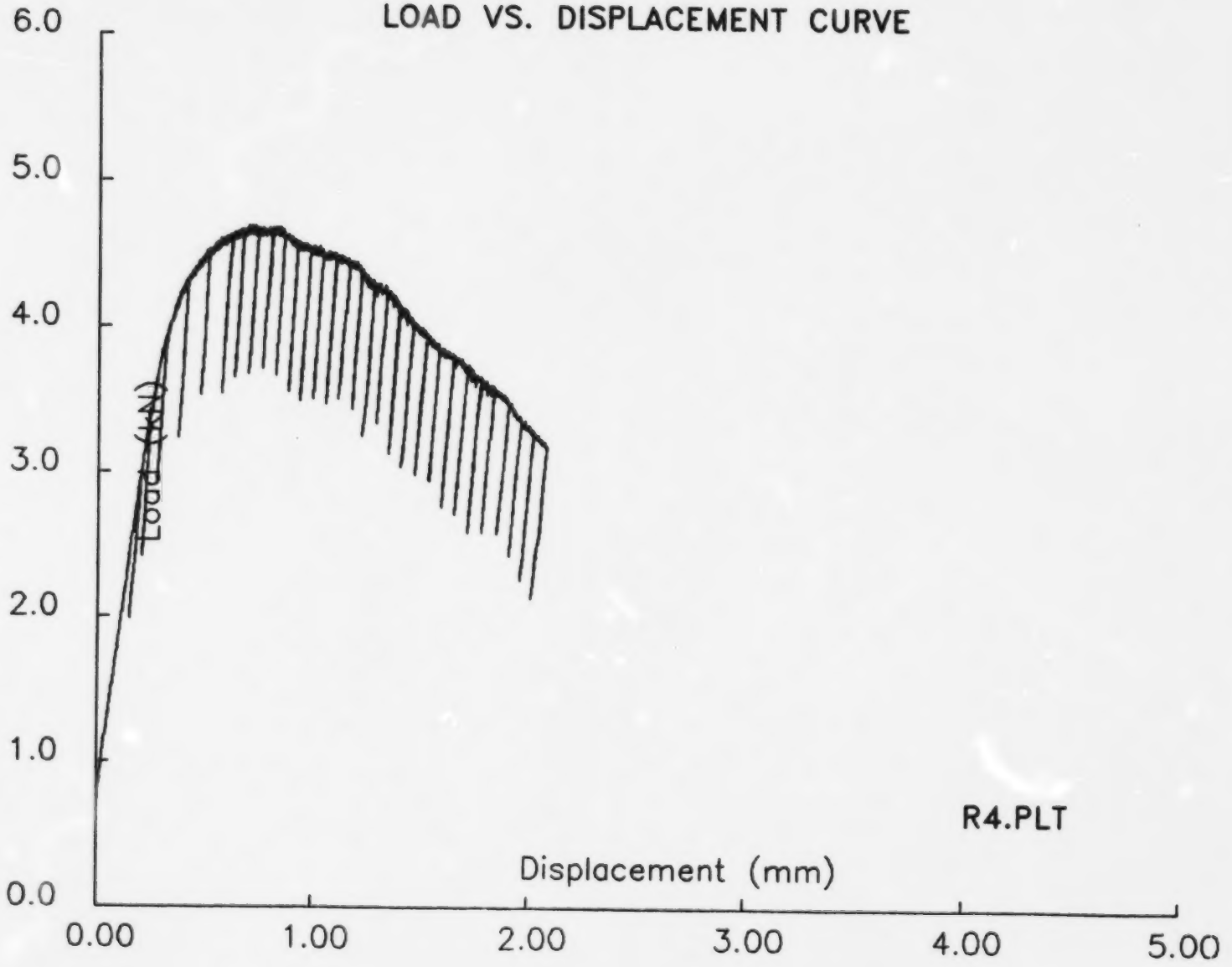
LOAD VS. DISPLACEMENT CURVE
6.0
5.0
4.0
3.0
2.0
1.0
0.0
Load (kN)
R4.PLT
Displacement (mm)
0.00
1.00
2.00
3.00
4.00
5.00

A33

89-135

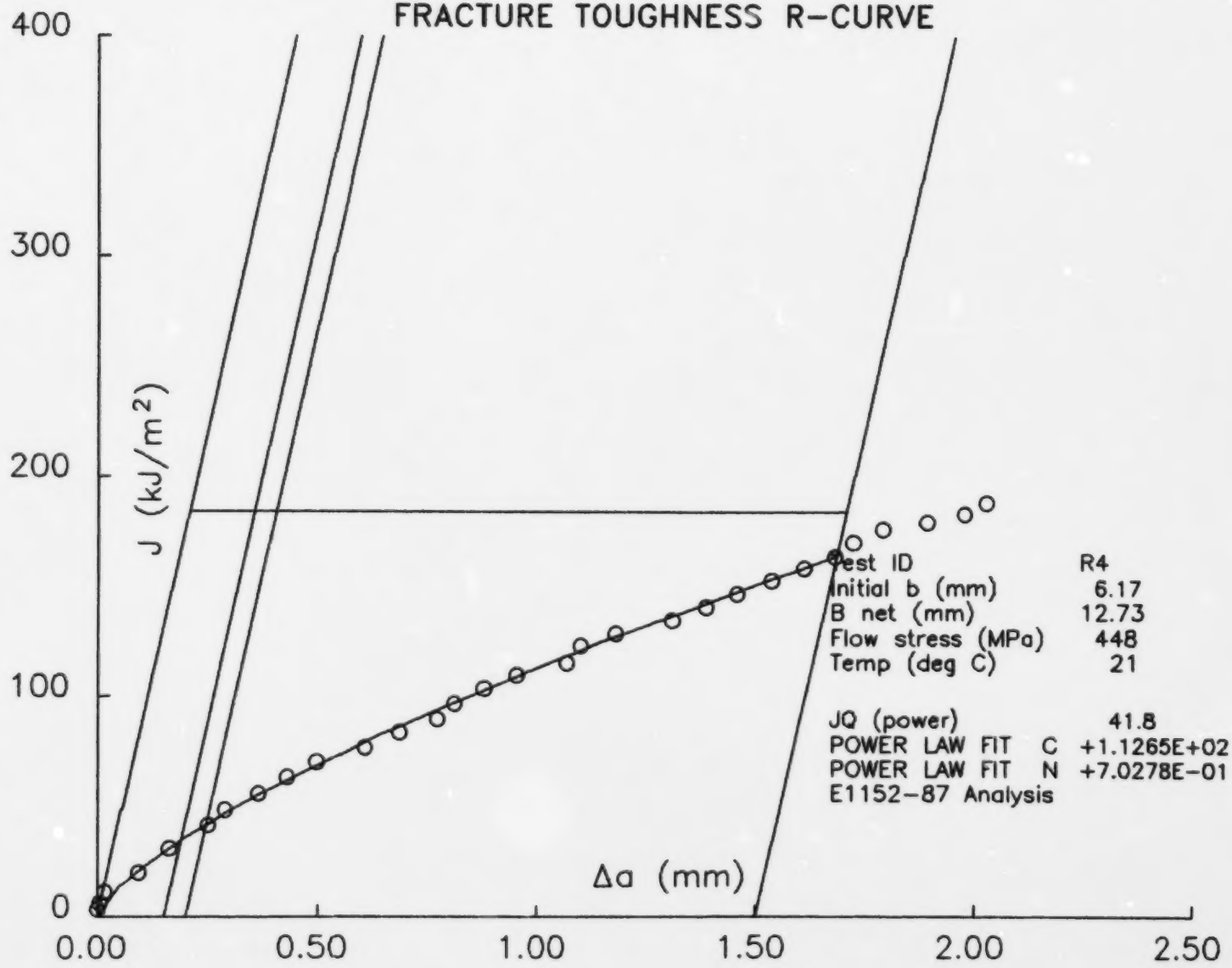
FRACTURE TOUGHNESS R-CURVE
400
300
200
100
0
J (kJ/m²)
Δa (mm)
0.00
0.50
1.00
1.50
2.00
2.50
Test ID R4
Initial b (mm) 6.17
B net (mm) 12.73
Flow stress (MPa) 448
Temp (deg C) 21
JQ (power) 41.8
POWER LAW FIT C +1.1265E+02
POWER LAW FIT N +7.0278E-01
E1152-87 Analysis

A34

89-135

ELASTIC-PLASTIC
FRACTURE TOUGHNESS ANALYSIS

Specimen Id.	R6	Geometry	SE(B)
Contract #	BHWP	Orientation	C-L
Material	A516 Gr 70	Flow stress (MPa)	448
Temperature (C)	21	Modulus (GPa)	192
Environment	AIR	Stroke rate (mm/min)	0.005
		Loading rate (min)	7.381

Specimen Dimensions (mm)

Thickness	15.90	Notch depth	8.00
Net thickness	12.79	Gage length	5.00
Width	15.87	Alpha ratio	1.008
Span	63.5		

Initial Ligament(s) (mm)

6.38	6.37	6.36	6.32	6.36	6.38	6.37	6.38	6.41

Final Ligament(s) (mm)

3.36	4.68	4.29	3.84	3.91	3.87	3.71	3.71	3.36

Precrack Parameters

Pmax (kN)	1.90	Stress ratio (R)	0.10
Final a (mm)	9.30	Kmax (MPa sqr[m])	14.24

Test Parameters

Initial ligament	(mm)	6.37	J1limit	(kJ/m^2)	190
Final ligament	"	3.92	J2limit	"	142
Delta a (actual)	"	2.45	J2limit	"	114
Delta a (EvB/P)	"	2.42	*JQ (813-81)	"	29
Delta a error	"	-0.03	*JQ (813-81)(NV)	"	29
Delta a error	(%)	-1.2	*JQ (813-87)	"	40
Compliance Adjustment		1.154	*JQ (813-87)(NV)	"	40
CTODi (mm)		0.034	Tearing modulus		75.7

POWER LAW REGRESSION CONSTANT C +1.0936E+02
POWER LAW REGRESSION EXPONENT N +7.2023E-01

Comments * Computed from E813-87 form for J

Tested December 22 1988.
Crk ext edge to ctr > 2% of W (sec 9.4.1.6)
Em differs from E by > 10%
Improper data group for E1152-87 (Sec 8.4.1)

Specimen Id. R6

Index	Load (kN)	Disp. (mm)	Delta a (mm)	CTOD (mm)	K399 (MPa sqr[m])	K813	J813-81	J813-87 (kJ/m^2)	J1152	Jmod
0	0.0	-0.020		0.000	0.0	0.0	0.0	0.0	0.0	0.0
1	2.3	0.046		0.002	19.2	14.8	1.3	1.1	1.1	1.1
2	2.8	0.067		0.004	23.4	21.3	2.6	2.4	2.4	2.4
3	3.3	0.088		0.006	27.6	27.1	4.2	3.8	3.8	3.8
4	3.8	0.119	0.000	0.011	31.8	35.0	6.8	6.4	6.4	6.4
5	4.3	0.174	0.047	0.019	36.4	47.4	12.3	11.7	11.7	11.7
6	4.6	0.268	0.124	0.033	39.6	64.5	22.5	21.7	21.8	22.0
7	4.8	0.366	0.225	0.049	42.4	79.1	33.6	32.5	32.8	33.3
8	4.9	0.441	0.248	0.061	43.5	89.2	42.8	41.4	42.0	42.5
9	4.9	0.519	0.341	0.074	44.6	98.5	51.9	50.5	51.0	52.2
10	4.9	0.597	0.420	0.087	45.5	107.0	61.1	59.6	60.2	62.0
11	4.9	0.680	0.506	0.101	46.5	115.4	70.9	69.3	69.9	72.5
12	4.8	0.762	0.587	0.115	46.5	123.1	80.5	78.8	79.5	83.0
13	4.8	0.840	0.683	0.129	47.7	129.8	89.3	87.6	88.2	93.0
14	4.7	0.921	0.795	0.143	48.2	136.4	98.0	96.8	96.9	103.3
15	4.5	1.004	0.911	0.157	47.6	142.8	106.7	106.0	105.6	114.0
16	4.4	1.090	1.071	0.172	48.7	148.6	114.4	114.9	113.2	124.6
17	4.2	1.173	1.212	0.188	48.5	154.1	121.8	123.5	120.7	135.0
18	4.1	1.259	1.350	0.203	49.3	159.3	129.2	131.9	128.1	145.5
19	3.9	1.343	1.487	0.219	48.9	164.1	136.1	140.1	135.0	155.8
20	3.7	1.431	1.647	0.235	48.8	168.8	142.2	148.2	141.1	166.3
21	3.6	1.517	1.785	0.251	49.7	172.9	148.3	155.5	147.1	176.4
22	3.4	1.605	1.899	0.268	48.8	177.2	155.0	163.2	153.8	186.8
23	3.2	1.689	2.035	0.284	48.1	180.8	159.8	170.0	158.6	196.2
24	3.1	1.774	2.149	0.301	48.5	184.2	165.2	176.5	164.0	205.7
25	2.9	1.862	2.312	0.317	48.2	187.6	168.4	183.0	167.2	215.2
26	2.8	1.948	2.416	0.335	48.4	190.6	173.3	189.0	172.1	224.4

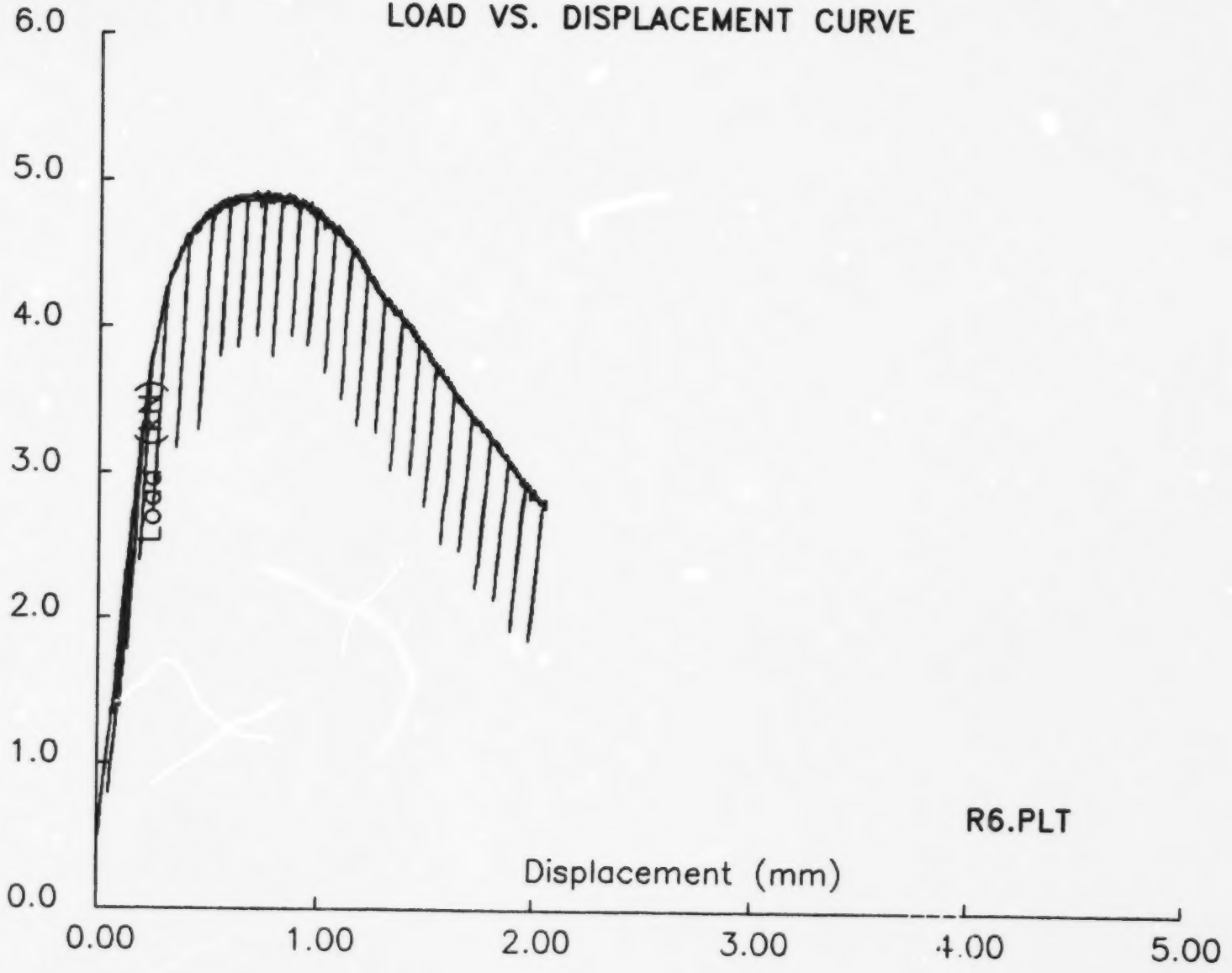
LOAD VS. DISPLACEMENT CURVE
6.0
5.0
4.0
3.0
2.0
1.0
0.0
Load (kN)
R6.PLT
Displacement (mm)
0.00
1.00
2.00
3.00
4.00
5.00

A37

89-135

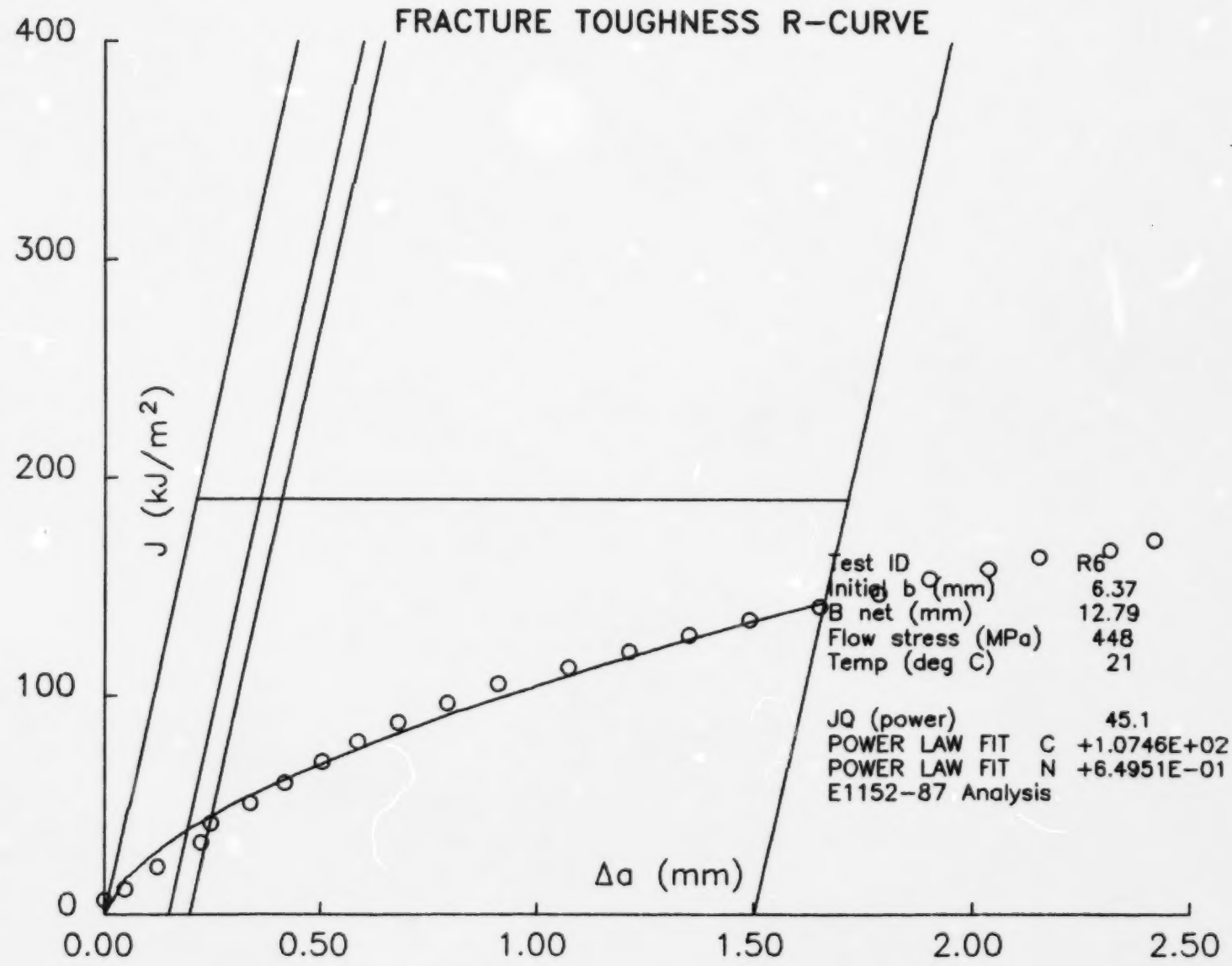
FRACTURE TOUGHNESS R-CURVE
400
300
200
100
0
J (kJ/m²)
Δa (mm)
0.00
0.50
1.00
1.50
2.00
2.50
Test ID R6
Initial b (mm) 6.37
B net (mm) 12.79
Flow stress (MPa) 448
Temp (deg C) 21
JQ (power) 45.1
POWER LAW FIT C +1.0746E+02
POWER LAW FIT N +6.4951E-01
E1152-87 Analysis

A38

89-135

ELASTIC-PLASTIC FRACTURE TOUGHNESS ANALYSIS

Specimen Id.	B3	Geometry	SE(B)
Contract #	BHWP	Orientation	C-R
Material	A516 Gr 70	Flow stress (MPa)	438
Temperature (C)	43	Modulus (GPa)	192
Environment	AIR	Stroke rate (mm/min)	0.005
		Loading rate (min)	5.236

Specimen Dimensions (mm)

Thickness	15.84	Notch depth	7.80
Net thickness	12.57	Gage length	5.00
Width	15.83	Alpha ratio	1.008
Span	63.5		

Initial Ligament(s) (mm)

5.97	5.89	5.88	5.87	5.86	5.85	5.96	5.96	6.05

Final Ligament(s) (mm)

3.46	3.94	4.11	4.13	4.16	4.44	4.35	3.84	3.86

Precrack Parameters

Pmax (kN)	1.90	Stress ratio (R)	0.10
Final a (mm)	9.00	Kmax (MPa sqr[m])	16.03

Test Parameters

Initial ligament	(mm)	5.91	J15limit	(kJ/m^2)	173
Final ligament	"	4.08	J20limit	"	129
Delta a (actual)	"	1.83	J25limit	"	104
Delta a (EvB/P)	"	1.62	*JQ (813-81)	"	0
Delta a error	"	-0.21	*JQ (813-81)(NV)	"	85
Delta a error	(%)	-11.7	*JQ (813-87)	"	0
Compliance Adjustment		1.636	*JQ (813-87)(NV)	"	269
CTODi (mm)		0.068	Tearing modulus		463.2

POWER LAW REGRESSION CONSTANT C +5.0456E+02
POWER LAW REGRESSION EXPONENT N +9.2515E-01

Comments

* Computed from E813-87 form for J

Tested February 1989.
Precrack load > 40% of limit load (Sec 7.6.2)
Less than 4 data pts for JIc fit (Sec 9.3.2)
Thickness < 25*JQ/flowstress (Sec 9.4.1.1)
Ligament < 25*JQ/flowstress (Sec 9.4.1.2)
Crk ext edge to ctr > 2% of W (sec 9.4.1.6)
Em differs from E by > 10%
Improper data group for E1152-87 (Sec 8.4.1)

Specimen Id. B3

Index	Load (kN)	Disp. (mm)	Delta a (mm)	CTOD (mm)	K399 (MPa sqr[m])	K813	J813-81	J813-87 (kJ/m^2)	J1152	Jmod
0	0.0	-0.015		0.000	0.0	0.0	0.0	0.0	0.0	0.0
1	3.0	0.023		0.001	28.4	10.1	0.9	0.5	0.5	0.5
2	3.5	0.048		0.004	33.2	22.3	3.1	2.6	2.6	2.6
3	4.0	0.077		0.007	37.9	32.0	6.0	5.4	5.4	5.4
4	4.5	0.170	0.000	0.020	42.6	55.1	16.7	15.8	15.8	15.8
5	4.7	0.270	0.038	0.035	45.0	73.3	29.0	28.0	28.0	28.1
6	4.9	0.371	0.026	0.048	46.7	88.7	42.2	41.0	41.1	41.1
7	5.1	0.466	0.034	0.063	48.7	101.5	54.9	53.6	53.8	53.9
8	5.3	0.562		0.077	50.6	113.5	68.5	67.1	67.5	67.6
9	5.4	0.664	0.083	0.092	52.3	125.0	82.7	81.4	81.3	81.9
10	5.6	0.764	0.108	0.107	54.6	135.7	97.3	95.9	95.9	96.8
11	5.8	0.865	0.140	0.123	57.0	146.0	112.6	111.1	111.0	112.4
12	5.9	0.967	0.168	0.139	58.4	156.1	128.5	126.9	126.8	128.8
13	6.1	1.062	0.178	0.154	60.6	165.1	144.0	142.0	142.3	144.4
14	6.2	1.159	0.215	0.170	62.2	174.0	159.7	157.8	157.8	160.8
15	6.3	1.261	0.252	0.186	63.8	183.0	176.4	174.5	174.5	178.4
16	6.4	1.362	0.303	0.202	65.7	191.6	192.9	191.3	190.8	196.2
17	6.4	1.460	0.347	0.218	66.5	199.7	209.1	207.9	207.0	213.9
18	6.5	1.557	0.349	0.234	67.6	207.6	226.9	224.5	224.7	231.7
19	6.5	1.659	0.381	0.249	68.2	215.6	244.6	242.1	242.4	250.5
20	6.5	1.757	0.423	0.266	69.0	222.9	261.1	258.9	258.7	268.7
21	6.5	1.859	0.483	0.281	70.1	230.2	277.4	276.2	275.0	287.6
22	6.5	1.962	0.558	0.299	71.6	237.4	293.2	293.6	290.6	306.9
23	6.5	2.065	0.584	0.316	72.2	244.4	311.6	311.4	309.0	326.7
24	6.5	2.162	0.642	0.332	73.4	250.8	327.0	327.8	324.4	345.2
25	6.5	2.260	0.691	0.349	74.4	257.1	343.2	344.5	340.4	364.2
26	6.5	2.363	0.727	0.366	75.2	263.6	361.2	362.1	358.4	384.4
27	6.4	2.461	0.768	0.382	75.0	269.7	377.8	379.0	375.0	403.7
28	6.4	2.559	0.805	0.399	75.8	275.5	394.4	395.5	391.6	422.9
29	6.4	2.662	0.818	0.415	76.1	281.6	413.9	413.1	411.0	443.3
30	6.4	2.764	0.870	0.432	77.3	287.3	430.0	430.1	427.1	463.4
31	6.4	2.867	0.886	0.449	77.7	293.1	449.5	447.7	446.5	484.1
32	6.3	2.970	0.915	0.466	77.1	298.8	467.6	465.3	464.6	504.8
33	6.3	3.073	0.955	0.484	78.1	304.2	484.5	482.3	481.4	525.2
34	6.3	3.176	0.982	0.501	78.7	309.6	502.7	499.5	499.6	545.8
35	6.2	3.274	1.010	0.518	78.1	314.7	519.6	516.0	516.5	565.5
36	6.1	3.378	1.041	0.535	77.6	319.9	537.1	533.2	534.0	586.2
37	6.0	3.481	1.094	0.552	77.6	324.8	551.6	549.7	548.5	606.3
38	6.0	3.584	1.124	0.570	78.4	329.6	568.4	566.0	565.3	626.5
39	5.9	3.688	1.144	0.587	77.6	334.4	586.6	582.8	583.5	647.0
40	5.9	3.785	1.167	0.605	78.1	338.8	602.9	598.0	599.8	666.0
41	5.9	3.888	1.181	0.622	78.5	343.3	621.5	614.2	618.3	686.3
42	5.8	3.991	1.236	0.639	78.5	347.7	634.4	630.2	631.2	706.3
43	5.8	4.094	1.221	0.657	78.1	352.2	656.9	646.4	653.7	726.7
44	5.6	4.194	1.309	0.674	77.6	356.3	663.7	661.6	660.5	745.6
45	5.5	4.292	1.361	0.690	77.6	360.2	674.9	676.1	671.7	764.2
46	5.5	4.395	1.398	0.707	78.6	364.1	689.2	690.9	685.9	783.7
47	5.4	4.499	1.421	0.724	77.7	368.2	705.6	706.3	702.4	803.6
48	5.3	4.607	1.524	0.742	79.0	372.0	709.5	721.2	706.1	823.4
49	5.2	4.716	1.557	0.760	78.4	376.0	724.8	736.7	721.5	844.1

Specimen Id. B3

Index	Load (kN)	Disp. (mm)	Delta a (mm)	CTOD (mm)	K399 (MPa sqr[m])	K813	J813-81	J813-87 (kJ/m^2)	J1152	Jmod
50	5.1	4.824	1.586	0.777	77.7	379.8	740.4	751.8	737.1	864.3
51	5.0	4.928	1.617	0.793	77.0	383.4	754.3	766.1	751.1	883.5

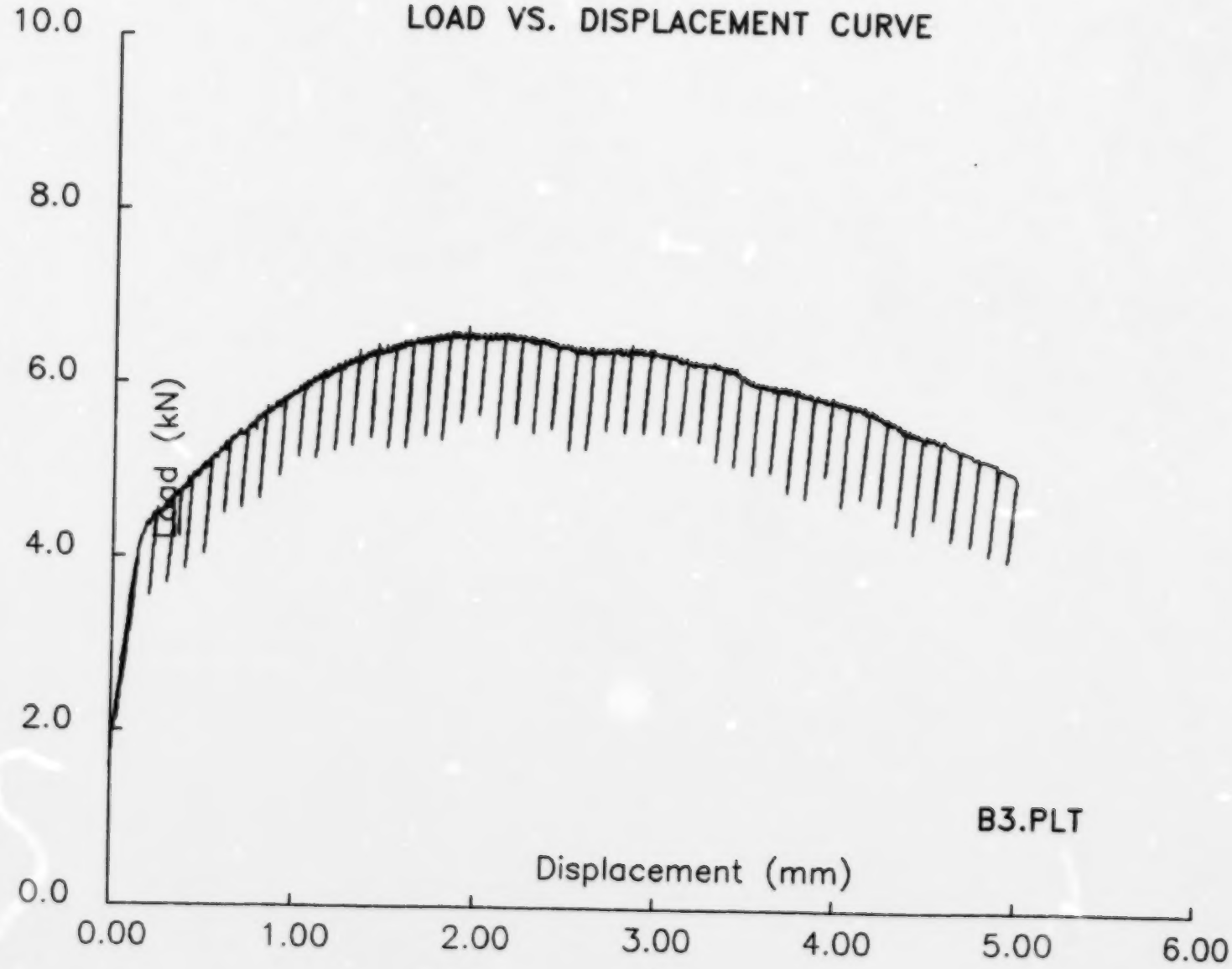
LOAD VS. DISPLACEMENT CURVE
10.0
8.0
6.0
4.0
2.0
0.0
Load (kN)
B3.PLT
Displacement (mm)
0.00
1.00
2.00
3.00
4.00
5.00
6.00

A42

89-135

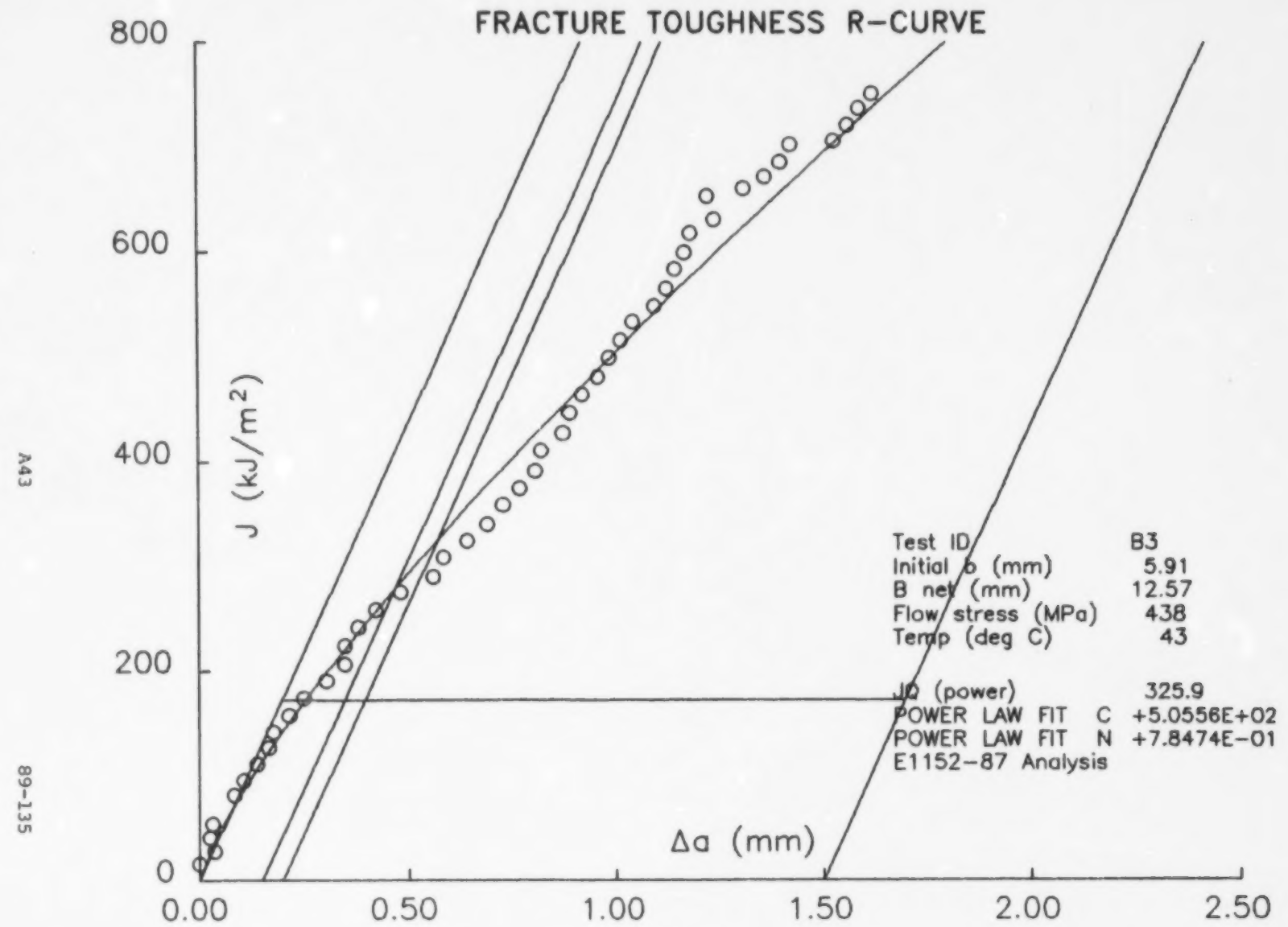
FRACTURE TOUGHNESS R-CURVE
800
600
400
200
0
J (kJ/m²)
Δa (mm)
0.00
0.50
1.00
1.50
2.00
2.50
Test ID B3
Initial b (mm) 5.91
B net (mm) 12.57
Flow stress (MPa) 438
Temp (deg C) 43
JQ (power) 325.9
POWER LAW FIT C +5.0556E+02
POWER LAW FIT N +7.8474E-01
E1152-87 Analysis
A43
89-135

ELASTIC-PLASTIC FRACTURE TOUGHNESS ANALYSIS

Specimen Id.	C7	Geometry	SE(B)
Contract #	BHWP	Orientation	C-R
Material	A516 Gr 70	Flow stress (MPa)	438
Temperature (C)	43	Modulus (GPa)	192
Environment	AIR	Stroke rate (mm/min)	0.005
		Loading rate (min)	5.429

Specimen Dimensions (mm)

Thickness	15.83	Notch depth	7.81
Net thickness	12.89	Gage length	5.00
Width	15.92	Alpha ratio	1.008
Span	63.5		

Initial Ligament(s) (mm)

6.47	6.36	6.45	6.43	6.51	6.44	6.46	6.45	6.57

Final Ligament(s) (mm)

3.66	4.21	4.11	4.22	4.34	4.35	4.38	4.32	3.86

Precrack Parameters

Pmax (kN)	1.90	Stress ratio (R)	0.10
Final a (mm)	9.00	Kmax (MPa sqr[m])	14.03

Test Parameters

Initial ligament	(mm)	6.45	J15limit	(kJ/m^2)	189
Final ligament	"	4.21	J20limit	"	141
Delta a (actual)	"	2.24	J25limit	"	113
Delta a (EvB/P)	"	1.97	*JQ (813-81)	"	0
Delta a error	"	-0.27	*JQ (813-81)(NV)	"	292
Delta a error	(%)	-12.1	*JQ (813-87)	"	0
Compliance Adjustment		1.549	*JQ (813-87)(NV)	"	368
CTODi (mm)		0.206	Tearing modulus		305.8

POWER LAW REGRESSION CONSTANT C +5.0155E+02
POWER LAW REGRESSION EXPONENT N +6.4672E-01

Comments * Computed from E813-87 form for J

Tested February 27 1989.
Less than 4 data pts for JIc fit (Sec 9.3.2)
Thickness < 25*JQ/flowstress (Sec 9.4.1.1)
Ligament < 25*JQ/flowstress (Sec 9.4.1.2)
Crk ext edge to ctr > 2% of W (sec 9.4.1.6)
Em differs from E by > 10%
Improper data group for E1152-87 (Sec 8.4.1)

Specimen Id. C7

Index	Load (kN)	Disp. (mm)	Delta a (mm)	CTOD (mm)	K399 (MPa sqr[mJ)	K813	J813-81	J813-87 (kJ/m^2)	J1152	Jmod
0	0.0	-0.015		0.000	0.0	0.0	0.0	0.0	0.0	0.0
2	3.9	0.015		0.005	31.9	6.7	0.7	0.2	0.2	0.2
3	4.4	0.026		0.008	36.0	15.2	1.8	1.2	1.2	1.2
4	4.9	0.042		0.012	40.1	23.8	3.7	3.0	3.0	3.0
5	5.4	0.107	0.000	0.023	44.2	45.6	11.7	10.8	10.8	10.8
6	5.7	0.202	0.038	0.039	47.1	66.7	24.2	23.2	23.2	23.3
7	6.0	0.292	0.028	0.056	49.4	82.9	37.0	35.8	35.9	35.9
8	6.3	0.387	0.023	0.073	51.8	97.7	51.2	49.7	50.0	50.0
9	6.5	0.484	0.042	0.090	53.7	111.2	66.0	64.5	64.7	64.8
10	6.8	0.579	0.076	0.108	56.7	123.4	80.9	79.4	79.5	79.9
11	6.9	0.678	0.086	0.125	57.6	135.5	97.4	95.6	95.9	96.4
12	7.1	0.776	0.054	0.143	58.9	146.7	114.5	112.2	113.0	113.1
13	7.2	0.876	0.140	0.161	60.9	157.2	130.4	128.9	128.7	130.3
14	7.4	0.973	0.160	0.179	62.9	167.1	147.3	145.6	145.6	147.5
15	7.4	1.071	0.215	0.196	63.8	176.7	163.9	162.7	162.1	165.2
16	7.5	1.166	0.224	0.213	64.8	185.6	181.3	179.6	179.5	182.8
17	7.6	1.266	0.277	0.231	66.5	194.5	198.5	197.2	196.5	201.3
18	7.7	1.366	0.281	0.248	67.5	203.4	217.6	215.5	215.6	220.5
19	7.8	1.466	0.273	0.267	68.2	211.9	237.3	234.0	235.2	239.9
20	7.8	1.564	0.376	0.285	70.0	219.7	252.5	251.6	250.3	258.7
21	7.9	1.659	0.374	0.302	70.9	227.4	271.7	269.5	269.4	277.8
22	7.9	1.761	0.428	0.320	71.8	235.3	289.8	288.4	287.5	298.1
23	8.0	1.861	0.430	0.339	72.8	242.9	310.2	307.5	307.9	318.6
24	8.0	1.959	0.509	0.357	74.3	250.0	326.3	325.6	323.9	338.5
25	7.9	2.059	0.514	0.374	73.4	257.2	346.7	344.8	344.3	359.2
26	7.9	2.162	0.576	0.392	74.6	264.2	364.3	363.8	361.8	380.2
27	7.9	2.265	0.585	0.410	74.8	271.2	385.3	383.3	382.8	401.6
28	7.9	2.362	0.698	0.429	77.1	277.3	397.9	400.6	395.3	421.3
29	7.8	2.463	0.713	0.447	76.4	283.8	418.2	419.7	415.6	442.6
30	7.7	2.563	0.805	0.465	77.3	289.8	432.5	437.7	429.8	463.3
31	7.5	2.670	0.890	0.483	77.1	296.1	448.2	456.9	445.6	485.4
32	7.4	2.771	0.970	0.502	77.7	301.7	462.6	474.4	459.9	505.9
33	7.3	2.877	1.025	0.521	77.9	307.5	479.9	492.8	477.2	527.7
34	7.2	2.976	1.080	0.539	78.0	312.8	495.6	509.9	492.9	548.1
35	7.1	3.082	1.133	0.558	78.1	318.2	512.5	527.8	509.8	569.7
36	7.1	3.184	1.169	0.577	78.9	323.3	530.2	544.8	527.3	590.6
37	7.1	3.282	1.207	0.596	79.8	328.2	546.7	561.2	543.8	610.8
38	7.0	3.382	1.252	0.615	79.7	333.1	562.9	578.1	560.0	631.6
39	6.9	3.487	1.289	0.633	79.4	338.0	580.7	595.5	577.7	653.1
40	6.8	3.593	1.340	0.653	79.4	342.9	596.6	612.7	593.7	674.6
41	6.7	3.698	1.405	0.673	79.8	347.6	610.6	629.5	607.6	695.9
42	6.6	3.803	1.417	0.692	78.9	352.2	630.4	646.4	627.5	717.3
43	6.4	3.911	1.529	0.712	79.2	356.7	637.8	662.9	634.9	738.5
44	6.2	4.014	1.617	0.732	78.8	360.8	646.7	678.4	643.7	758.6
45	6.1	4.119	1.672	0.752	78.9	364.9	659.9	693.7	656.9	778.9
46	6.0	4.225	1.743	0.772	79.4	368.8	670.7	708.7	667.7	799.3
47	5.9	4.324	1.825	0.792	80.2	372.4	678.3	722.5	675.2	818.3
48	5.8	4.430	1.847	0.812	79.4	376.2	695.7	737.6	692.7	838.9
49	5.7	4.536	1.804	0.833	76.9	380.2	722.7	753.1	719.8	859.8
50	5.6	4.640	1.838	0.853	76.4	383.7	737.1	767.4	734.3	879.4

Specimen Id. C7

Index	Load (kN)	Disp. (mm)	Delta a (mm)	CTOD (mm)	K399 (MPa sqr[m])	K813	J813-81	J813-87 (kJ/m^2)	J1152	Jmod
51	5.6	4.738	1.907	0.873	78.2	386.9	744.4	779.9	741.4	897.4
52	5.5	4.839	1.968	0.892	78.4	390.1	753.2	793.1	750.2	916.1

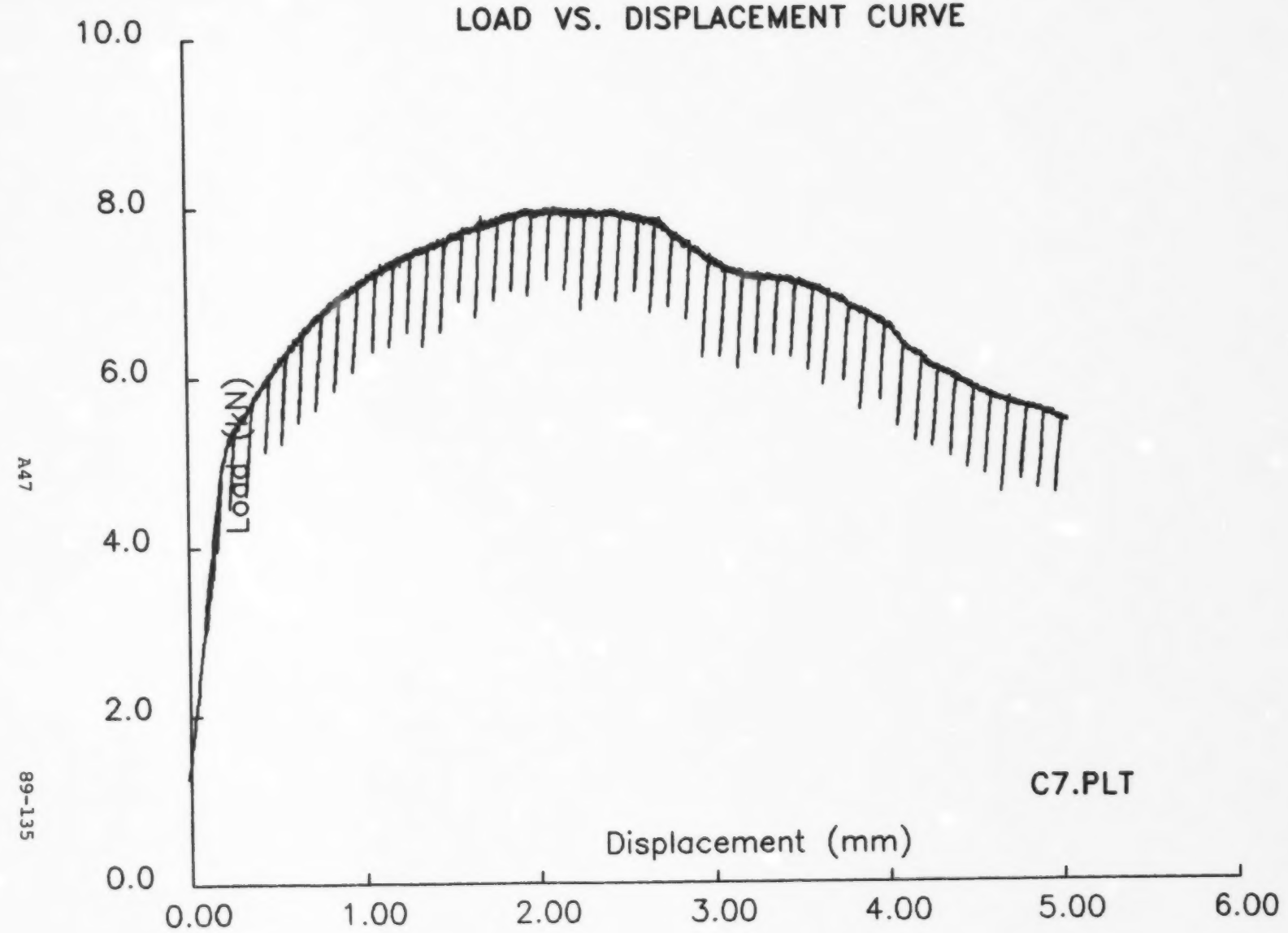
LOAD VS. DISPLACEMENT CURVE
10.0
8.0
6.0
4.0
2.0
0.0
Load (kN)
0.00
1.00
2.00
3.00
4.00
5.00
6.00
Displacement (mm)
C7.PLT
A47
89-135

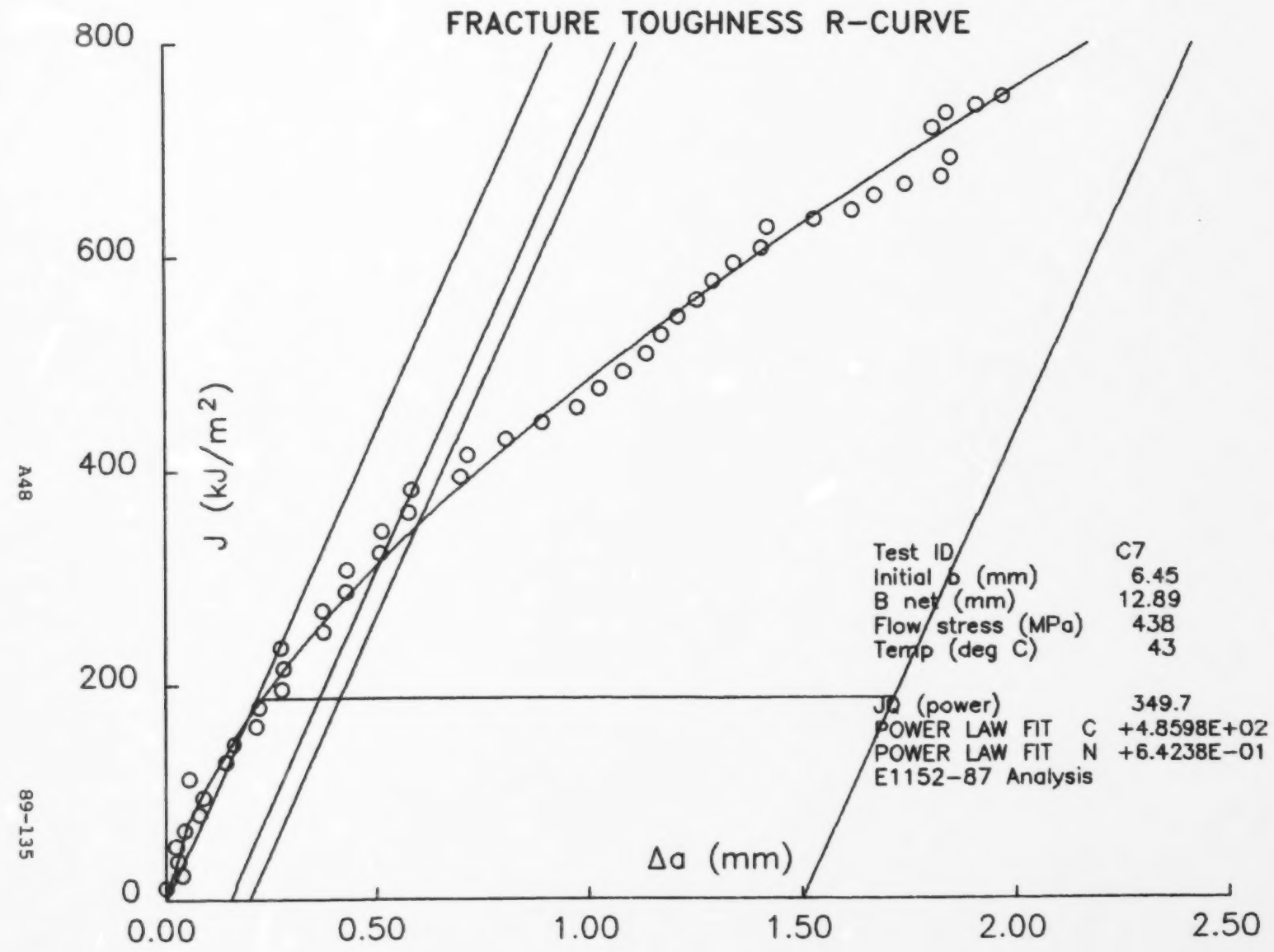
FRACTURE TOUGHNESS R-CURVE
800
600
400
200
0
J (kJ/m²)
Δa (mm)
0.00
0.50
1.00
1.50
2.00
2.50
Test ID C7
Initial b (mm) 6.45
B net (mm) 12.89
Flow stress (MPa) 438
Temp (deg C) 43
JQ (power) 349.7
POWER LAW FIT C +4.8598E+02
POWER LAW FIT N +6.4238E-01
E1152-87 Analysis
A48
89-135

ELASTIC-PLASTIC FRACTURE TOUGHNESS ANALYSIS

Specimen Id.	C	Geometry	SE(B)
Contract #	BHWP	Orientation	C-R
Material	A516 Gr 70	Flow stress (MPa)	438
Temperature (C)	43	Modulus (GPa)	192
Environment	AIR	Stroke rate (mm/min)	0.005
		Loading rate (min)	5.595

Specimen Dimensions (mm)

Thickness	15.89	Notch depth	7.85
Net thickness	12.80	Gage length	5.00
Width	15.97	Alpha ratio	1.008
Span	63.5		

Initial Ligament(s) (mm)

5.91	5.82	5.79	5.74	5.73	5.73	5.81	5.88	6.05

Final Ligament(s) (mm)

3.27	3.80	3.96	3.94	3.96	4.02	3.89	3.93	3.80

Precrack Parameters

Pmax (kN)	1.90	Stress ratio (R)	0.10
Final a (mm)	9.50	Kmax (MPa sqr[m])	16.41

Test Parameters

Initial ligament	(mm)	5.81	J15limit	(kJ/m^2)	170
Final ligament	〃	3.88	J20limit	〃	127
Delta a (actual)	〃	1.93	J25limit	〃	102
Delta a (EvB/P)	〃	1.81	*JQ (813-81)	〃	42
Delta a error	〃	-0.12	*JQ (813-81)(NV)	〃	39
Delta a error	(%)	-6.2	*JQ (813-87)	〃	0
Compliance Adjustment		1.579	*JQ (813-87)(NV)	〃	70
CTODi (mm)		0.044	Tearing modulus		141.6

POWER LAW REGRESSION CONSTANT C +1.7882E+02
POWER LAW REGRESSION EXPONENT N +7.4068E-01

Comments * Computed from E813-87 form for J

Tested March 1 1989.
Precrack load > 40% of limit load (Sec 7.6.2)
Improper data group for JIc (Sec 9.2.2)
Crk ext edge to ctr > 2% of W (sec 9.4.1.6)
Em differs from E by > 10%
Improper data group for E1152-87 (Sec 8.4.1)

Specimen Id. C

Index	Load (kN)	Disp. (mm)	Delta a (mm)	CTOD (mm)	K399 (MPa sqr[m])	K813	J813-81	J813-87 (kJ/m^2)	J1152	Jmod
0	0.0	-0.015		0.000	0.0	0.0	0.0	0.0	0.0	0.0
1	3.6	0.012	0.000	0.005	34.6	3.2	0.6	0.1	0.1	0.1
3	4.2	0.151		0.026	40.4	52.5	15.1	14.4	14.4	14.4
4	4.8	0.265	0.027	0.045	46.5	73.2	28.9	27.9	27.9	28.0
5	4.9	0.366	0.079	0.060	48.2	88.5	41.8	40.8	40.8	41.1
6	5.0	0.466	0.186	0.076	50.6	101.4	54.5	53.5	53.4	54.3
7	5.1	0.562	0.263	0.091	52.7	112.6	67.2	66.1	65.9	67.6
8	5.2	0.663	0.319	0.107	54.5	123.7	81.2	79.7	79.8	82.0
9	5.2	0.760	0.402	0.123	55.8	133.4	94.3	92.8	92.8	96.2
10	5.2	0.863	0.471	0.138	56.9	143.2	108.5	106.8	107.0	111.5
11	5.0	0.965	0.603	0.154	56.9	152.0	121.0	120.3	119.5	126.5
12	5.0	1.067		0.170	56.9	162.2	136.3	137.1	141.6	148.5
14	4.8	1.276	0.918	0.204	60.0	175.2	158.2	160.0	156.2	172.1
15	4.7	1.356	1.035	0.218	61.0	180.5	166.4	169.7	164.4	183.8
16	4.6	1.437	1.101	0.230	61.0	185.7	176.4	179.7	174.4	196.0
17	4.6	1.520	1.162	0.243	62.2	190.7	186.8	189.5	184.7	208.4
18	4.6	1.598	1.210	0.257	63.1	195.3	196.9	198.8	194.8	220.2
19	4.5	1.678	1.234	0.270	62.3	200.2	208.2	208.8	206.2	232.6
20	4.5	1.756	1.301	0.284	63.7	204.4	217.1	217.7	214.9	244.2
21	4.5	1.839	1.363	0.297	65.0	208.8	227.0	227.3	224.8	256.9
22	4.4	1.924	1.427	0.311	65.0	213.4	237.0	237.3	234.7	269.9
23	4.3	2.004	1.481	0.325	64.7	217.6	246.5	246.7	244.2	282.2
24	4.2	2.090	1.560	0.339	65.0	221.7	254.9	256.2	252.6	294.9
25	4.1	2.171	1.593	0.353	64.2	225.7	265.3	265.4	263.1	307.2
26	4.0	2.251	1.673	0.366	64.5	229.3	272.2	273.9	269.9	318.8
27	3.8	2.338	1.808	0.380	64.4	233.0	275.8	282.9	273.5	331.1

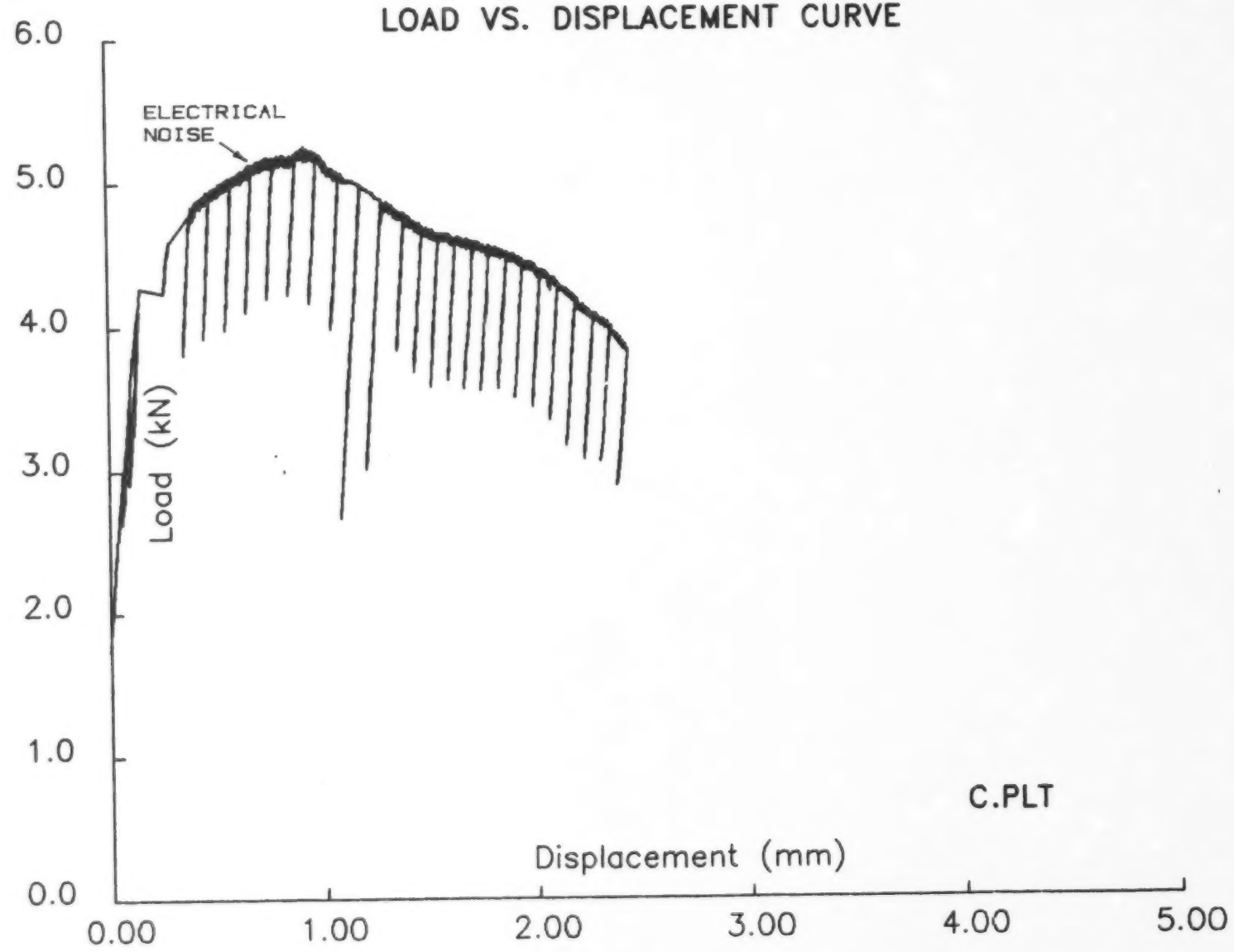
LOAD VS. DISPLACEMENT CURVE
ELECTRICAL NOISE
Load (kN)
6.0
5.0
4.0
3.0
2.0
1.0
0.0
0.00
1.00
2.00
3.00
4.00
5.00
Displacement (mm)
C.PLT

A51

89-135

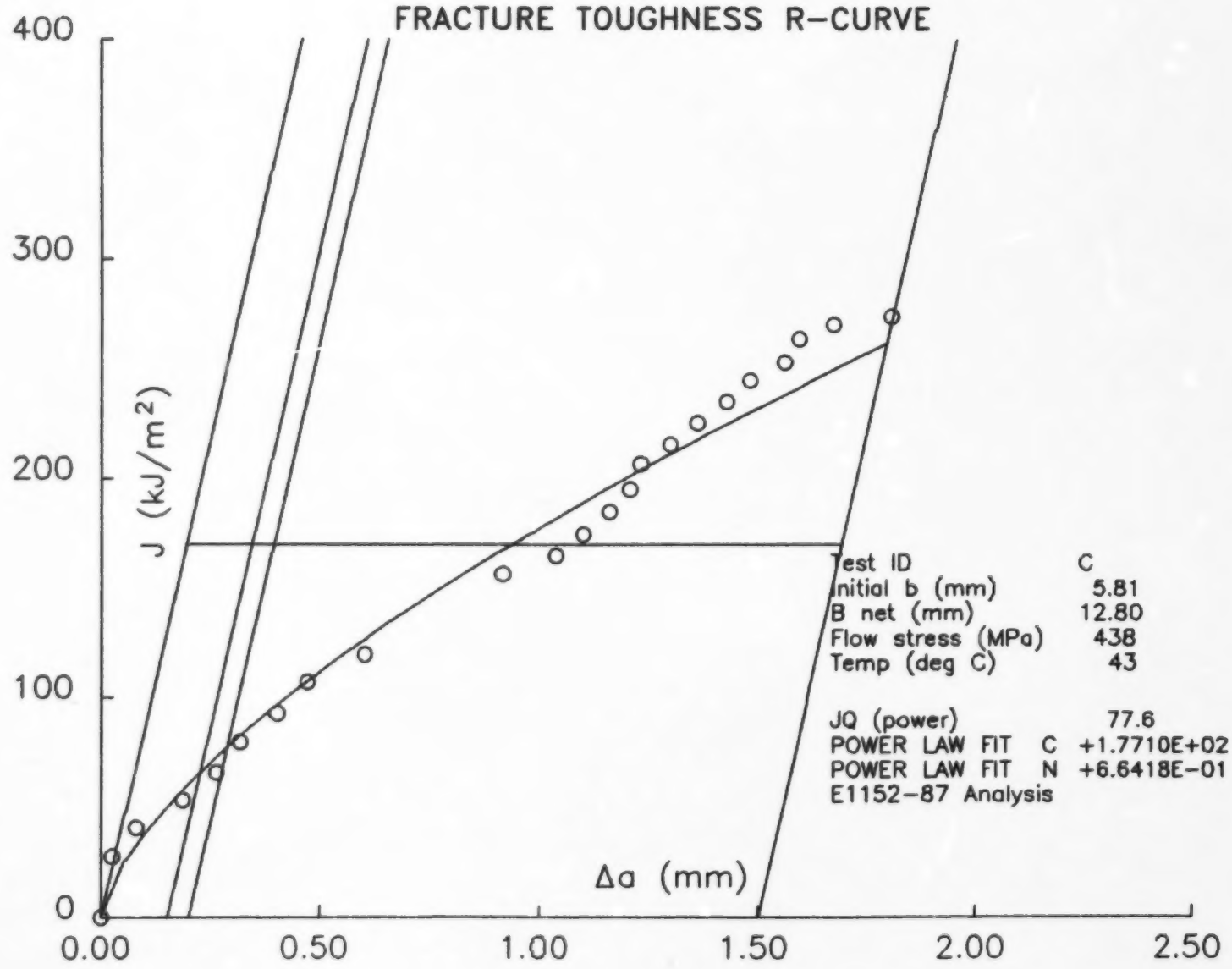
FRACTURE TOUGHNESS R-CURVE
400
300
200
100
0
J (kJ/m²)
Δa (mm)
0.00
0.50
1.00
1.50
2.00
2.50
Test ID C
Initial b (mm) 5.81
B net (mm) 12.80
Flow stress (MPa) 438
Temp (deg C) 43
JQ (power) 77.6
POWER LAW FIT C +1.7710E+02
POWER LAW FIT N +6.6418E-01
E1152-87 Analysis

A52

89-135

APPENDIX B

Fracture Surfaces of All Tests

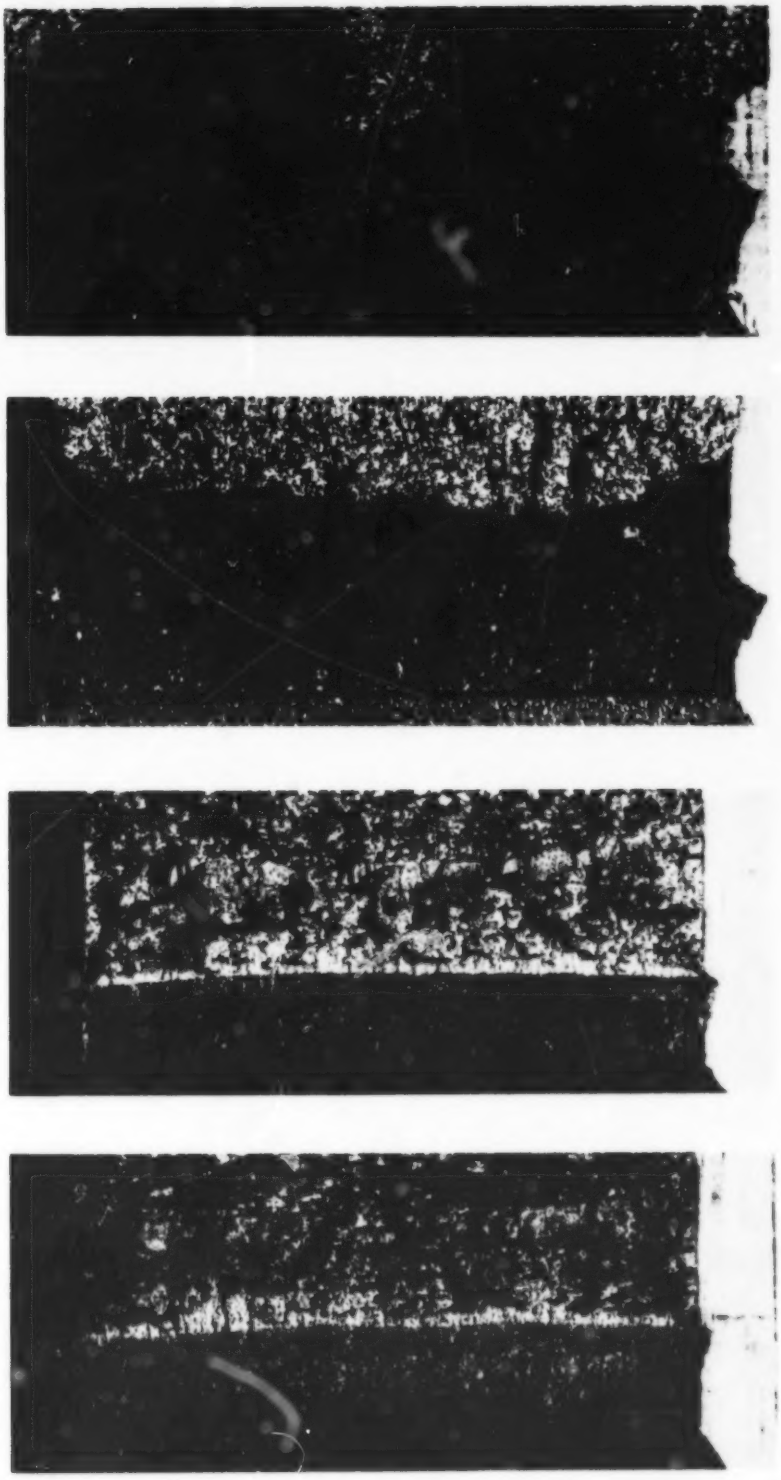

FIGURE B1 Fracture Surfaces of Unblistered Specimens Tested at 21°C.

D2

FIGURE B2 Fracture Surface of Unblistered Specimen Tested at 21°C.

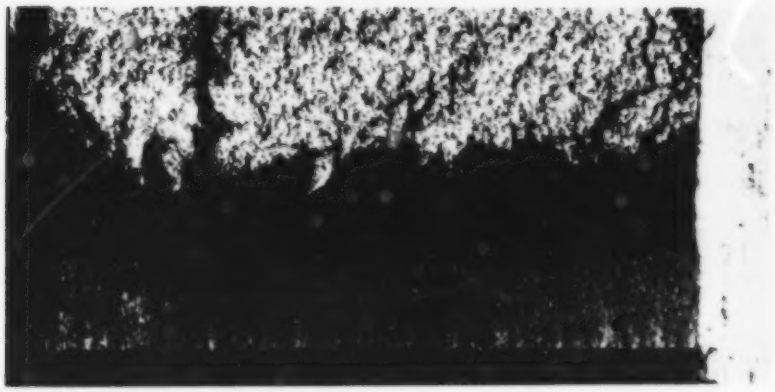

R8

R6

FIGURE B3 Fracture Surfaces of Blistered Specimens Tested at 21°C.

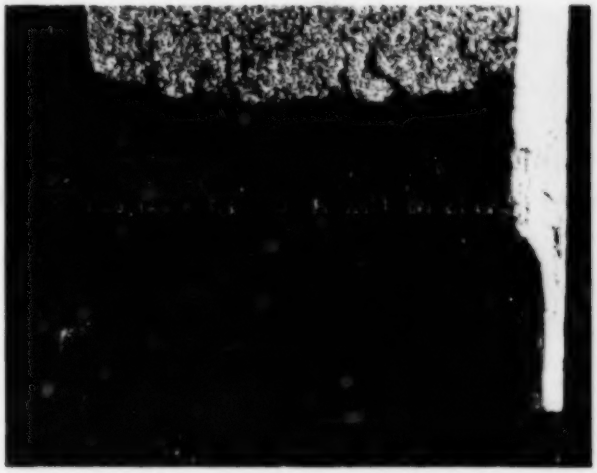

R1

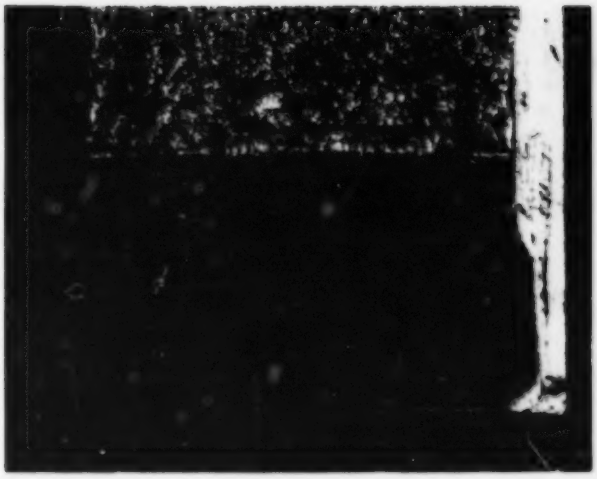

R4

FIGURE B4 Fracture Surfaces of Blistered Specimens Tested at 21°C.

B3

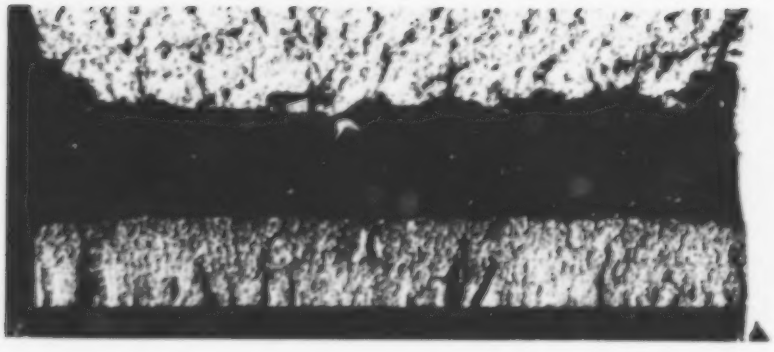

C7

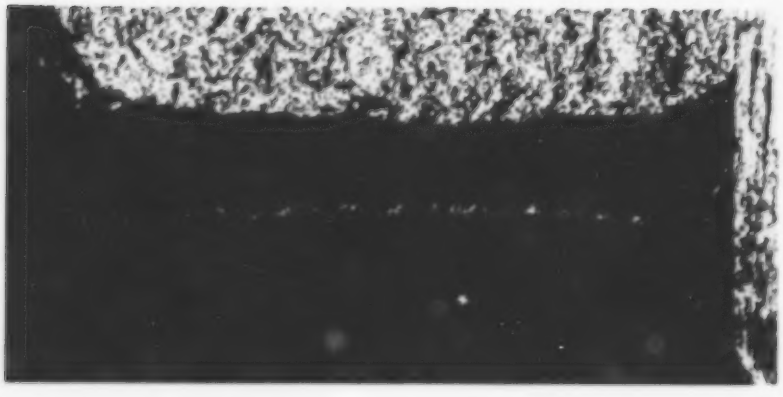

C

FIGURE B5 Fracture Surfaces of Specimens Tested at 43°C.